ENGINEERING EXPERIMENT STATION
DEPARTMENT OF MECHANICAL
AND INDUSTRIAL ENGINEERING
ME-TR-395-1

JET MIXING UNDER THE INFLUENCE OF A PRESSURE GRADIENT

by

D. F. BRINK and W. L. CHOW

FLUID DYNAMIC AND HEAT TRANSFER
ASSOCIATED WITH MODERN PROPULSIVE SYSTEMS

Research Grant No. NASA - NGL 14-005-140

UNIVERSITY OF ILLINOIS
AT URBANA - CHAMPAIGN
URBANA, ILLINOIS 61801
APRIL, 1971

FOREWORD

This research was carried out under Research Grant NASA NGL 14-005-140 entitled "Fluid Dynamic and Heat Transfer Problems Associated with Modern Propulsive Systems." This present report deals with the problem of jet mixing under non-constant pressure conditions.

UNCLASSIFIED
BIBLIOGRAPHICAL CONTROL SHEET

1. Originating Agency and Monitoring Agency
   O.A. University of Illinois at Urbana-Champaign
   Urbana, Illinois 61801
   M.A. NASA, Office of Research Grants and Contracts

2. Originating Agency and Monitoring Agency Report Number
   O.A. ME-TR-395-1
   M.A.

3. Title and Classification of Title
   Jet Mixing under the Influence of a Pressure Gradient

4. Personal Authors
   Brink, D. F., Chow, W. L.

5. Date of Report
   April 1971

6. Pages: 108

7. Illustrative Material: Twenty-four (24) figures

8. Prepared for Contract No.: NASA Research Grant NGL 14-005-140

9. Prepared for Project Code and/or No:

10. Security Classification: Unclassified

11. Distribution Limitation: None

12. Abstract

The problem of jet mixing under a non-constant pressure condition is examined in detail by theoretical analysis. The system of the non-similar boundary layer equations governing the flow phenomenon is solved by the asymptotic method of integrations. The analytical results provided sufficient evidence to the validity of the locally similar approximations under these flow conditions. The problem of relaxation from an initially non-similar flow field toward the final asymptotically similar flow has also been examined and discussed.

NOMENCLATURE

a	coefficients of series in Eq. (2.24)
A	coefficients of series in Eq. (2.34)
b	coefficients of series defined by Eq. (2.38)
C	coefficients of series in Eq. (2.33)
C_p	specific heat at constant pressure
Cr	Crocco number
d	coefficients of series in Eq. (2.36) or viscosity index
e	coefficients of series in Eq. (2.36)
f	stream function in transformed plane
F	defined by Eq. (2.26)
h	coefficients of series defined by Eq. (2.39)
L	reference length
m	dimensionless pressure gradient
p	pressure
Pr	Prandtl number
Re_L	Reynolds number based on length L
T	temperature
u,v	velocity components in x- and y-directions, respectively
x,y	coordinates along and normal to dividing streamline, respectively
γ	ratio of specific heats
$\Gamma(n)$	gamma function
$\Gamma(n,x)$	incomplete gamma function
ε	kinematic viscosity
η	transformed coordinate defined by Eq. (2.12)

β	ρ_{1a}/ρ, density ratio or T/T_{1a} the temperature ratio
λ	defined by Eq. (2.18)
Λ	T_o/T_{o1a}, total temperature ratio
Λ_b	T_{o1b}/T_{o1a}, freestream total temperature ratio
μ	dynamic viscosity
ν	kinematic viscosity
ξ	transformed coordinate defined by Eq. (2.11)
ρ	density
τ	variable of integration defined by Eq. (2.33)
ϕ	u/u_{1a}, velocity ratio or function defined by Eq. (2.28)
ϕ_b	u_{1b}/u_{1a}, freestream velocity ratio
ψ	stream function in physical plane
Ω	function defined by Eq. (2.31)

Subscripts

a	above dividing streamline
b	below dividing streamline
i	initial condition
j	dividing streamline
o	stagnation condition
1	edge of mixing layer

TABLE OF CONTENTS

1: INTRODUCTION

Intensive studies carried out within the last twenty years on separated flows have led to a better understanding of flow problems in this field. It was recognized that for flow past bluff bodies, the viscous layer cannot cope with the eventual pressure rise and breaks away together with the freestream from the wall, thereby forming a wake behind the body. The fluid within the shear layer can thus be energized through the jet mixing action and prepare itself for the subsequent reattachment or realignment of the flow. The interacting interplay between the viscid and the inviscid streams controls and determines the overall flow field. Flow problems associated with the phenomenon of the determination of the flow pattern through such viscid-inviscid interaction mechanisms are now classified as "strong interactions." The fact that the flow conditions downstream of separation contribute equally to the overall flow determination, including its influence on the location of the point of separation, properly illustrates the typical elliptic behavior of all separated flow problems, which is in sharp contrast with the classical boundary layer theory enunciated by Prandtl in its original form.

However, the boundary layer concept is very important and useful for all separated flow problems. Indeed, studies of these strong interaction problems are based entirely on the boundary layer concept; the pressure field is impressed and dictated by the adjacent freestream. The need to correct this basic interacting link between

the viscid and inviscid flows only arises when the effect of streamline curvature is no longer negligible.

Since jet mixing is one of the important flow components in separated flow, many investigations have been carried out to study constant pressure jet mixing, as a major portion of the wake boundary is under an essentially constant pressure condition. With idealized approaching flow (the initial condition for jet mixing), this mixing flow field exhibits similarity; the governing partial differential equations can be reduced into an ordinary differential equation through suitable transformations, and the solution of the flow problem is thereby greatly simplified.

There are many practical situations where mixing occurs while the pressure varies in the main direction of flow. For example, within an ejector system the inviscid interaction between the primary and secondary streams produces changes in the flow properties along the course of the flow. Thus, the mixing between the primary (faster moving stream) and the secondary (slower stream) flow is precisely such a variable pressure mixing. A previous method of dealing with such a flow problem [1]† was based on a purely speculative approach that the flow at each location has a locally similar profile, despite the fact that the flow is truthfully non-similar. Although this local similarity concept gives a reasonable estimation of this effect, the validity of this approach was never properly assessed. Thus, one basic motivation for studying jet mixing under the influence of a pressure gradient is to obtain the correct or

†Numbers in brackets refer to entries in REFERENCES.

more nearly exact solution, so that the result from any other approximate analysis to this problem may be compared and evaluated.

A modern concept in air breathing propulsion, conceived recently for propulsive systems under supersonic flight conditions such as a scramjet, relies on a successful combustion process occurring within a supersonic flow field. As combustion within a flow field must depend on the diffusive process within the jet mixing region, it is a necessity that the mixing process under the influence of a pressure gradient must be understood, since the pressure within such flow fields varies considerably.

It was also expected that the understanding of jet mixing with a pressure gradient may lead to the possibility of attacking flow reattachment onto the solid wall since all these types of problems involve non-similar flow fields. It is known that the method of dealing with partial differential equations of the boundary layer type would be much more complicated than that for ordinary differential equations when similar situations prevail.

A considerable amount of theoretical and experimental work on jet mixing problems has been performed previously. Chapman [2] obtained laminar jet mixing similar profiles. Crane [3] calculated turbulent similar flow solutions. Studies of developing flow under constant pressure conditions were all based on an integral approach or finite difference calculation [4,5,6]. There are also many other calculations for constant pressure jet mixing problems and they are not mentioned here.

One of the earliest studies of jet mixing with a pressure gradient was done by Napolitano and Pozzi [7] for laminar incompressible flows. They defined a velocity defect function and found the solutions for particular types of pressure gradient from the first two terms of the assumed infinite series. Their results for zero pressure gradient was compared favorably with other exact numerical results. Other studies of mixing between infinite stream and finite jet or wake with pressure gradient [8,9] relied the linearization of the momentum equation. Sabin [10] also obtained the approximate solution for incompressible turbulent mixing between two infinite streams with a pressure gradient. Perhaps a more thorough study of mixing under variable pressure conditions was carried out by Greenberg [11]. In the interest on the effectiveness of the cooling gas ejected into the stagnation region of a re-entry body, he studied first the mixing near the stagnation point and within the region where the effect of the boundary layer on the wall influences the mixing region. In the stagnation region, the jet mixing problem was recognized to possess a similar solution which was solved by using Meksyn's method for boundary layer flows [12]. In the second region of mixing downstream of the stagnation point, the flow is governed by the full non-similar equation. It was recognized that Meksyn's method could not sufficiently approximate the initial mixing region near the stagnation point and a series solution resembling the Blasius series for the non-similar boundary layer flow was incorporated. Some calculations were also made using a

finite difference technique for each of the two mixing regions and compared with the series solution; in both cases the agreement was reasonably good.

It should be pointed out that Greenberg did not follow Meksyn's scheme in the evaluation of the integrals by the series inversion technique. Since this series inversion would improve the convergence of the resulting series, it is an important part of Meksyn's "asymptotic method of integration." Therefore, the potential of studying non-similar jet mixing by Meksyn's method was never properly explored.

The present investigation of jet mixing with a pressure gradient is a part of the overall effort in the study of separated flow problems at the University of Illinois. Previous studies concerning constant pressure jet mixing of turbulent flows employed the integral momentum technique after adopting the error function for the fully developed flow profiles [13,14]. The turbulent flow structure of such flow fields has also been discussed [15]. A numerical integration has also been applied to the ordinary differential equation for a similar flow field [16]. In a recent investiation [17], Meksyn's method of solving boundary layer problems was applied to studying mixing problems with similarity. It was also recognized that this method has the potential to study non-similar flow problems and therefore Meksyn's technique forms the basic method for the present investigations.

The general scheme in dealing with such problems of steady,

compressible, non-isoenergetic jet mixing for either laminar or turbulent flows is presented in Chapter 2. To assess the validity of the method of solution, the case of constant pressure jet mixing has been presented in the following chapter and compared with another solution from numerical integrations. In Chapter 4 the solution to the problem of compressible, laminar jet mixing under the influence of a streamwise pressure gradient is derived. Finally, the problem of incompressible, constant pressure jet mixing is examined in Chapter 5 when the initial mixing profile is non-uniform, resulting in an asymptotic development toward the fully developed flow far downstream.

2. BASIC FORMULATION AND DERIVATION OF THE TWO-DIMENSIONAL JET MIXING BETWEEN TWO PARALLEL STREAMS UNDER THE INFLUENCE OF A PRESSURE GRADIENT

2.1 FUNDAMENTAL EQUATIONS AND DISCUSSIONS OF SIMILARITY

If one agrees that the present jet mixing problem can be treated within the framework of the boundary layer concept, the basic differential equations governing the flow phenomena are the system of boundary layer equations, namely,

$$\frac{\partial(\rho u)}{\partial x} + \frac{\partial(\rho v)}{\partial y} = 0 \tag{2.1}$$

$$\rho\left(u\,\frac{\partial u}{\partial x} + v\,\frac{\partial u}{\partial y}\right) = -\frac{\partial p}{\partial x} + \frac{\partial}{\partial y}\left(\varepsilon\rho\,\frac{\partial u}{\partial y}\right) \tag{2.2a}$$

$$\frac{\partial p}{\partial y} = 0 \tag{2.2b}$$

and

$$\rho C_p\left(u\,\frac{\partial T}{\partial x} + v\,\frac{\partial T}{\partial y}\right) = u\,\frac{\partial p}{\partial x} + \frac{\partial}{\partial y}\left(K\,\frac{\partial T}{\partial y}\right) + \varepsilon\rho\left(\frac{\partial u}{\partial y}\right)^2 \tag{2.3}$$

where ε is the kinematic viscosity ν for the laminar flows and the "eddy" kinematic viscosity for turbulent flows. The energy equation can be combined with the momentum equation and written as

$$\rho\left(u\,\frac{\partial T_o}{\partial x} + v\,\frac{\partial T_o}{\partial y}\right) = \frac{\partial}{\partial y}\left\{\frac{\varepsilon\rho}{Pr}\left[\frac{\partial T_o}{\partial y} + (Pr - 1)\,\frac{\partial}{\partial y}\left(\frac{u^2}{2C_p}\right)\right]\right\} \tag{2.4}$$

where the Prandtl number, $Pr = C_p \varepsilon\rho/k$, and the specific heat C_p have been assumed to be constant. The initial conditions considered here are (referring to Fig. 1),

$$u(0,y) = u_{1ai} = u_{1a}(0), \quad T_o(0,y) = T_{o1a}, \quad y > 0$$

$$u(0,y) = u_{1bi} = u_{1b}(0), \quad T_o(0,y) = T_{o1b}, \quad y < 0 \tag{2.5}$$

The boundary conditions take the form

$$u(x,\infty) = u_{1a}(x) \qquad T_o(x,\infty) = T_{o1a},$$

$$u(x,-\infty) = u_{1b}(x), \qquad T_o(x,-\infty) = T_{o1b}, \tag{2.6}$$

$$v(x,0) = 0$$

with

$$\frac{dp}{dx} = -\rho_1 u_1 \frac{du_1}{dx}$$

A usual practice of solving this system of partial differential equations is to seek suitable transformations and combinations of the dependent and independent variables of the problem so that a "similarity"† solution can be found and the system of equations transforms into ordinary differential equations.

†"Similarity" usually refers to similarity of velocity profiles, *i.e.*, the velocity profiles within the region can be represented by a single profile in the transformed plane.

This has been studied exhaustfully for wall boundary layer flows (*e.g.*, [18]) and it was found that for the existence of similarity not only must the boundary conditions and the initial conditions be "compatible," the pressure gradient associated with the flow problem is also restricted to specific types of functions.

When a similarity situation does exist for wall boundary layer flows, the unknown function $f'(\eta)$, (η is a combination of the x- and y-coordinates) associated with the velocity profiles, invariably satisfies the boundary conditions

$$f'(\eta = 0) = \frac{u(x,y = 0)}{u_1(x)} = 0$$

$$f'(\eta \to \infty) = \frac{u(x,y \to \infty)}{u_1(x)} = 1$$

For the present problem of jet mixing the boundary conditions imposed on the velocity profiles are

$$\frac{u(x,y \to \infty)}{u_{1a}(x)} = 1$$

and

$$\frac{u(x,y \to -\infty)}{u_{1a}(x)} = \frac{u_{1b}(x)}{u_{1a}(x)} = \phi_b(x)$$

as a result of the existence of the pressure gradient. Thus, for the same transformations as employed for wall boundary layer flows,

the function f' cannot be a function of η alone, since f' must approach a value of $\phi_b(x)$ as $y \to -\infty$. It may, therefore, be concluded that in general the velocity profiles of the jet mixing region under the influence of a pressure gradient would not exhibit similarity.

There is one specific flow case which has the possibility to exhibit similarity and has been discussed by Napolitano, Libby, and Ferri [19].† The two compressible streams must have the same stagnation pressure but different stagnation temperatures. At any station of the flow, the Mach numbers of the two streams are the same and the value of ϕ_b will be a constant under a non-zero pressure gradient. The stagnation temperature ratio and the velocity ratio cannot be independently selected. This particular flow case does not occur frequently in separated flows where jet mixing usually occurs between streams of unequal stagnation pressures.

Perhaps it may be argued that the meaning of "similarity" should not be restricted to velocity profiles. If one chooses the stagnation pressure as the dependent variable, the boundary conditions imposed on the stagnation pressure would be

$$\frac{p_o(x, y \to \infty)}{p_{o1a}} = 1$$

and

---

†The stagnation flow studied by Greenberg [11] belongs to this category.

$$\frac{p_o(x,y \to -\infty)}{p_{o1a}} = \frac{p_{o1b}}{p_{o1a}} = \text{constant}$$

However, flow problems with different pressure gradients with the same terminal values of stagnation pressure ratios at $y = \pm \infty$ would have different stagnation pressure profiles in between. This fact implies that the stagnation pressure profiles also will not exhibit similarity.

As a result of these discussions and in view of the considerations already made elsewhere [19], no serious attempt has been made to find transformations such that a similar solution in a more general sense may possibly be found for the flow with a non-zero pressure gradient. Instead the usual boundary layer transformations based on the velocity potential and stream function for the inviscid main freestream have been used and the resulting partial differential equations solved. The study undertaken in this chapter is for the general case of compressible, non-isoenergetic jet mixing between two parallel streams of the same composition for laminar or turbulent flows, with special cases being examined in the succeeding chapters.

The basic scheme upon which the present analysis is based is to divide the flow field into two regions of flow along the streamline which separates the two streams. It is recognized that each of these two regions resembles a "boundary layer type" of flow; the velocity changes rapidly from the value at the dividing

streamline and approaches the freestream value asymptotically. Therefore, a boundary layer method is used to solve each of the two problems, and the conditions that the velocity, temperature, and their gradients should be matched are subsequently applied to join the two streams along the dividing streamline.

The Meksyn method [12] is used to obtain the solution for each of the boundary layer flow problems. His method essentially consists of assuming a power series solution of η with the coefficients as functions of ξ (transformed x variable). Treating the non-linear partial differential equation as a non-homogeneous linear differential equation in the second derivative of the function, one may integrate twice, and the resulting integral is evaluated by the method of steepest descent. This calculation will produce a set of ordinary differential equations for the coefficient functions of the assumed series for mixing with a pressure gradient (non-similar flow case) or a set of algebraic equations for cases of similar jet mixing (constant pressure condition is necessary but not sufficient). After these coefficient functions are evaluated, the velocity and temperature profiles can be established through additional straightforward calculations.

2.2 THE EQUIVALENT TWO STREAMS AND THEIR MATCHING

As it has been mentioned in the preceding section, the mixing region is now split into two subregions (Fig. 2a) along the dividing (or separating) streamline; each is identified with a subscript "a"

(above) or "b" (below). If one employs a simple transformation for the b stream by

$$x_b = x, \quad y_b = -y, \quad u_b = u, \quad v_b = -v, \quad T_b = T, \qquad (2.7)$$

one would recognize that the individual flow problems associated with the two streams (Fig. 2b) will be governed by the same differential equations, Eqs. (2.1), (2.2) and (2.4) and the same types of initial and boundary conditions, (thus the subscript a or b is superfluous here) which are given as

$$u(0,y) = u_1(0), \quad T_o(0,y) = T_{o1}, \quad y \geq 0 \qquad (2.8)$$

and

$$u(x,\infty) = u_1(x), \quad T_o(x,\infty) = T_{o1},$$

$$u(x,0) = u_j(x), \quad T_o(x,0) = T_{oj}(x) \qquad (2.9)$$

$$v(x,0) = 0$$

with

$$\frac{dp}{dx} = -\rho_1 u_1 \frac{du_1}{dx}$$

where $u_j(x)$ and $T_{oj}(x)$ are the velocity and total temperature of

the dividing streamline, respectively.

The two individual flow problems are necessarily related to each other due to the fact that the velocity, velocity gradient, temperature, and temperature gradient must be the same for each stream along the dividing streamline. Therefore, the following four matching conditions must also hold

$$
\begin{aligned}
&u_{j\,a}(x) = u_{j\,b}(x) \\
&\left.\frac{\partial u}{\partial y}\right)_a (x,0) = \left.\frac{\partial u}{\partial y}\right)_b (x,0) \\
&T_{j\,a}(x) = T_{j\,b}(x) \\
&\left.\frac{\partial T}{\partial y}\right)_a (x,0) = \left.\frac{\partial T}{\partial y}\right)_b (x,0)
\end{aligned}
\tag{2.10}
$$

2.3 TRANSFORMATIONS FOR LAMINAR OR TURBULENT FLOWS

For the individual flow problems under consideration, the coordinate transformations are introduced according to

$$\xi = \int_0^{x^*} \frac{\varepsilon}{\nu_{o\,la}\,\beta^{2-d}} \left(\frac{\rho_{la}}{\rho_{o\,la}}\right)^2 \frac{u_{la}}{u_{lai}}\, d\left(\frac{x}{L}\right) \tag{2.11}$$

$$\eta = \sqrt{\frac{Re_L}{2\xi}}\, \frac{u_{la}}{u_{lai}} \int_0^{y^*} \frac{\rho}{\rho_{o\,la}}\, d\left(\frac{y}{L}\right) \tag{2.12}$$

with

$$Re_L = \frac{u_{1ai} L}{\nu_{ola}}$$

and

$$\beta = \frac{\rho_{1a}}{\rho} = \frac{T}{T_{1a}}$$

It is stipulated that ε/β^{2-d} is a function of x only, and the index d is introduced for the convenience of adapting any commonly used viscosity law for both laminar or turbulent flows into the analysis. L is an arbitrary reference length.

Introducing

$$\psi = \sqrt{\frac{2\xi}{Re_L}}\, u_{1ai} L\, f(\xi,\eta) \qquad (2.13)$$

and

$$\Lambda(\xi,\eta) = \frac{T_o}{T_{ola}}\,, \qquad (2.14)$$

one may easily establish that

$$u = \frac{\rho_{ola}}{\rho} \frac{\partial \psi}{\partial y} = u_{1a}\, f_\eta \qquad (2.15)$$

and

$$-v = \frac{\rho_{ola}}{\rho}\frac{\partial \psi}{\partial x} = \frac{\rho_{ola}}{\rho}\frac{u_{lia}L}{\sqrt{Re_L}}\left[\left(\frac{f}{\sqrt{2\xi}} + \sqrt{2\xi}\, f_\xi\right)\frac{\partial \xi}{\partial x} + \sqrt{2\xi}\, f_\eta \frac{\partial \eta}{\partial x}\right] \quad (2.16)$$

where the subscripts η and ξ indicate partial differentiation.

The momentum and energy equations, Eqs. (2.2a) and (2.3), are now, respectively, transformed into

$$\frac{\partial}{\partial \eta}\left(\beta^{-d} f_{\eta\eta}\right) + f f_{\eta\eta} = \lambda(\beta - f_\eta^2) + 2\xi(f_\eta f_{\eta\xi} - f_\xi f_{\eta\eta}) \quad (2.17)$$

where

$$\lambda = \frac{-2\xi}{u_{la}}\frac{du_{la}}{d\xi} \quad (2.18)$$

and

$$\frac{\partial}{\partial \eta}\left(\beta^{-d}\Lambda_\eta\right) + Pr\, f\Lambda_\eta + (Pr - 1)\, Cr_{la}^2 \frac{\partial}{\partial \eta}\left[\beta^{-d}\frac{\partial}{\partial \eta}(f_\eta)^2\right]$$

$$= 2Pr\xi\,(f_\eta \Lambda_\xi - f_\xi \Lambda_\eta) \quad (2.19)$$

where Cr_{la}^2 is the square of the Crocco number of the main freestream and

$$\beta = \frac{\Lambda - Cr_{la}^2 f_\eta^2}{1 - Cr_{la}^2} \quad (2.20)$$

holds for an ideal gas.

The initial conditions can now be written as

$$f_\eta(0,\eta) = \frac{u_1(0)}{u_{1ai}} \quad \text{and} \quad \Lambda(0,\eta) = \frac{T_{o1}}{T_{o1a}} . \tag{2.21}$$

The boundary conditions become

$$\begin{aligned} f_\eta(\xi,\infty) &= \frac{u_1(x)}{U_{1a}(x)} & \Lambda(\xi,\infty) &= \frac{T_{o1}}{T_{o1a}} \\ f_\eta(\xi,0) &= \frac{u_j(x)}{u_{1a}(x)} & \Lambda(\xi,0) &= \frac{T_{oj}(x)}{T_{o1a}} \end{aligned} \tag{2.22}$$

$$f(\xi,0) = 0$$

$$f_\xi(\xi,0) = 0$$

Finally the matching conditions are

$$f_{a\eta}(\xi,0) = f_{b\eta}(\xi,0)$$

$$f_{a\eta\eta}(\xi,0) = -f_{b\eta\eta}(\xi,0)$$

$$\Lambda_a(\xi,0) - Cr_{1a}^2[f_{a\eta}(\xi,0)]^2 = \Lambda_b(\xi,0) - Cr_{1a}^2[f_{b\eta}(\xi,0)]^2 \tag{2.23}$$

$$\Lambda_{a\eta}(\xi,0) - 2Cr_{1a}^2 f_{a\eta}(\xi,0) f_{a\eta\eta}(\xi,0)$$

$$= -[\Lambda_{b\eta}(\xi,0) - 2Cr_{1a}^2 f_{b\eta}(\xi,0) f_{b\eta\eta}(\xi,0)]$$

The last two equations in Eq. (2.23) can be simplified into

$$\Lambda_a(\xi,0) = \Lambda_b(\xi,0)$$

and (2.23a)

$$\Lambda_{a\eta}(\xi,0) = -\Lambda_{b\eta}(\xi,0)$$

It is appropriate to point out now that the transformation introduced in Eqs. (2.11) and (2.12) are a generalization of the Illingworth-Stewartson transformation [20] so that all mixing problems, whether laminar or turbulent, can be treated by a single formulation. For turbulent mixing when the original exchange coefficient concept by Gortler is extended to compressible flows so that the average value of the eddy diffusivity across the flow is utilized, *i.e.*, $\varepsilon = \varepsilon(x)$, one needs only to set $d = 2$ in the analysis. On the other hand, stipulation of $\varepsilon/\beta^2(x)$ has been introduced by Ting and Libby [21] and Alber and Lees [22] for turbulent flows to expedite mathematical transformations, and one needs again only set $d = 0$ for these situations. Another eddy diffusivity model suggested by Ferri, Libby, and Zakkay [23] is $\mu_t = \mu_t(x)$ and one may adopt this model into the present analysis by setting $d = 1$.

Indeed, setting $d = 0$ covers all flow cases for laminar jet mixing since the expression

$$\frac{\varepsilon}{\beta^2}(x) = \frac{\rho\mu}{\rho_{1a}^2}(x)$$

is effectively the relationship

$$\frac{\mu}{\mu_{ola}} = b(x) \frac{T}{T_{ola}}$$

introduced by Chapman for laminar compressible flow to decouple the energy and momentum equations. For these flow cases the transformations, Eqs. (2.11) and (2.12) become

$$\xi = \int_0^{x^*} b(x) \frac{p(x)}{p_{oa}} \frac{u_{1a}(x)}{u_{lai}} d\left(\frac{x}{L}\right)$$

and

$$\eta = \sqrt{\frac{Re_L}{2\xi}} \frac{u_{1a}}{u_{lai}} \int_0^{y^*} \frac{\rho}{\rho_{ola}} d\left(\frac{y}{L}\right)$$

which is precisely the Illingworth-Stewartson transformation.

It is worthwhile to remark that the value of d may also be evaluated according to any viscosity-temperature relationship such as Sutherland's formula.

2.4 METHOD OF SOLUTION

For each of the two streams, series solutions are assumed for the stream function f and the dimensionless stagnation temperature Λ. They are given by

$$f(\xi,\eta) = \sum_{n=1}^{\infty} \frac{a_n(\xi)}{n!} \eta^n = a_1(\xi)\eta + \frac{a_2(\xi)}{2!} \eta^2 + \cdots \quad (2.24)$$

and

$$\Lambda(\xi,\eta) = \sum_{n=0}^{\infty} \frac{\theta_n(\xi)}{n!}\eta^n = \theta_o(\xi) + \theta_1(\xi)\,\eta + \cdots \quad (2.25)$$

Two of the boundary conditions, Eq. (2.22), are automatically satisfied as a result of the assumed form of the series.

Upon substituting the series, Eqs. (2.24) and (2.25), into the differential equations, Eqs. (2.17) and (2.19), the coefficients a_3, a_4, $\cdots$ and θ_2, θ_3 $\cdots$ can be found as functions of a_1, a_2, θ_o, θ_1, and their derivatives. It is found that

$$a_3 = \frac{1}{\theta_o - Cr_{1a}^2 a_1^2}\left[d\,a_2(\theta_1 - 2Cr_{1a}^2 a_1 a_2) + \frac{1}{(1 - Cr_{1a}^2)^d}\right.$$

$$\left.\cdot\left(\lambda\frac{\theta_o - Cr_{1a}^2 a_1^2}{1 - Cr_{1a}^2} - \lambda a_1^2 + 2\xi a_1 a_1'\right)(\theta_o - Cr_{1a}^2 a_1^2)^{d+1}\right]$$

$$a_4 = \frac{1}{\theta_o - Cr_{1a}^2 a_1^2}\left\{d[\theta_2 a_2 - 2Cr_{1a}^2(a_1 a_3 + a_2^2)\,a_2\right.$$

$$+ \theta_1 a_3 - 2Cr_{1a}^2 a_1 a_2 a_3] - (\theta_1 - 2Cr_{1a}^2 a_1 a_2)\,a_3$$

$$+ \frac{1}{(1 - Cr_{1a}^2)^d}\left\{\left(\lambda\frac{\theta_o - Cr_{1a}^2 a_1^2}{1 - Cr_{1a}^2} - \lambda a_1^2 + 2\xi a_1 a_1'\right)\right.$$

$$\cdot\left[\sum_{n=1}^{\infty}\frac{(d+1)\,d\cdots(d+2-n)}{(n-1)!}(\theta_o - Cr_{1a}^2 a_1^2 - 1)^{n-1}\right.$$

$$\left.\left.\cdot(\theta_1 - 2Cr_{1a}^2 a_1 a_2)\right] + \left(-a_1 a_2 + \lambda\frac{\theta_1 - 2Cr_{1a}^2 a_1 a_2}{1 - Cr_{1a}^2}\right.\right.$$

$$\left.\left.\left. - 2\lambda a_1 a_2 + 2\xi a_1 a_2'\right)(\theta_o - Cr_{1a}^2 a_1^2)^{d+1}\right\}\right\}$$

$$\theta_2 = \frac{1}{\theta_o - Cr_{1a}^2 a_1^2}\Big[d(\theta_1 - 2Cr_{1a}^2 a_1 a_2)\,\theta_1 - 2(Pr-1)$$
$$\cdot Cr_{1a}^2(\theta_o - Cr_{1a}^2 a_1^2)(a_1 a_3 + a_2^2)$$
$$+ 2d(Pr-1)\,Cr_{1a}^2(\theta_1 - 2Cr_{1a}^2 a_1 a_2)\,a_1 a_2$$
$$+ \frac{2Pr\,\xi}{(1 - Cr_{1a}^2)^d}(\theta_o - Cr_{1a}^2 a_1^2)^{d+1}\,a_1\theta_o'\Big]$$

$$\theta_3 = \frac{1}{\theta_o - Cr_{1a}^2 a_1^2}\Big\{d[\theta_2 - 2Cr_{1a}^2(a_1 a_3 + a_2^2)]\,\theta_1$$
$$+ d[\theta_1 - 2Cr_{1a}^2 a_1 a_2]\,\theta_2$$
$$- 2(Pr-1)\,Cr_{1a}^2[(\theta_1 - 2Cr_{1a}^2 a_1 a_2)(a_1 a_3 + a_2^2)$$
$$+ (\theta_o - Cr_{1a}^2 a_1^2)(a_1 a_4 + 3a_2 a_3)]$$
$$+ 2d(Pr-1)\,Cr_{1a}^2\Big\{[\theta_2 - 2Cr_{1a}^2(a_1 a_3 + a_2^2)]\,a_1 a_2$$
$$+ [\theta_1 - 2Cr_{1a}^2 a_1 a_2](a_1 a_3 + a_2^2)\Big\} - (\theta_1 - 2Cr_{1a}^2 a_1 a_2)\,\theta_2$$
$$+ \frac{1}{(1 - Cr_{1a}^2)^d}\Big\{[-Pr\,a_1\theta_1 + 2Pr\,\xi(a_1\theta_1' + a_2\theta_o')$$
$$- 2Pr\,\xi a_1'\theta_1]\,(\theta_o - Cr_{1a}^2 a_1^2)^{d+1} + 2Pr\,\xi a_1\theta_o'$$
$$\cdot\Big[\sum_{n=1}^{\infty}\frac{(d+1)\,d\cdots(d+2-n)}{(n-1)!}$$
$$\cdot\,(\theta_o - Cr_{1a}^2 a_1^2 - 1)^{n-1}\,(\theta_1 - 2Cr_{1a}^2 a_1 a_2)\Big]\Big\}\Big\}$$

The momentum equation is first integrated with an integrating factor $e^{F(\xi,\eta)}$, where

$$F(\xi,\eta) = \int_0^{\eta} \beta^d f\,d\eta \qquad (2.26)$$

and the resulting expression may be written as

$$f_{\eta\eta} = e^{-F}\phi(\xi,\eta) \tag{2.27}$$

where

$$\phi(\xi,\eta) = \beta^{d}\Big\{a_2[\beta(\xi,0)]^{-d} + \int_0^{\eta} e^{F}[\lambda(\beta - f_{\eta}^{2}) + 2\xi\,(f_{\eta}f_{\eta\xi} - f_{\xi}f_{\eta\eta})]\,d\eta\Big\} \tag{2.28}$$

A second integration yields

$$\frac{u_1}{u_{1a}} - a_1 = \int_0^{\infty} e^{-F}\,\phi(\xi,\eta)\,d\eta \tag{2.29}$$

Following a similar manipulation for the energy equation, one obtains

$$\Lambda_{\eta} = e^{-Pr\,F}\,\Omega(\xi,\eta) \tag{2.30}$$

where

$$\Omega(\xi,\eta) = \beta^{d}\Big\{\theta_1[\beta(\xi,0)]^{-d} + \int e^{Pr\,F}\Big[2Pr\,\xi(f_{\eta}\Lambda_{\xi} - f_{\xi}\Lambda_{\eta}) + (Pr - 1)\,Cr_{1a}^{2}\,\frac{\partial}{\partial\eta}\,(2\beta^{-d}\,f_{\eta}f_{\eta\eta})\Big]d\eta\Big\} \tag{2.31}$$

$$\frac{T_{o1}}{T_{o1a}} - \theta_o = \int_0^{\infty} e^{-Pr\,F}\,\Omega(\xi,\eta)\,d\eta \tag{2.32}$$

The integrals given in Eqs. (2.29) and (2.32) are evaluated by the method of steepest descent. Meksyn pointed out that, due to the special character of the boundary layer problems, the velocity and temperature gradients are rapidly decaying functions away from the ξ-axis. The main contribution of the integrals comes from the region near $\eta = 0$, the stationary point of F. Only a few terms in the series are needed and the low radius of convergence of the series is thus unimportant.

To evaluate the integrals in Eqs. (2.29) and (2.32), the series for F is first inverted by defining

$$F = \tau = \eta^2 \sum_{n=0}^{\infty} C_n \eta^n \tag{2.33}$$

where the coefficients C_n may be found by carrying out the integration in Eq. (2.26), and

$$I = \sum_{m=0}^{\infty} \frac{A_m}{m+1} \tau^{(m+1)/2} \tag{2.34}$$

The coefficients A_m have been found to be given by

$$\begin{aligned} A_o &= C_o^{-1/2} \\ A_1 &= -\frac{C_1}{C_o^2} \\ A_2 &= -\frac{3}{2}\frac{C_2}{C_o^{5/2}} + \frac{15}{8}\frac{C_1^2}{C_o^{7/2}} \end{aligned} \tag{2.35}$$

The integrands of Eqs. (2.29) and (2.32) must be expressed also as functions of τ. For this purpose, it is convenient to define (see [12] for details)

$$\phi \frac{d\eta}{d\tau} = \tau^{-1/2} \sum_{m=0}^{\infty} d_m \tau^{m/2}$$
$$\Omega \frac{d\eta}{d\tau} = \tau^{-1/2} \sum_{m=0}^{\infty} e_m \tau^{m/2} \tag{2.36}$$

The coefficients d_m and e_m have been found to be given by

$$d_o = \frac{b_o A_o}{2} \qquad e_o = \frac{h_o A_o}{2}$$
$$d_1 = \frac{b_o A_1}{2} + \frac{b_1 A_o^2}{2} \qquad e_1 = \frac{h_o A_1}{2} + \frac{h_1 A_o^2}{2} \tag{2.37}$$

where the coefficients b_n and h_n are the coefficients of the expansion of ϕ and Ω in η, namely,

$$b_n = \frac{\partial^n \phi}{\partial \eta^n} (\xi, \eta = 0) \tag{2.38}$$

$$h_n = \frac{\partial^n \Omega}{\partial \eta^n} (\xi, \eta = 0) \tag{2.39}$$

and can be evaluated from Eqs. (2.27) and (2.30).

Equation (2.29) may now be written as

$$\frac{u_1}{u_{1a}} - a_1 = \int_0^\infty e^{-\tau}\, \tau^{-1/2} \left(\sum_{m=0}^{\infty} d_m \tau^{m/2} \right) d\tau \tag{2.40}$$

which becomes, upon integrating,

$$\frac{u_1}{u_{1a}} - a_1 = \sum_{m=0}^{\infty} \Gamma\left(\frac{m+1}{2}\right) d_m(\xi) \tag{2.41}$$

Likewise for the energy relationship, Eq. (2.32) becomes

$$\frac{T_{o1}}{T_{o1a}} - \theta_o = \int_0^\infty e^{-Pr\tau}\, \tau^{-1/2} \left(\sum_{m=0}^{\infty} e_m \tau^{m/2} \right) d\tau \tag{2.42}$$

which yields

$$\frac{T_{o1}}{T_{o1a}} - \theta_o = \sum_{m=0} \Gamma\left(\frac{m+1}{2}\right) Pr^{-(m+1)/2}\, e_m(\xi) \tag{2.43}$$

where $\Gamma[(m+1)/2]$ is the Gamma function.

The above equations hold for either of the two streams. Therefore, Eqs. (2.41) and (2.43) yield four relations, two for each stream. These equations contain basically eight unknown functions: a_{1a}, a_{2a}, a_{1b}, a_{2b}, θ_{oa}, θ_{1a}, θ_{ob}, and θ_{1b}. The remaining four equations needed to obtain a solution are the following four matching conditions:

$$a_{1a}(\xi) = a_{1b}(\xi)$$
$$a_{2a}(\xi) = -a_{2b}(\xi) \qquad (2.44)$$
$$\theta_{oa}(\xi) = \theta_{ob}(\xi)$$

and

$$\theta_{1a}(\xi) = -\theta_{1b}(\xi)$$

Once the eight coefficient functions are evaluated (often through numerical integrations), the velocity and total temperature profiles within the mixing region can be found from

$$\frac{u}{u_{1a}} = a_1 + \sum_{m=0}^{\infty} \Gamma\left(\frac{m+1}{2}, \tau\right) d_m(\xi) \qquad (2.45)$$

and

$$\frac{T_o}{T_{o1a}} = \theta_o + \sum_{m=0}^{\infty} \Gamma\left(\frac{m+1}{2}; \tau\right) Pr^{-(m+1)/2} e_m(\xi) \qquad (2.46)$$

where $\Gamma[(m+1)/2,\tau]$ is the incomplete Gamma function and the η,τ relationship given by Eq. (2.34) is needed if the results are to be interpreted in the ξ,η plane. The additional transformation relationship between η and y given by

$$\frac{Y}{L}\sqrt{Re_L} = \sqrt{2\xi}\,\frac{u_{1a_i}}{u_{1a}}\,\frac{\rho_{oi\,a}}{\rho_{1a}}\int_0^{\eta} \beta\, d\eta \qquad (2.47)$$

is also needed in order to obtain the profiles in the physical plane.

It should be stressed that, in locating the profiles within the physical plane, certain boundary (or constraint) conditions assumed by the inviscid streams have to be known [e.g., $v_a(\xi,\eta = \infty) = 0$ or $v_b(\xi,\eta = -\infty) = 0$]. The system of coordinates within which the solution of the present problem is described is intrinsic and it can only be localized after the trajectory of the dividing streamline is known in the physical plane.

3. SIMILAR, NON-ISOENERGETIC, CONSTANT PRESSURE JET MIXING

The general analysis presented in Chapter 2 can easily be reduced to cases of similar, non-isoenergetic, constant pressure jet mixing for either laminar or turbulent flows. The conditions that the pressure be constant (zero pressure gradient) and the uniform flow entrance condition compatible with the boundary conditions would assure the similarity (see [24]) of the velocity profiles. The stream function f thus depends on η only; the unknown coefficient functions become numerical constants which are related now by algebraic equations reduced from Eqs. (2.41) and (2.44).

3.1 BASIC EQUATIONS FOR CONSTANT PRESSURE JET MIXING

Equation (2.17) is now reduced into

$$\frac{d}{d\eta}\left(\frac{f'''}{\beta^d}\right) + ff'' = 0 \tag{3.1}$$

and the energy equation, Eq. (2.19), becomes, for unity Prandtl number,

$$\frac{d}{d\eta}\left(\frac{\Lambda'}{\beta^d}\right) + f\Lambda' = 0 \tag{3.2}$$

An obvious solution which satisfies the energy equation is

$$\Lambda = Af' + B$$

which is, of course, the Crocco integral relationship. After one

evaluates the constants A and B in the above expression according to the boundary conditions, it becomes

$$\Lambda = 1 + \frac{\Lambda_b - 1}{1 - \phi_b}(1 - f') \tag{3.3}$$

Since

$$\beta = \frac{\Lambda - Cr_{1a}^2 f'^2}{1 - Cr_{1a}^2}$$

Eq. (3.1) becomes

$$f''' + \left[\frac{1 + \frac{\Lambda_b - 1}{1 - \phi_b}(1 - f') - Cr_{1a}^2 f'^2}{1 - Cr_{1a}^2}\right]^d ff'' - \frac{df''^2\left(\frac{1 - \Lambda_b}{1 - \phi_b} - 2Cr_{1a}^2 f'\right)}{1 + \frac{\Lambda_b - 1}{1 - \phi_b}(1 - f') - Cr_{1a}^2 f'^2} = 0 \tag{3.4}$$

The coefficients a_3, a_4, $\cdots$, C_o, C_1, $\cdots$, are now given by

$$a_3 = -\frac{da_2^2(Q + 2Cr_{1a}^2 a_1)}{1 + Q(1 - a_1) - Cr_{1a}^2 a_1^2}$$

$$a_4 = \frac{(1-Cr_{1a}^2)^d[(1-2d)(Q+2Cr_{1a}^2 a_1)a_2 a_3 - 2dCr_{1a}^2 a_2^3] - (1+\gamma_1)^{d+1} a_1 a_2}{(1 - Cr_{1a}^2)^d [1 + Q(1 - a_1) - Cr_{1a}^2 a_1^2]} \tag{3.5}$$

$$C_o = \frac{(1 + \gamma_1)^d \; a_1}{2(1 - Cr_{1a}^2)^d}$$

$$C_1 = \frac{(1 + \gamma_1)^d \; \frac{a_2}{2!} + \left[\sum_{n=1}^{\infty} \frac{d(d-1)\cdots(d+1-n)}{n!} \; n \; \gamma_1^{n-1} \; \gamma_2\right] a_1}{3(1 - Cr_{1a}^2 \; a_1^2)^d} \qquad (3.6)\dagger$$

where

$$Q = \frac{\Lambda_b - 1}{1 - \phi_b}$$

$$\gamma_1 = Q(1 - a_1) - Cr_{1a}^2 \; a_1^2$$

$$\gamma_2 = -Qa_2 - 2Cr_{1a}^2 \; a_1 a_2$$

Finally, the coefficients b_n and d_n are

$$b_o = a_2$$

$$b_1 = a_3$$

$$b_2 = a_4 + \left[\frac{Q(1 - a_1) + 1 - Cr_{1a}^2 \; a_1^2}{1 - Cr_{1a}^2}\right]^d a_1 a_2 \qquad (3.7)$$

$$\cdots$$

†For integer values of d, the infinite series in these equations have a finite number of terms.

and

$$
\begin{aligned}
d_o &= \frac{b_o}{2\sqrt{C_o}} \\
d_1 &= -\frac{b_o C_1}{C_o^2} + \frac{b_1}{2C_o} \\
d_2 &= \frac{15}{16}\frac{b_o C_1^2}{C_o^{7/2}} - \frac{3}{4}\frac{b_o C_2}{C_o^{5/2}} - \frac{3}{4}\frac{b_1 C_1}{C_o^{5/2}} + \frac{b_2}{4C_o^{3/2}}
\end{aligned}
\tag{3.8}
$$

For the two streams under consideration (identified with subscripts a and b), Eq. (2.41) gives

$$
\begin{aligned}
1 - a_{1a} &= \Gamma\left(\frac{1}{2}\right) d_{oa} + \Gamma(1)\, d_{1a} + \Gamma\left(\frac{3}{2}\right) d_{2a} + \cdots \\
\phi_b - a_{1b} &= \Gamma\left(\frac{1}{2}\right) d_{ob} + \Gamma(1)\, d_{1b} + \Gamma\left(\frac{3}{2}\right) d_{2b} + \cdots
\end{aligned}
\tag{3.9}
$$

The matching conditions given by Eq. (2.44) reduce into

$$a_{1b} = a_{1a}$$

and

$$a_{2b} = -a_{2a}$$

The four unknowns a_{1a}, a_{2a}, a_{1b}, and a_{2b} can be found from the above four algebraic equations.

It should be mentioned that, for turbulent jet mixing under the condition of constant pressure, the eddy diffusivity formulation usually assumes the form of

$$\frac{\varepsilon}{\beta^{2-d}}(x) = \frac{1}{4\sigma^2} \times u_{1a}$$

where σ is the spread rate parameter. The value of σ for incompressible flow has been established to be around 12. It is also known that σ increases with the freestream Mach number, indicating a smaller spread rate, although the precise variation of σ is still subject to speculation. This information is needed, however, in order to interpret the results of the calculations and its comparison with experimental data in the physical plane as dictated by Eq. (2.47).

3.2 RESULTS

The infinite series of the right side of Eq. (3.9) is the asymptotic representation of the integrated functions and the resulting values of a_1 and a_2 depend upon the number of terms employed in the calculations, although the series showed rapid convergence for nearly all cases investigated.

These equations were programmed on a digital computer and values of a_1 and a_2 were found by using Newton's iteration method of solving a system of nonlinear equations. With given values of ϕ_b, Λ_b, Cr_{1a}^2, and the index d, values of a_1 and a_2 were calculated for successively larger numbers of terms from the infinite series.* In Figs. 3 and 4, a comparison of the results for a_1, which represents the velocity of the dividing streamline, and a_2, the velocity gradient at the dividing streamline, is shown for different numbers of terms from the infinite series with $\phi_b = 0.0$ and 0.8 and $\Lambda_b = 1.0$. They

*It is not necessary to take the same number of terms from the two infinite series in Eq. (3.9); however, it is expedient for numerical calculation purposes that same number of terms are always used from the two series.

indicate that the convergence is poorer for larger values of Crocco number and viscosity index d. However, for the larger values of velocity ratio ϕ_b, the convergence improves markedly. Such an example is also shown in the same figure for $\phi_b = 0.8$ where only the one- and two-term results are presented for cases of d = 0 and 2. The four-term results agreed very well (usually up to the third digit after the decimal point) with those obtained from numerical integration of the ordinary differential equation, Eq. (3.1), given in [16]. Figure 5 shows the results of a_1 for various values of Λ_b indicating the convergence of the series and its relative insensitivity with respect to the stagnation temperature ratio.

Results of these calculations for many other cases have been obtained and are not reported here. In general, taking three terms from the series would give good results. The series showed convergence except for larger values of ϕ_b and Cr_{1a}^2 where the fourth term assumes a larger value than the third term, although they all remain small.

The velocity profiles have been calculated and plotted against the similarity variable η. Figure 6 shows such a calculation for various viscosity index values. It is interesting to observe that all profiles shown in that figure seem to pass through a common point; its physical significance is, however, not obvious. Figure 7 also shows velocity profiles for various values of ϕ_b (d = 1.0, Λ_b = 1.0, Cr_{1a}^2 = 0.5). In Fig. 8, the effect of the main freestream Crocco number is illustrated for a velocity ratio of 0.5 (Λ_b = 1.0, d = 1.0). The width of the mixing region in the η plane is seen to decrease as the mainstream Crocco number increases.

4. TWO STREAM LAMINAR JET MIXING WITH A PRESSURE GRADIENT

In many of the practical situations, turbulent jet mixing occurs within a non-constant pressure flow field and a study of the turbulent flow case would be more suitable for application purposes. However, one should remember that, due to a lack of basic knowledge in turbulent flows, the prediction of eddy diffusivity under the influence of a pressure gradient can only be based on speculations and it would be difficult to interpret the result in the physical plane.

The main purpose of studying laminar flow cases in this chapter is to investigate the mathematical method for such flow conditions. The knowledge gained in this study can no doubt be equally applicable to turbulent flow cases.

It has been shown in Chapter 2 that, if one sets d = 0, one obtains

$$\frac{\varepsilon}{\beta^2} = \frac{\varepsilon}{\beta^2}(x)$$

which is equivalent to the statement that $\rho\mu$ is a function of x only. This is the assumption usually introduced to solve laminar flow problems. We now set d = 0 and the momentum and the energy equations become

$$f_{\eta\eta\eta} + ff_{\eta\eta} = \lambda(\beta - f_\eta^2) + 2\xi(f_\eta f_{\xi\eta} - f_\xi f_{\eta\eta}) \tag{4.1}$$

and

$$\Lambda_{\eta\eta} + Pr\, f\, \Lambda_\eta + (Pr - 1)\, Cr_{la}^2 (f_\eta)_{\eta\eta}^2 = 2Pr\, \xi(f_\eta \Lambda_\xi - f_\xi \Lambda_\eta) \tag{4.2}$$

where

$$\xi = \int_0^{x^*} b(x) \frac{p(x)}{p_{o1a}} \frac{u_{1a}(x)}{u_{1a_i}} d\ \frac{x}{L} \tag{4.3}$$

$$\lambda = -\frac{2\xi}{u_{1a}} \frac{du_{1a}}{d\xi} \tag{4.4}$$

and

$$\beta = \frac{\Lambda - Cr_{1a}^2\ f_\eta^2}{1 - Cr_{1a}^2} \tag{4.5}$$

As already presented in Chapter 2, one would obtain Eqs. (2.41) and (2.43) which are to be written with subscripts a and b and solved with the matching conditions given in Eqs. (2.44).

For this case, the coefficient functions for the series in Eqs. (2.24) and (2.25) become

$$\begin{aligned} a_3 &= \lambda \left(\frac{\theta_o - Cr_{1a}^2\ a_1^2}{1 - Cr_{1a}^2} - a_1^2 \right) + 2\xi\ a_1 a_1' \\ a_4 &= -a_1 a_2 + \lambda \left(\frac{\theta_1 - 2Cr_{1a}^2\ a_1 a_2}{1 - Cr_{1a}^2} - 2a_1 a_2 \right) + 2\xi\ a_1 a_2' \\ &\cdots \end{aligned} \tag{4.6}$$

and

$$\begin{aligned} \theta_2 &= -2Cr_{1a}^2 (Pr - 1)\ (a_1 a_3 + a_2^2) + 2Pr\ \xi a_1 \theta_o' \\ \theta_3 &= -Pr\ a_1 \theta_1 - 2Cr_{1a}^2 (Pr - 1)\ (a_1 a_4 + 3a_2 a_3) \\ &\quad + 2Pr\ \xi (a_1 \theta_1' + a_2 \theta_o' - a_1' \theta_1) \\ &\cdots \end{aligned} \tag{4.7}$$

where the primes indicate differentiation with respect to ξ. The coefficients C_n in Eq. (2.33) can be written as

$$C_n = \frac{a_{n+1}}{(n+2)!}, \quad n = 0, 1, 2, \cdots \tag{4.8}$$

Finally, the coefficients for Eqs. (2.38) and (2.39) are found to be given by

$$\begin{aligned} b_o &= a_2 & h_o &= \theta_1 \\ b_1 &= a_3 & h_1 &= \theta_2 \\ b_2 &= a_1 a_2 + a_4 & h_2 &= \mathrm{Pr}\, a_1 \theta_1 + \theta_z \\ &\cdots & &\cdots \end{aligned} \tag{4.9}$$

and Eqs. (2.41) and (2.43) can be written for each of the two streams as

$$\frac{u_1}{u_{1a}} - a_1 = \Gamma\left(\frac{1}{2}\right) d_o + \Gamma(1)\, d_1 + \Gamma\left(\frac{3}{2}\right) d_2 + \cdots \tag{4.10}$$

$$\frac{T_o}{T_{ola}} - \theta_o = \Gamma\left(\frac{1}{2}\right) \mathrm{Pr}^{-1/2}\, e_o + \Gamma(1)\, \mathrm{Pr}^{-1}\, e_1 + \Gamma\left(\frac{3}{2}\right) \mathrm{Pr}^{-3/2}\, e_2 + \cdots \tag{4.11}$$

with

$$\begin{aligned} d_o &= \frac{a_2}{2}\sqrt{\frac{2}{a_1}} \\ d_1 &= -\frac{1}{3}\left(\frac{a_2}{a_1}\right)^2 + \frac{a_3}{a_1} \\ d_2 &= \frac{5a_2^3}{192}\left(\frac{2}{a_1}\right)^{7/2} - \frac{5a_2 a_3}{8}\left(\frac{2}{a_1}\right)^{5/2} + \frac{(a_1 a_2 + a_4)}{4}\left(\frac{2}{a_1}\right)^{3/2} \end{aligned} \tag{4.12}$$

and

$$
\begin{aligned}
e_o &= \frac{\theta_1}{2}\sqrt{\frac{2}{a_1}} \\
e_1 &= -\frac{\theta_1 a_2}{3a_1^2} + \frac{\theta_2}{a_1} \\
e_2 &= \frac{5}{192}\theta_1 a_2^3\left(\frac{2}{a_1}\right)^{7/2} - \frac{\theta_1 a_3}{32}\left(\frac{2}{a_1}\right)^{5/2} - \frac{\theta_2 a_2}{8}\left(\frac{2}{a_1}\right)^{5/2} \\
&\quad + \frac{(\mathrm{Pr}\, a_1\theta_1 + \theta_3)}{4}\left(\frac{2}{a_1}\right)^{3/2}
\end{aligned}
\tag{4.13}
$$

with matching conditions

$$
\begin{aligned}
a_{1a} &= a_{1b} \\
a_{2a} &= -a_{2b} \\
\theta_{oa} &= \theta_{ob} \\
\theta_{1a} &= -\theta_{1b}.
\end{aligned}
\tag{4.14}
$$

4.1 METHOD OF CALCULATION

With the given initial condition (two uniform flows) and the prescribed pressure gradient (represented by the function λ), a_{1a}, a_{1b}, a_{2a}, a_{2b}, θ_{oa}, θ_{ob}, θ_{1a}, and θ_{1b} are to be found from Eqs. (4.10) and (4.11) and the matching conditions (4.14).

Perhaps it is proper to mention that the arbitrarily prescribed pressure gradient may be either generated due to the variation of the external inviscid streams (inviscid interactions) or may be induced

due to the mixing action itself (viscid interaction). In general, the inviscid flows are usually subjected to the constraint that a natural boundary condition is imposed, (e.g., $v_a(\xi,\infty) = 0$) on the jet mixing region so that the location of the profiles in the physical plane can be determined [16]. It is also worthwhile to mention that the static pressure across such a mixing region is by no means constant although the difference is indeed small. Nevertheless, within the framework of the boundary layer concept, one considers for the present flow problem that the pressure field is prescribed and is constant across the mixing region.

Additional manipulations on the ξ and λ variables are introduced by defining

$$u^*_{1a} = \frac{u_{1a}}{u_{1ai}}$$

$$p^* = \frac{p}{\rho_{01a} u_{1ai}^2}$$

$$X^* = \frac{X}{L}$$

Bernoulli's equation is now given by

$$\frac{dp^*}{dX^*} = \left(1 - Cr_{1ai}^2 u_{1a}^{*2}\right)^{1/\gamma-1} u^*_{1a} \frac{du^*_{1a}}{dX^*} \tag{4.15}$$

It may be shown that ξ and λ can be expressed as

$$\xi = \int_{1}^{u^*_{1a}} \left(1 - Cr^2_{1ai}\, u^{*2}_{1a}\right)^{(\gamma+1)/(\gamma-1)} u^{*2} \frac{b(X^*)}{\left(-\frac{dp^*}{dX^*}\right)}\, du^*_{1a} \qquad (4.16)$$

and

$$\lambda = -\frac{2}{b(X^*)} \frac{-\frac{dp^*}{dX^*}}{u^{*3}_{1a}\left(1 - Cr^2_{1ai}\, u^{*2}_{1a}\right)^{(\gamma+1)/(\gamma-1)}} \qquad (4.17)$$

Thus, for given initial velocity ratio between the two streams ϕ_{bi} $(=u_{1bi}/u_{1ai})$, stagnation temperature ratio $\Lambda_b (=T_{01b}/T_{01a})$, Prandtl number, initial Crocco number of the main stream, viscosity coefficient function b(x) and the pressure gradient (-dp/dx), the problem may be solved by integrating the system of Eqs. (4.10) and (4.11) incorporating the matching conditions (Eq. (4.14)).

It is important to note that if only the first term from the series in Eqs. (4.10) and (4.11) is employed, the system of equations becomes algebraic and is independent of ξ and λ leading to the same one term "similar" solution for constant pressure jet mixing already discussed in Chapter 3. With the first two terms from the series included into the considerations, first derivatives of a_1 and θ_0 appear. The derivatives of a_2 and θ_1 will also appear if one additional term is added, and the second derivatives of a_1 and θ_0 will appear when the fourth term is included. It is usually expected that the second derivatives are relatively small, at least in part of the domain [25] and thus one may neglect its contribution;

justification can only be supported by checking the results obtained.

Considering that the three-term representation of the infinite series would give fairly accurate results, one now needs to know the initial values of the first derivatives of a_1, a_2, θ_o, and θ_1 at the origin ($\xi = 0$) in order to carry out effectively the integration. Inspection of Eqs. (4.10) and (4.11) shows that these derivatives are always multiplied by ξ, indicating the singular behavior of the system at the origin. However, these derivatives may be found from the following consideration: when one sets $\xi = 0$, the resulting algebraic equations will again yield the results for $a_1(0)$, $a_2(0)$, $\theta_o(0)$, and $\theta_1(0)$ which correspond to the similar mixing solution (zero pressure gradient solution). Although there are discontinuities in the velocity and temperature profiles at the origin, one should take these values as the correct initial conditions for a_1, a_2, θ_o, and θ_1, and the derivatives of these functions at the origin may then be found from limiting considerations by L'Hospital's rule. These procedures can also be adopted to find $a_{1a}''(0)$ and $\theta_o''(0)$ when four terms are employed from the series. One should be aware, however, that in such situations the pressure field should have continuous second derivatives at the origin.

Equations (4.10) and (4.11) can now be integrated numerically to establish the coefficient functions $a_1(\xi)$, $a_2(\xi)$, $\theta_o(\xi)$, and $\theta_1(\xi)$. These equations were programmed on a digital computer and

solved by using a predictor-corrector integration technique with the Runga-Kutta method for starting the solution.

One difficulty in carrying out the numerical integration was that it was usually not possible to solve for the desired derivatives explicitly from the differential equations. It was necessary to use a Newton-Raphson iterative technique for this purpose.

The velocity and temperature profiles were calculated also by using a digital computer. From the coefficient functions $a_1(\xi)$, $a_2(\xi)$, $\theta_o(\xi)$, and $\theta_1(\xi)$, all the coefficients needed in Eqs. (2.45), (2.46), (2.47), and (2.34) to establish the desired profiles in both the transformed and physical planes can be determined.

4.2 RESULTS

Calculations were carried out using a constant pressure gradient. It was thought that for any arbitrary pressure distribution one may always approximate this function by segmented straight lines within each small increment in ξ. Thus restricting the flow to the case of a constant pressure gradient would simplify the analysis, yet it does retain the essential features of the system of equations. Denoting

$$-\frac{dp}{dX} = K \tag{4.18}$$

where k is a constant, one may write in dimensionless form

$$\frac{dp^*}{dX^*} = m \tag{4.19}$$

$$m = \frac{KL}{\rho_{01a} u_{1ia}^2} \tag{4.20}$$

The reference length L may be so chosen that $|m| = 1$. Thus, $m = +1$ indicates a favorable pressure gradient while $m = -1$ is for an adverse pressure gradient. Unity Prandtl number was used throughout all calculations. Also, b(x) was chosen as unity.

Figure 9 presents the coefficient functions a_{1a}, a_{2a}, and a_{3a} for the specific flow case of $\phi_{bi} = 0.5$ and $\Lambda_b = 1.0$. The results are shown for cases where one, two and three terms were used from the series in Eq. (4.10) and Eq. (4.11) for initial Mach numbers of 0.0 and 1.0. It is interesting to note that for both cases the values of a_{1a} for the two and three term results are nearly the same. However, for the coefficient a_{2a} the three term results appear to deviate away from the two term results. It should also be mentioned that for the case of a constant adverse pressure gradient, the secondary stream will decelerate to zero velocity near $x^* = 0.0727$ for an intial main stream Mach number of 1.0 and near $x^* .0.125$ for incompressible flow. Similarly, for a favorable pressure gradient, the main stream will accelerate to an infinite

Mach number (unity Crocco number) near $x^* = 0.4528$ for an initial Mach number of 1.0. No such limit exists for incompressible flow.

For boundary layer flow problems, the curvature of the velocity profile has a particular meaning since it may be easily seen from the equation of motion that the change of mechanical energy of the fluid is closely related with its curvature; a postive curvature indicates an increase while negative curvature implies a decrease in mechanical energy. Since the coefficient a_3 is directly proportional to the curvature of the velocity profile at the dividing streamline, the values of a_3 are also presented in Fig. 9.

The velocity profiles of these flow cases are presented in Fig. 10. Since the profiles are not greatly different for the one, two and three term results, only representative profiles (three term results) are shown for various locations in the flow field. It should be noted that the velocity profiles may differ little between the one, two and three term results; however, the thickness of the mixing region may be quite different.

It should also be noted that a smooth velocity profile is presented in this figure as the initial condition. One should, however, be aware of the fact that the mixing layer has no thickness at this initial section, thus the profile actually shows a discontinuity in the physical plane.

Results of these calculations seem to indicate that the infinite series in Eqs. (4.10) and (4.11) converges quickly and calculations with three terms from these series would be adequate.

Other results presented here were produced from this same scheme of calculations.

The curves in Fig. 11 are the results for isoenergetic mixing with a favorable pressure gradient. They are given for three initial velocity ratios of 0.1, 0.5, and 0.9 for incompressible flow. Also shown are curves for initial Mach numbers of 0.0, 0.5, 1.0, and 1.5 with an initial velocity ratio of 0.5.

The effect of non-isoenergetic mixing, i.e., $\Lambda_b \neq 1$, is shown in Figs. 12, 13, 14, and 15. It should be pointed out that for large values of Λ_b ($\Lambda_b >> 1$), when two inviscid streams expand through the same pressure ratio, the initially slower stream ($\phi_{bi} < 1$) may assume a larger velocity than the initially faster stream. Thus, the value of ϕ_b may be greater than one. One should not be surprised to find that a_{1a} may be greater than one (naturally a_{2a} will be negative) when Λ_b is much greater than one. Values of ϕ_b for those cases are presented in Fig. 12.

The coefficient a_1, a_2, θ_o, and θ_1 are presented in Fig. 13. The results are plotted up to the point where the Crocco number Cr_{1a} is close to unity ($x^* = 0.4528$). The velocity and temperature profiles are plotted as a function of η in Figs. 14 and 15, respectively, for an initial Mach number of 1.0 and an initial velocity ratio of 0.5 for mixing with a favorable pressure gradient.

It has been mentioned in the INTRODUCTION that the motivation of making such a detailed mathematical study is to set up a standard, or to obtain a solution in a more nearly exact fashion if possible,

for such flow problems so that the merit of any other approximate method may be assessed and evaluated. One such simple and convenient approximation which is based more on physical grounds is the "locally similar" solution. A locally similar profile is defined for a certain location x^* as the profile resulting from a constant pressure jet mixing starting from the origin--the pressure being the local value. It is expected that this approximation should give reasonable results from the considerations that

(1) This profile satisfies the correct boundary conditions at $\eta = \pm \infty$ and

(2) Any difference in the upstream flow conditions tends to disappear as the governing system of equations is parabolic in nature.

Indeed, the present investigation does support this conjecture when locally similar solutions (produced by the method discussed in Chapter 3) are compared with the results from the present detailed mathematical calculations.

Figure 16 shows a plot of a_1, the velocity ratio for the dividing streamline, and a_2, the velocity gradient at the dividing streamline, as a function of x^* and ϕ_b. The curves are given for both favorable (m = +1) and adverse (m = -1) pressure gradients for an incompressible flow. Recalling that the initial velocity profile is similar, the deviation between the locally similar and non-similar values of a_1 and a_2 is initially zero. The results of flow cases with different initial freestream Mach number are shown in Fig. 17. The curves are for isoenergetic mixing with an

initial velocity ratio of 0.5 and initial Mach numbers of 0.0, 0.5, 1.0, and 1.5 for both m = +1 and m =

It is evident from the results of these numerical calculations that the locally similar flow concept provides adequate approximations to the actually non-similar flow situations. It is pertinent to remark that the results for different initial freestream Mach number (Figs. 17b and 17d) do not differ significantly from each other when plotted against ϕ_b so that they are presented by one single curve. Since d is zero for these calculations, the compressible flows are transformed into the corresponding incompressible flows and thus the results for different freestream Mach numbers should fall into one single curve. The effect of compressibility should, of course, be noticeable when the results are transformated into the physical system of coordinates. The last series of curves, Fig. 19, illustrates the effect of different stagnation temperature ratios for the case of $M_{1ai} = 1.0$, $\phi_{bi} = 0.5$, and m = +1. The locally similar results again provide good approximations to the non-similar solutions, except in the extreme case with $\Lambda_b = 10.0$ where the difference is not negligible. It is also noteworthy to remark that the values of a_1 and a_2 for locally similar solutions, when presented as functions of ϕ_b should appear as one single curve for all stagnation temperature ratios.

For any practical problems, the pressure gradient would not have a constant value and the calculations by this scheme of

analysis should not present any difficulties. One may approximate this pressure distribution by segmented straight lines. If a fixed L is employed as a reference length throughout the analysis, different segments would have different values of m. A step by step calculation with different m values would provide the results for the problem. Early investigations by assuming segmented parabolic pressure distributions for incompressible flows do not produce significantly different results.

5. THE DEVELOPMENT OF INCOMPRESSIBLE, NON-SIMILAR JET MIXING TOWARD THE ASYMPTOTIC SIMILAR SOLUTION

The problem of constant pressure jet mixing between two incompressible parallel streams,† where the velocity profile at some initial section ξ_o is not similar, is considered here. This initial non-similar profile could possibly result from a non-zero pressure gradient upstream of ξ_o or from the separation of the boundary layer from a bluff based body. In the latter case, the velocity profile at the point of separation (or slightly downstream) is considered as an initial mixing profile. The lower stream is stagnant, and the velocity and its slope at the separating streamline are also zero. One has to ignore the small pressure gradient which exists in the vicinity of the point of separation. For such a type of flow $\lambda = 0$ and the momentum equation, Eq. (2.17), becomes

$$f_{\eta\eta\eta} + ff_{\eta\eta} = 2\xi(f_\eta f_{\xi\eta} - f_\xi f_{\eta\eta}) \tag{5.1}$$

with an initial velocity profile $f_\eta(\xi_o,\eta)$ specified.†† The non-similarity comes, of course, from the existence of the non-similar

---

†Since the compressible flow can be transformed into incompressible flow under isobaric conditions, we are essentially dealing with equivalent incompressible flow problems.

††From the analysis in Chapter 4, one should see that when $a_1(\xi_o)$ and $a_2(\xi_o)$ at ξ_o are known, the detailed profile within the viscous layer (whether it is a wall boundary layer or mixing layer) is completely determined.

profile at the location $\xi = \xi_o$ (ξ_o is non-zero). This type of flow is similar to any relaxation process, and it is appropriate to label this flow as a "dynamically relaxating flow."

5.1 DEVELOPMENT OF THE AUTONOMOUS EQUATION

Following the same manipulations presented in Chapter 4 by setting $\lambda = 0$, Eqs. (5.1) together with the matching conditions would yield

$$1 - a_1 = \sqrt{\pi}\frac{a_2}{\sqrt{2a_1}} + \left(2\xi a_1' - \frac{a_2^2}{3a_1^2}\right) + \frac{\sqrt{\pi}}{2}\left(\frac{5\sqrt{2}}{24}\frac{a_2^3}{a_1^{7/2}} - \frac{5\sqrt{2}}{4}\frac{a_2}{a_1^{3/2}}\xi a_1' + \sqrt{2}\xi\frac{a_1'}{a_1^{1/2}}\right)$$
$$+ \left(\frac{1}{15}\frac{a_2^2}{a_1^2} - \frac{4}{5}\xi\frac{a_2 a_2'}{a_1^2} - \frac{4}{3}\xi^2\frac{a'^2}{a_1} + 2\frac{a_2^2}{a_1^3}\xi a_1' - \frac{8}{27}\frac{a_2^4}{a_1^5} + 2\xi a_1' + \frac{4}{3}\xi^2 a_1''\right) + \cdots$$

and (5.2)

$$\phi_b - a_1 = -\sqrt{\pi}\frac{a_2}{\sqrt{2a_1}} + \left(2\xi a_1' - \frac{a_2^2}{3a_1^2}\right) - \frac{\sqrt{\pi}}{2}\left(\frac{5\sqrt{2}}{24}\frac{a_2^3}{a_1^{7/2}} - \frac{5\sqrt{2}}{4}\frac{a_2}{a_1^{3/2}}\xi a_1' + \sqrt{2}\xi\frac{a_1'}{a_1^{1/2}}\right) +$$

Upon examining the solution for various numbers of terms on the right side of Eq. (5.2), it is interesting to observe again that the one term solution is identical with that from the similar analysis. The functions a_1 and a_2 are constants which are given by

$$a_1 = \frac{1}{2}(1 + \phi_b)$$
$$a_2 = \sqrt{\frac{a_1}{2\pi}}(1 - \phi_b) = \sqrt{\frac{1 + \phi_b}{\pi}}\frac{1 - \phi_b}{2} \tag{5.3}$$

Using two terms in the right side of Eqs. (5.2), one obtains a differential equation in a_1 given by

$$\xi \frac{da_1}{d\xi} = \frac{da_1}{d\ln\xi} = \frac{1}{2}(1 - a_1) - \frac{1}{4}(1 - \phi_b) + \frac{(1 - \phi_b)^2}{12\pi a_1} \tag{5.4}$$

and an algebraic relation for a_2 in terms of a_1 which is expressed by

$$a_2 = \sqrt{\frac{a_1}{2\pi}}(1 - \phi_b) ; \tag{5.5}$$

the latter also holds for the one term solution. The asumptotic similar condition, corresponding to fully developed mixing flow, can be obtained by setting $a_1' = 0$. Denoting such a condition by the subscript 'e', Eq. (5.4) can be rewritten as

$$\frac{a_1}{\ln\xi} = \frac{a_{1e} - a_1}{2}\left[1 + \frac{(1 - \phi_b)}{6\pi}\frac{1}{a_1 a_{1e}}\right] \tag{5.6}$$

with

$$a_{1e} = \frac{1 + \phi_b}{4}\left[1 + \sqrt{1 + \frac{8}{3\pi}\left(\frac{1 - \phi_b}{1 + \phi_b}\right)^2}\right]$$

This two term solution shows that a stable condition results which is typical for all relaxation processes. Since the bracketed quantity in Eq. (5.6) is always positive, any a_1 value different from a_{1e} would produce a change which is proportional to the difference and is in a direction to reduce this difference. If a_1 is less than the asymptotic solution a_{1e}, Eq. (5.6) shows that $da_1/d \ln \xi$ is positive and a_1 will therefore increase with ξ toward a_{1e}. If a_1 is greater than a_{1e}, $da_1/d \ln \xi$ is negative and a_1 will decrease toward a_{1e}. Thus, for any given initial value of a_1 at ξ_o corresponding to a non-similar initial velocity profile, the resulting mixing process is such that the similar solution (fully developed profile) will be reached asymptotically.

By taking three terms on the right side of Eq. (5.2), two first order, ordinary differential equation in a_1 and a_2 result. Since ξ appears only with derivatives, they may be rearranged to yield

$$\frac{\xi \dfrac{da_2}{d\xi}}{\xi \dfrac{da_1}{d\xi}} = \frac{da_2}{da_1} = \frac{\dfrac{1 - \phi_b}{\sqrt{2\pi}\sqrt{a_1}} + \dfrac{5}{8}\dfrac{1 + \phi_b}{2}\dfrac{a_2}{a_1} - \dfrac{13}{8}a_2}{\dfrac{1}{2}\left[\dfrac{1 + \phi_b}{2} - a_1 + \dfrac{1}{3}\left(\dfrac{a_2}{a_1}\right)^2\right]} \qquad (5.7)$$

which is a differential equation between a_1 and a_2 only. The

"autonomous" character of the original equation is illustrated by the successful elimination of ξ in Eq. (5.7). One now recognizes that a_2 can be considered as a function of a_1, or vice versa. The asymptotic condition, corresponding to $a_1' = 0$ and $a_2' = 0$, is obtained when both numerator and denominator are zero. To be specific, they correspond to the constant pressure jet mixing solution when three terms are used from the infinite series in Eq. (3.9). These asymptotic conditions are presented in Fig. 20.

To integrate Eq. (5.7) initial values of $a_1(\xi_o)$ and $a_2(\xi_o)$ are needed. This is in contrast to the above mentioned cases where the one term solution is independent of the initial velocity profile and the two term solution requires an initial value of a_1 only. For the four term solution it can be seen from Eq. (5.2) that values of a_1, a_2, and a_1' are required. However, the second (or higher) derivatives are usually small and can be neglected [25]. The ξ variable can again be eliminated and a_2 can be found as a function of a_1 only.

5.2 DEVELOPMENT OF FLOW AFTER SEPARATION FROM THE SOLID BODY

Particular attention is now given to the flow development after it separates from the bluff based body. The resulting downstream flow can be considered as an isobaric mixing between the approaching freestream and the quiescent fluid within the wake. Under such a condition, the velocity ratio between the main and the secondary freestreams is approximately zero.

The one-term results as given by Eq. (5.8) are $a_1 = 0.5$ and $a_2 = 0.282$. For the two-term solution, the relation between a_1 and a_2

can easily be established through Eq. (5.5). For any initial value of a_1, jet mixing action will take place such that a_1 (and thus a_2) will change toward the final asymptotic value ($a_{1e} = 0.590$, $a_{2e} = 0.306$). It must be kept in mind that for inversion of the infinite series of η to be valid, the first term involving a_1 must not be small. Therefore, the solutions given above do not hold for the region near $a_1 = 0$. Thus, the two-term solution presented in Fig. 21 is not shown near the origin.

For the integration of the differential equation, Eq. (5.7), which was obtained from the three-term representation of the original series, it was found that there were definite regions in the a_1, a_2 plane where convergence of the series was a problem. This is in addition to the region near the a_1 axis where a_1 is small. On the other hand it was found that in certain regions the values of a_1 and a_2 were such that the convergence of the series (now represented by the first three terms) was as good or even better than the point corresponding to the similar solution. By examining the third term, it was found that its magnitude becomes zero when

$$a_2 = \sqrt{\frac{a_1}{2\pi}}$$

this, of course, is identical with that from the two-term solution. Near the similar point, it was found that the first term is never smaller than the second term; therefore, in the region near this point the series convergence is good. When the magnitude of the

second term is small, poor convergence results, unless the third term is even smaller. The second term is zero for $a_1 = 0.5$ for $\phi_b = 0$.

When calculations were made for a_1 and a_2 values away from the above mentioned regions where convergence of the series was observed, it was found that often the convergence of the series was very poor. For example, at the point $a_1 = 0.15$ and $a_2 = 0.50$, the three terms gave values of 1.624, 0.350, and -1.124, respectively, as compared to 0.461, -0.078, and 0.039 for the corresponding terms at the asymptotic limiting point.

Figure 22 shows various regions in the a_1, a_2 plane where the series converges quickly, slowly, or diverges.

To avoid the trouble of the divergence of the series, the summation scheme proposed by Euler, and used extensively by Meksyn, was tried. When Eqs. (5.2) were integrated using Euler's summation scheme, the convergence improved greatly. For example, for the above mentioned point where $a_1 = 0.15$ and $a_2 = 0.50$, after applying Euler's scheme once, the three terms gave values of 0.812, 0.494, and 0.150, respectively, seemingly to indicate convergence of the series. When Euler's summation scheme is indiscriminately applied, one obtains the integral curves in the a_1, a_2 plane and its final asymptotic value of $a_1 = 0.560$, $a_2 = 0.335$ as shown in Fig. 23.

However, it is known that the Euler's scheme is not needed in the region (including its asymptotic limit) where the original series is convergent. It was therefore necessary that the Euler's sum be applied only when the series appears to be divergent. An

arbitrary scheme had to be developed such that the change over from one calculating scheme to another (with or without Euler's summation procedure) would give smooth trajectories in the a_1, a_2 plane. This is accomplished by the following considerations:

After application of Euler's summation procedure to the infinite series in Eq. (5.2), one obtains

$$\frac{da_2}{da_1} = \frac{4\sqrt{\frac{2a_1}{\pi}} - \frac{33}{4}a_2 + \frac{5}{8}\frac{a_2}{a_1}}{\frac{1}{2} - a + \frac{a_2^2}{6a_1^2}} \qquad (5.8)$$

In order to obtain smooth integral curves in the a_1, a_2 plane, it is obvious that the change over between the two calculating schemes should be made at points where they yield the same slope. Equating da_2/da_1 from Eqs. (5.7) and (5.8), one has

$$\frac{3}{4}\sqrt{\frac{2a_1}{\pi}}(1 - 2a_1) - \frac{5}{4}(1 - 2a_1)a_2 + \frac{7}{12}\sqrt{\frac{2a_1}{\pi}}\frac{a_2^2}{a_1^2} - \left(\frac{53}{48}a_1 - \frac{5}{96}\right)\left(\frac{a_2}{a_1}\right)^3 = 0 \qquad (5.9)$$

Points with a_1, a_2 values satisfying the above expression are joined in Fig. 23 by curve "A" which should obviously pass through the two asymptotic limiting points. Since these two points are quite close to each other, points along this curve usually are within the region where the original series converges. Furthermore, any error introduced from this arbitrary scheme of manipulation is expected to decay due to the parabolic nature of the system.

There is another region in the a_1, a_2 plane where a_1 is small while a_2 is finite, which also presents a convergence problem after Euler's summation is applied once. Although this region does not seem to be physically realistic, it is nevertheless tacitly suggested that when the first term equals the second term of the series, the regular summation scheme should be applied.

The final integral trajectories (phase tracks) are presented in Fig. 24. It should be noted that although information of the ξ values is not needed in establishing these curves, the corresponding velocity profiles of this developing flow field cannot be computed until the precise variation of ξ is known.

5.3 EXAMPLE OF THE CALCULATION OF A DEVELOPING FLOW FIELD

Schubauer [26] performed an experimental investigation of low speed air flow past an elliptic cylinder. Meksyn [1] performed calculations based on Schubauer's data and produced the velocity profile and ξ value at the point of separation. Employing this information as the given initial condition for the subsequent flow field, one may easily establish the path of integration of Eq. (5.7) in the a_1, a_2 plane.

Another numerical scheme based on finite difference (see the APPENDIX for details) has also been worked out for this problem. Results of these calculations are also presented in Fig. 24. Reasonably good agreement between the results seem to support the considerations discussed in this chapter.

6. SUMMARY AND CONCLUSIONS

The method developed by Meksyn in dealing with boundary layer flow problems is certainly interesting and useful. It provides an effective tool to solve boundary layer flow problems, especially when a non-similarity situation prevails. The present problem of jet mixing under the influence of a pressure gradient is one of these non-similar flow situations, and the application of this method has successfully produced results which also supported the locally similar concept.

However, in some situations such as the flow case discussed in Chapter 5, the infinite series resulting from the integration by the method of steepest descent, diverges in certain parts of the domain. To evaluate this series, one has to resort to Euler's transformation. No knowledge is available as to the extent and number of times which the Euler transformation should be applied, and the arbitrariness of decision was thus necessarily introduced in performing any practical numerical calculations.

However, even in the problem discussed in Chapter 5 where poor convergence of the series has been observed, the qualitative character of the flow development toward the final asymptotic solution is fully illustrated by such an analytical scheme. This feature probably cannot be easily illustrated by finite difference numerical calculations.

REFERENCES

1. Chow, W. L. and Addy, A. L., "Interaction Between Primary and Secondary Streams of Supersonic Ejector Systems and Their Performance Characteristics," AIAA J., Vol. 2, April 1964, pp. 686-695.

2. Chapman, D. R., "Laminar Mixing of a Compressible Fluid," NACA TN 1800, 1949.

3. Crane, L. J., "The Laminar and Turbulent Mixing of Jets of Compressible Fluid," Part II: The Mixing of Two Semi-Infinite Streams," J. Fluid Mech., Vol. 3, October 1957, pp. 81-92.

4. Hill, W. G., Jr. and Page, R. H., "Initial Development of Turbulent, Compressible Free Shear Layers," Trans. of ASME, J. of Basic Engr., Vol. 91, March 1969, pp. 67-73.

5. Lamb, J. P., "An Approximate Theory for Developing Turbulent Free Shear Layers," Trans. of ASME, J. of Basic Engr., Vol. 89, September 1967, pp. 633-642.

6. Denison, M. R. and Baum, E., "Compressible Free Shear Layer with Finite Initial Thickness," AIAA J., Vol. 1, February 1963, pp. 342-349.

7. Napolitano, L. G. and Pozzi, A., "Laminar Mixing in the Presence of Axial Pressure Gradients," J. Aerospace Sci., Vol. 28, Jan. 1961, pp. 73-75.

8. Steiger, M. H. and Bloom, M. H., "Linearized Viscous Free Mixing with Streamwise Pressure Gradients," AIAA J., Vol. 2, Feb. 1964, pp. 263-266.

9. Schetz, J. A. and Jannone, J., "Planar Free Turbulent Mixing with an Axial Pressure Gradient," Trans. of ASME, J. of Basic Engr., Vol. 87, December 1967, pp. 707-714.

10. Sabin, C. M., "An Analytical and Experimental Study of the Plane, Incompressible, Turbulent Free-Shear Layer with Arbitrary Velocity Ratio and Pressure Gradient," Trans of ASME, J. of Basic Engr., Vol. 87, June 1965, pp. 421-428.

11. Greenberg, R. A., "Laminar Mixing of Two Streams in a Pressure Gradient," M.I.T., Aerophysics Laboratory, TR 117, February 1966.

12. Meksyn, D., New Methods in Laminar Boundary-Layer Theory, Pergamon Press, New York, 1961.

13. Korst, H. H., Page, R. H. and Childs, M. E., "Compressible Two-Dimensional Jet Mixing at Constant Pressure," ME-TN-392-1, Engineering Experiment Station, University of Illinois, April 1954.

14. Korst, H. H. and Chow, W. L., "Non-Isoenergetic Turbulent (Pr_t = 1) Jet Mixing Between Two Compressible Streams at Constant Pressure," NASA CR-419, April 1966, also ME-TN-393-2, Engineering Experiment Station, University of Illinois, April 1965.

15. Chow, W. L. and Korst, H. H., "On the Flow Structure Within a Constant Pressure Compressible Turbulent Jet Mixing Region," NASA TN-D-1894, April 1963, also ME-TN-393-1, Engineering Experiment Station, University of Illinois, July 1962.

16. Korst, H. H. and Chow, W. L., "On The Correlation of Analytical and Experimental Free Shear Layer Similarity Profiles by Spread Rate Parameters," ASME Paper 70-WA/FE-12, to be appearing in Trans. of ASME, J. of Basic Engr.

17. Chow, W. L., "Study of Jet Mixing Problems by Meksyn's Method," AIAA J., Vol. 6, December 1968, pp. 2422-2424.

18. Schlichting, H., Boundary-Layer Theory, Sixth Edition, McGraw-Hill, Inc., 1968, 137-141.

19. Napolitano, L. G., Libby, P. A. and Ferri, A., "Recent Work on Mixing at the Polytechnic Institute of Brooklyn," Combustion and Propulsion, Third AGARD Colloquium, Pergamon Press, 1958, pp. 118-152.

20. Schlichting, H., Boundary-Layer Theory, Sixth Edition, McGraw-Hill, Inc., 1968, p. 324.

21. Ting, L. and Libby, P. A., "Remarks on the Eddy Viscosity in Compressible Mixing Flows," J. of Aerospace Sci., Vol. 27, Oct. 1960, pp. 797-798.

22. Alber, I. E. and Lees, L., "Integral Theory for Supersonic Turbulent Base Flows," AIAA J., Vol. 6, July 1968, pp. 1343-1351.

23. Ferri, A., Libby, P. A. and Zakkay, V., "Theoretical and Experimental Investigation of Supersonic Combustion," Third ICAS Conference, Stockholm, 1962.

24. Chao, B. T., "Selected Topics on Fundamentals of Convective Heat Transfer," Advanced Heat Transfer, University of Illinois Press, Urbana, Ill. 1967.

25. Chow, W. L. and Chao, B. T., "Slip Flow Past a Semi-Infinite Flat Plate," Sixth Int. Symposium on Rarefied Gas Dynamics, Vol. I, pp. 441-450.

26. Schubauer, G. B., "Air Flow in a Separating Laminar Boundary Layer," NACA TR 527, 1934.

FIGURES

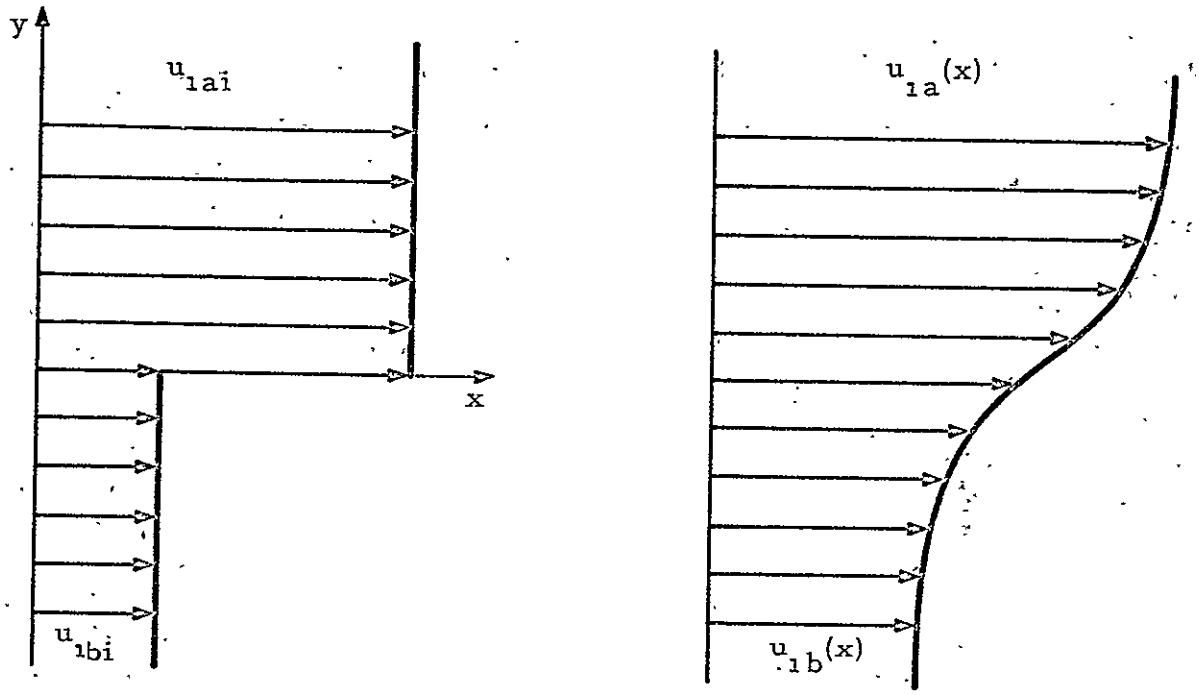

Figure 1 Illustration of the initial and boundary conditions of the jet mixing problem

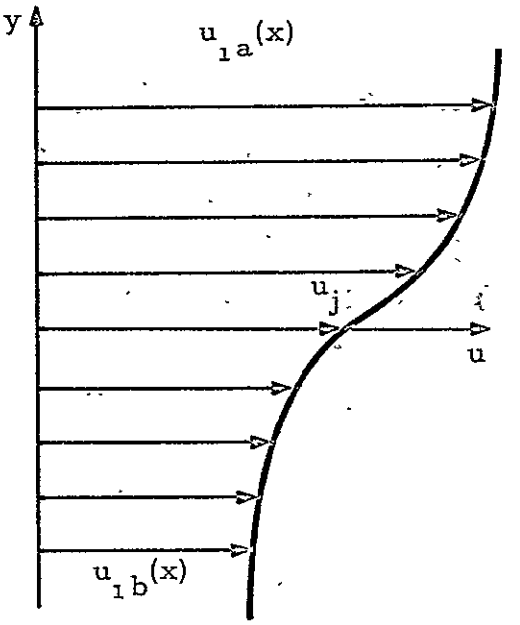

'igure 2a Mixing profile

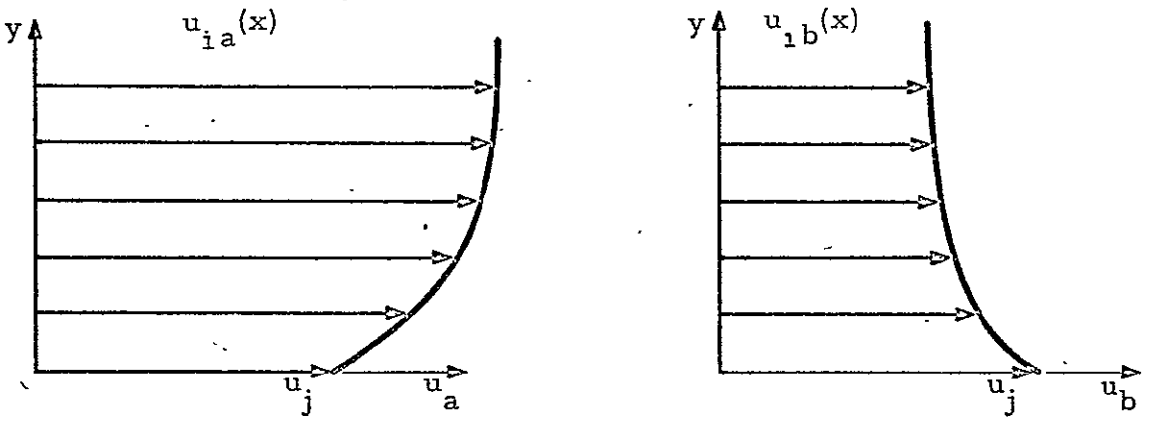

Above dividing streamline

Below dividing streamline

Figure 2b Corresponding two boundary layer flow problems

Figure 2 Illustration of the mixing profile and its corresponding two boundary layer flow problems

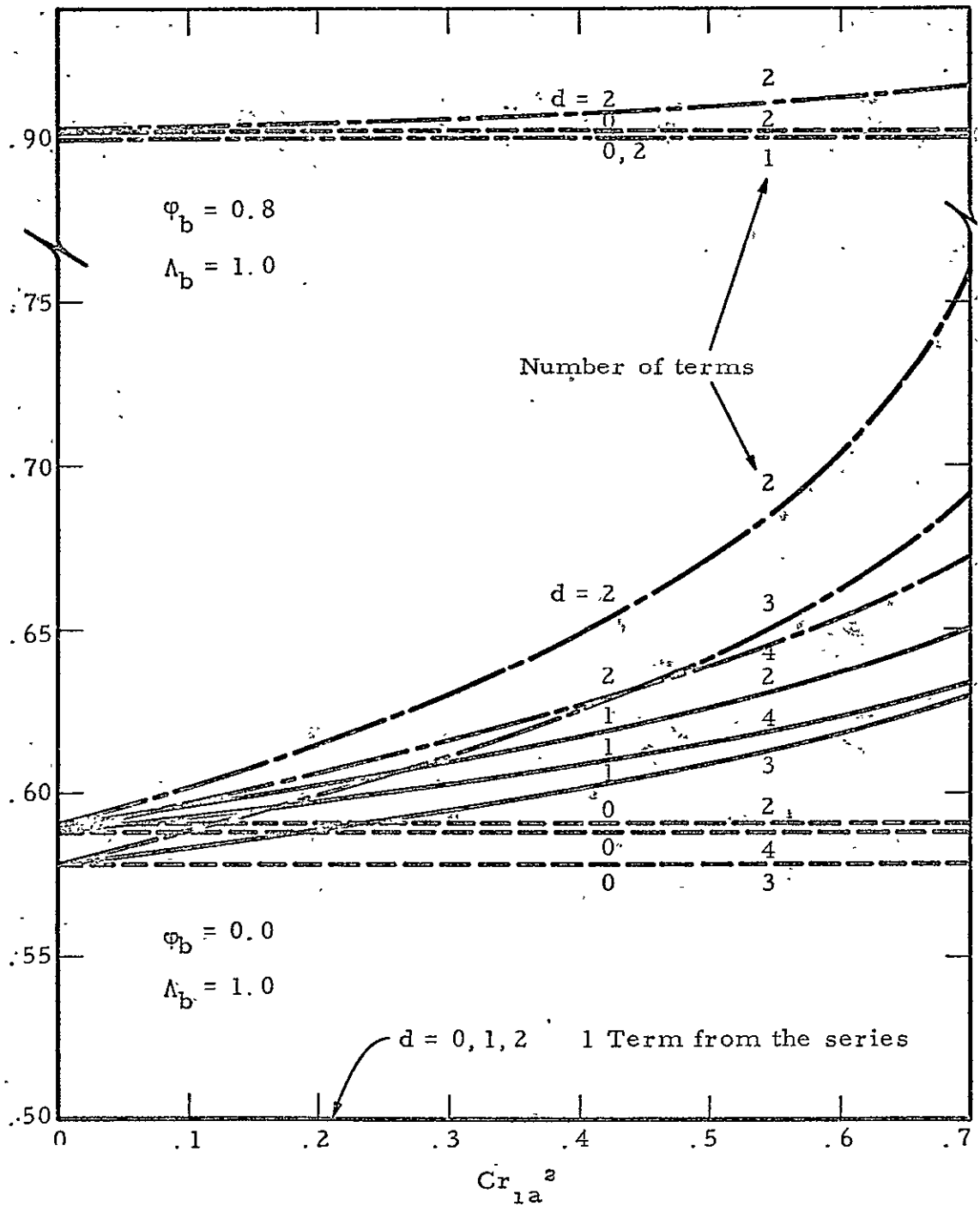

Figure 3 Isoenergetic results of a_1 for isobaric mixing

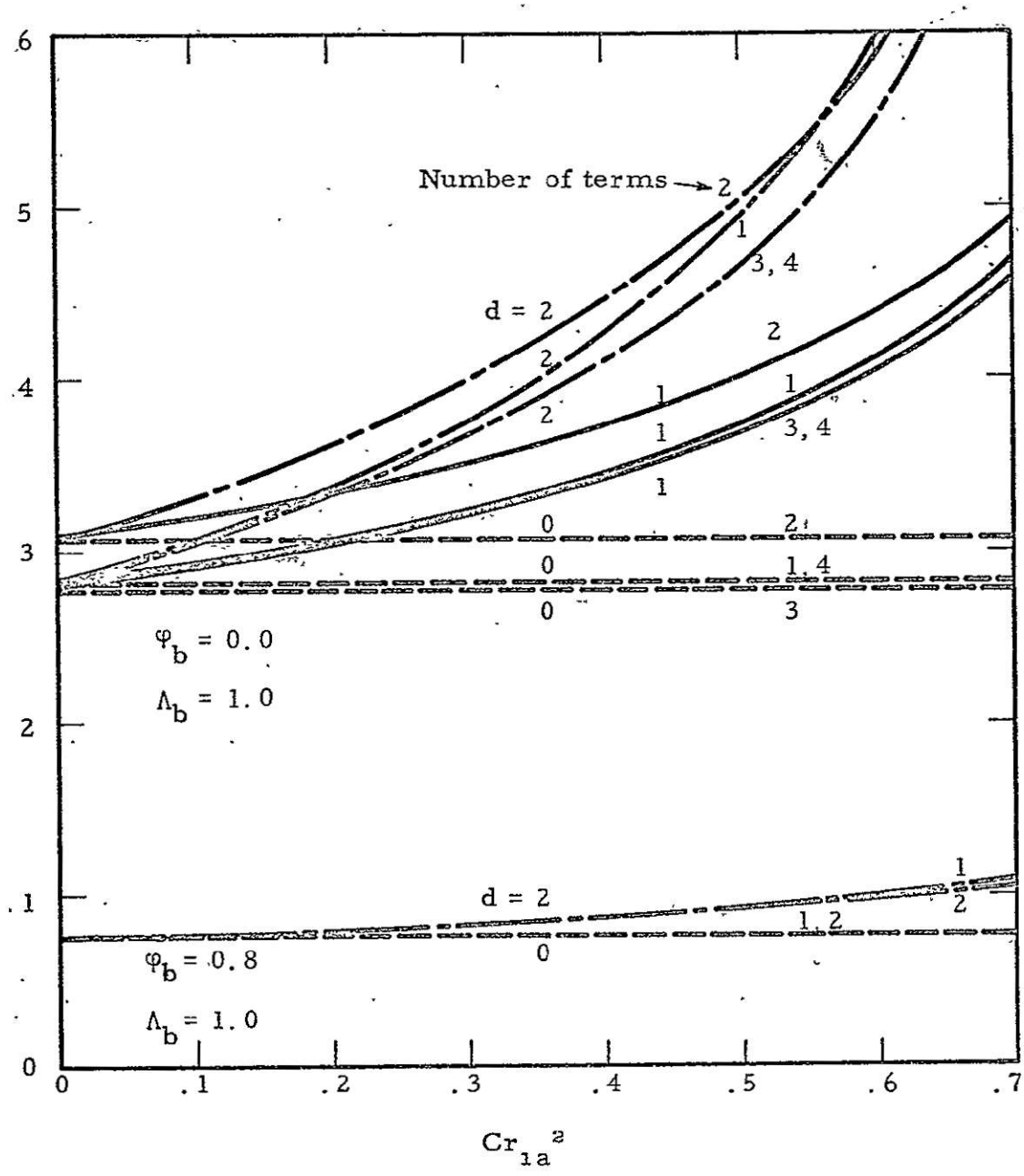

Figure 4 Isonenergetic results of a_2 for isobaric mixing

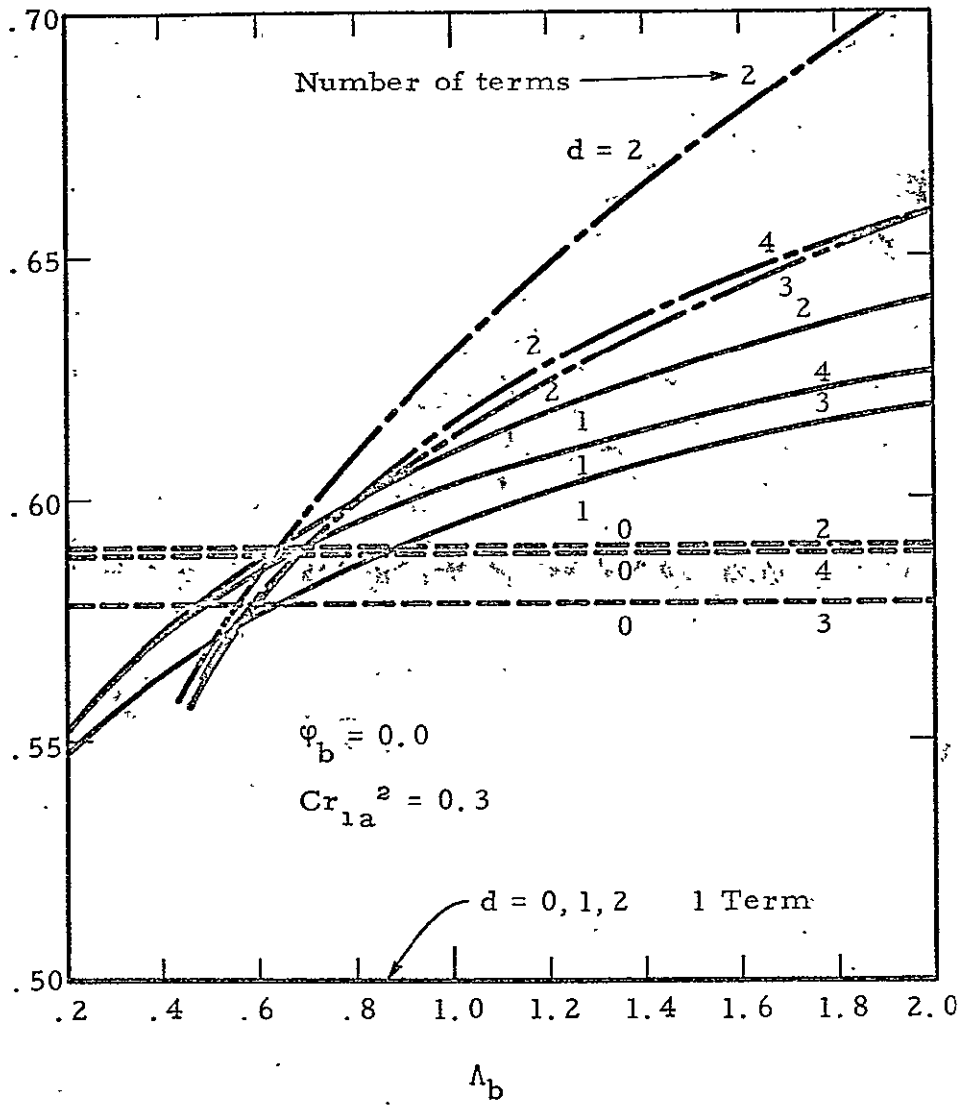

Figure 5 Non-isoenergetic results of a_1 for isobaric mixing

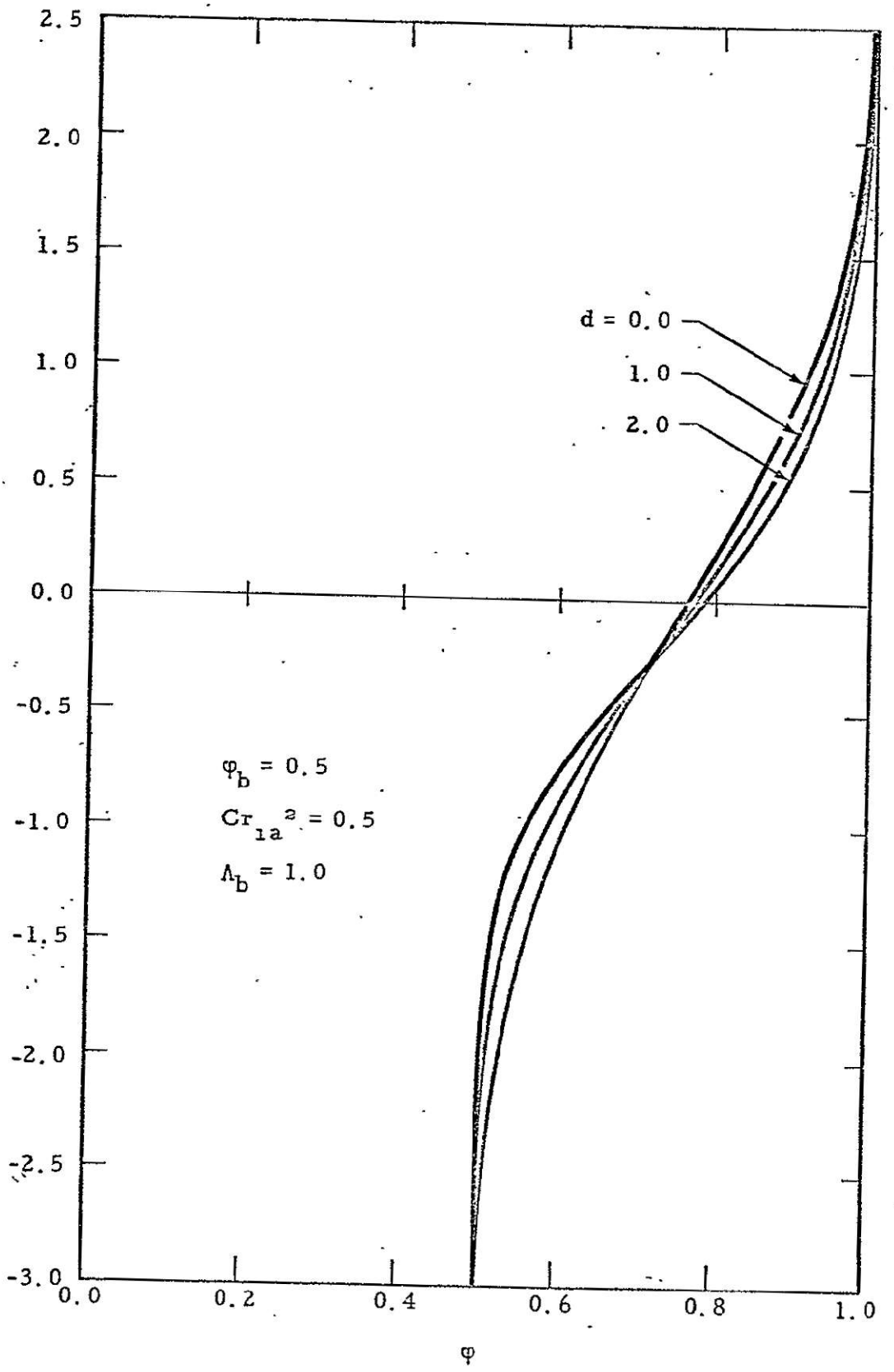

Figure 6 Velocity profiles for various values of index d

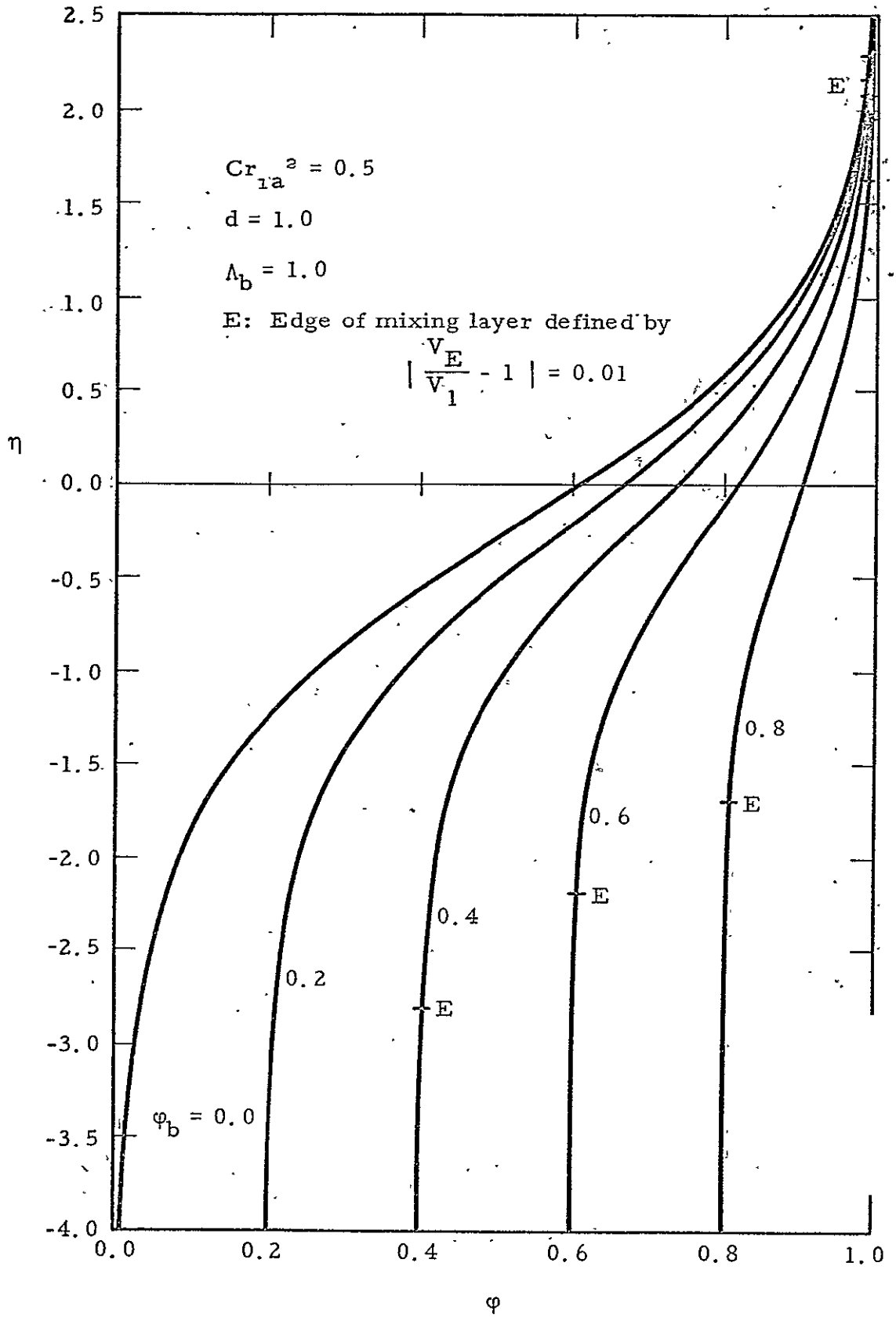

Figure 7 Turbulent velocity profiles for various velocity ratio

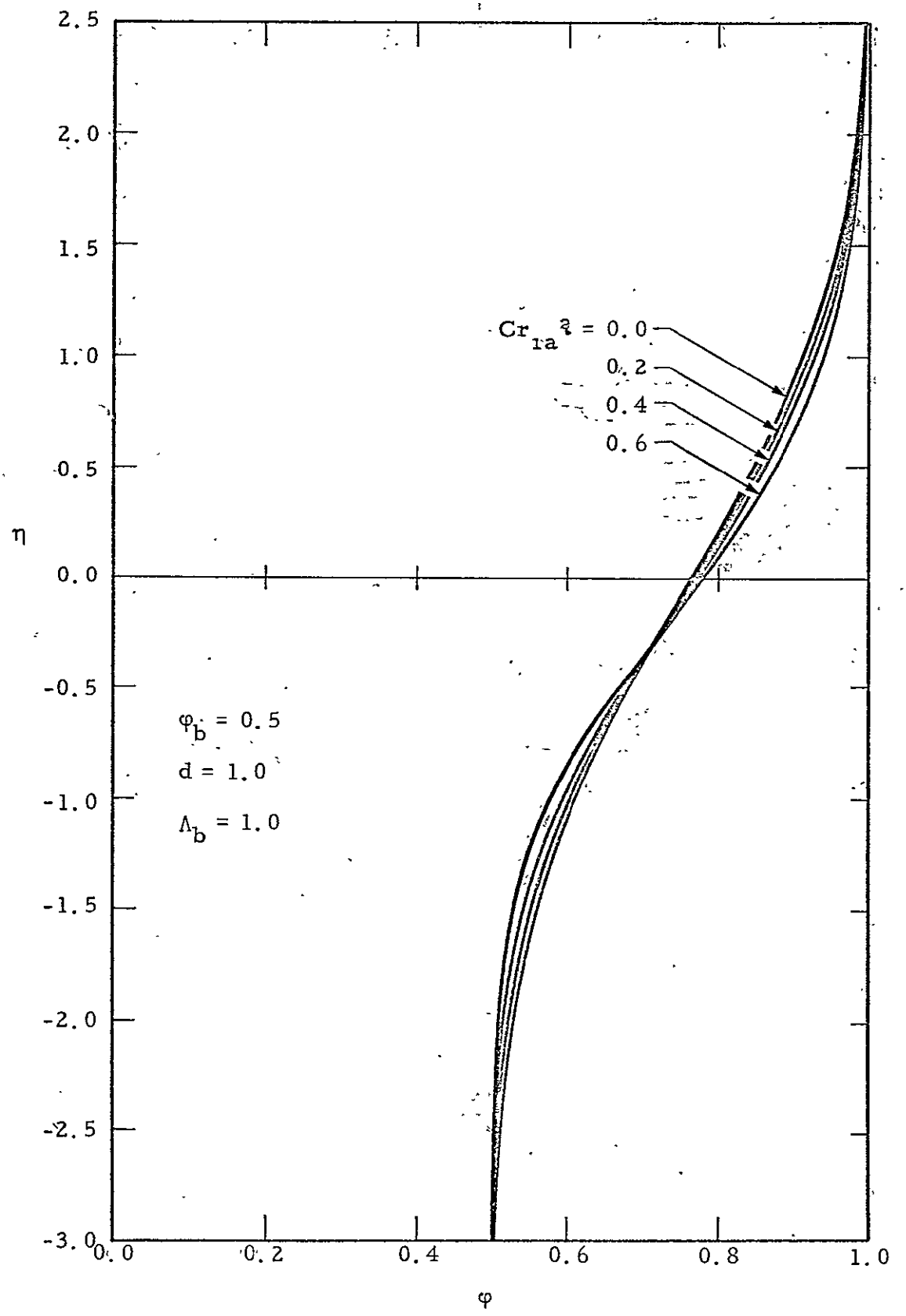

Figure 8 Turbulent velocity profiles for various freestream Crocco numbers

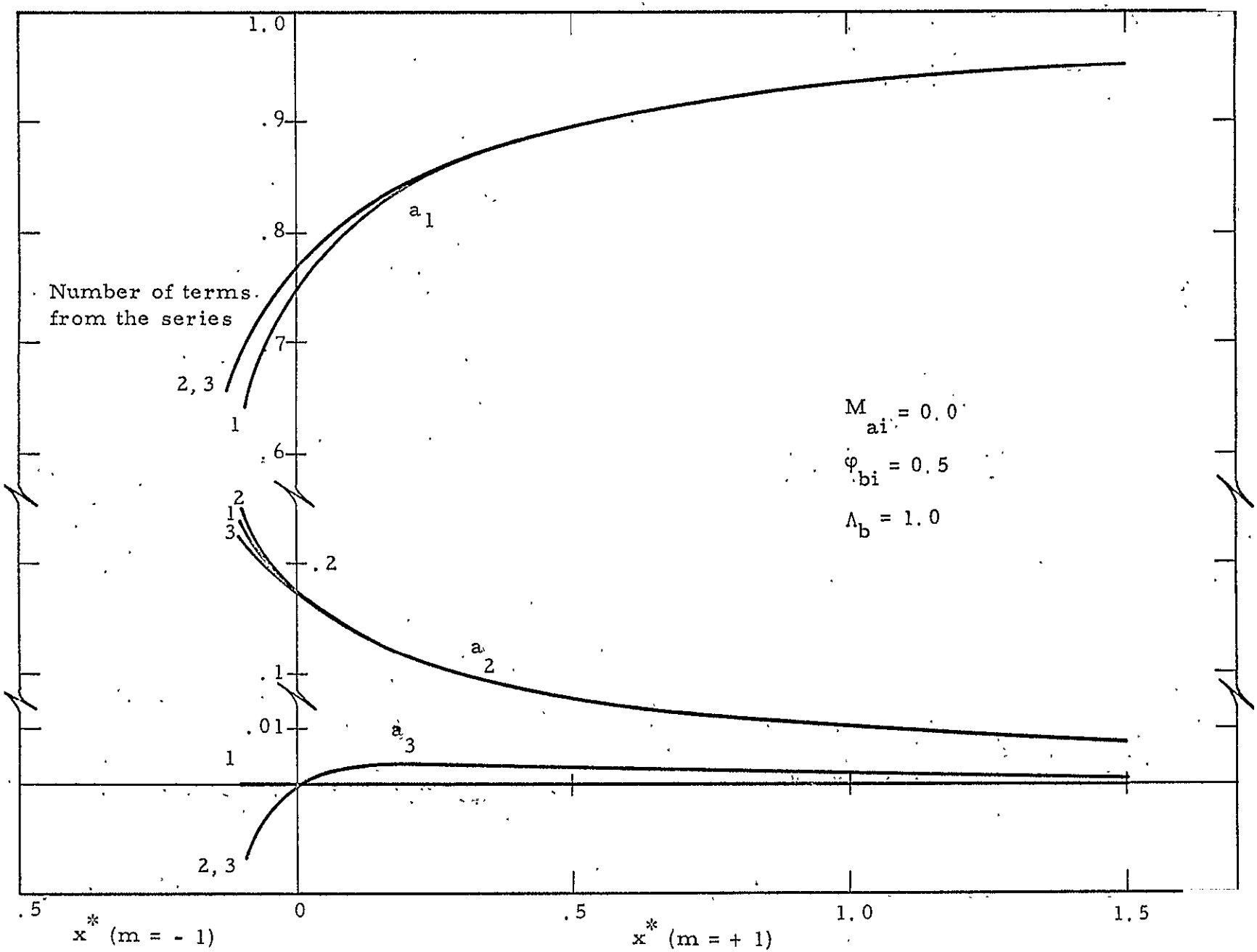

Figure 9a Coefficients a_{-}, a_{-}, and a_{-} as a function of x^*

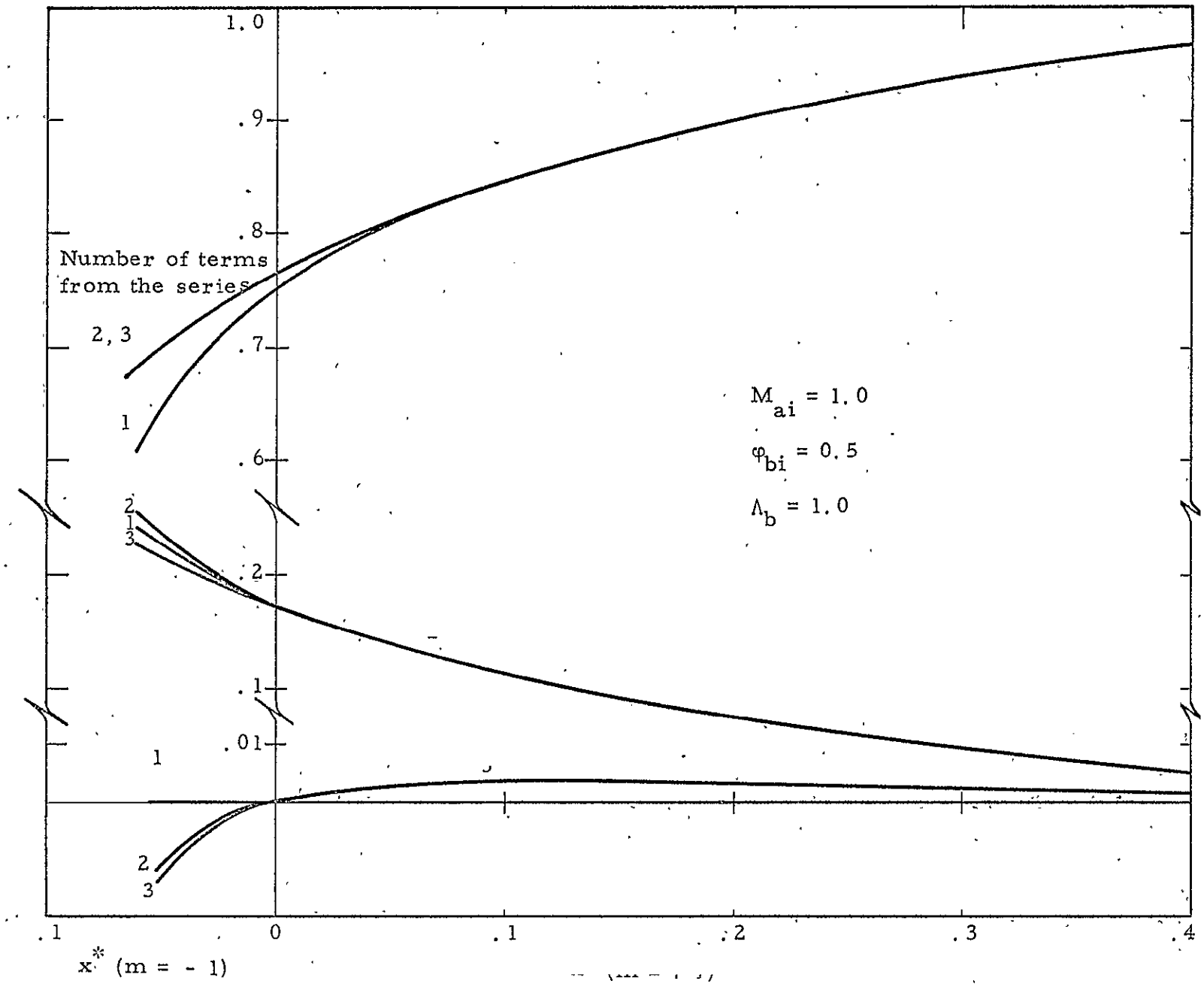

Figure 9b Coefficients a_1, a_2, and a_3 as a function of x^*

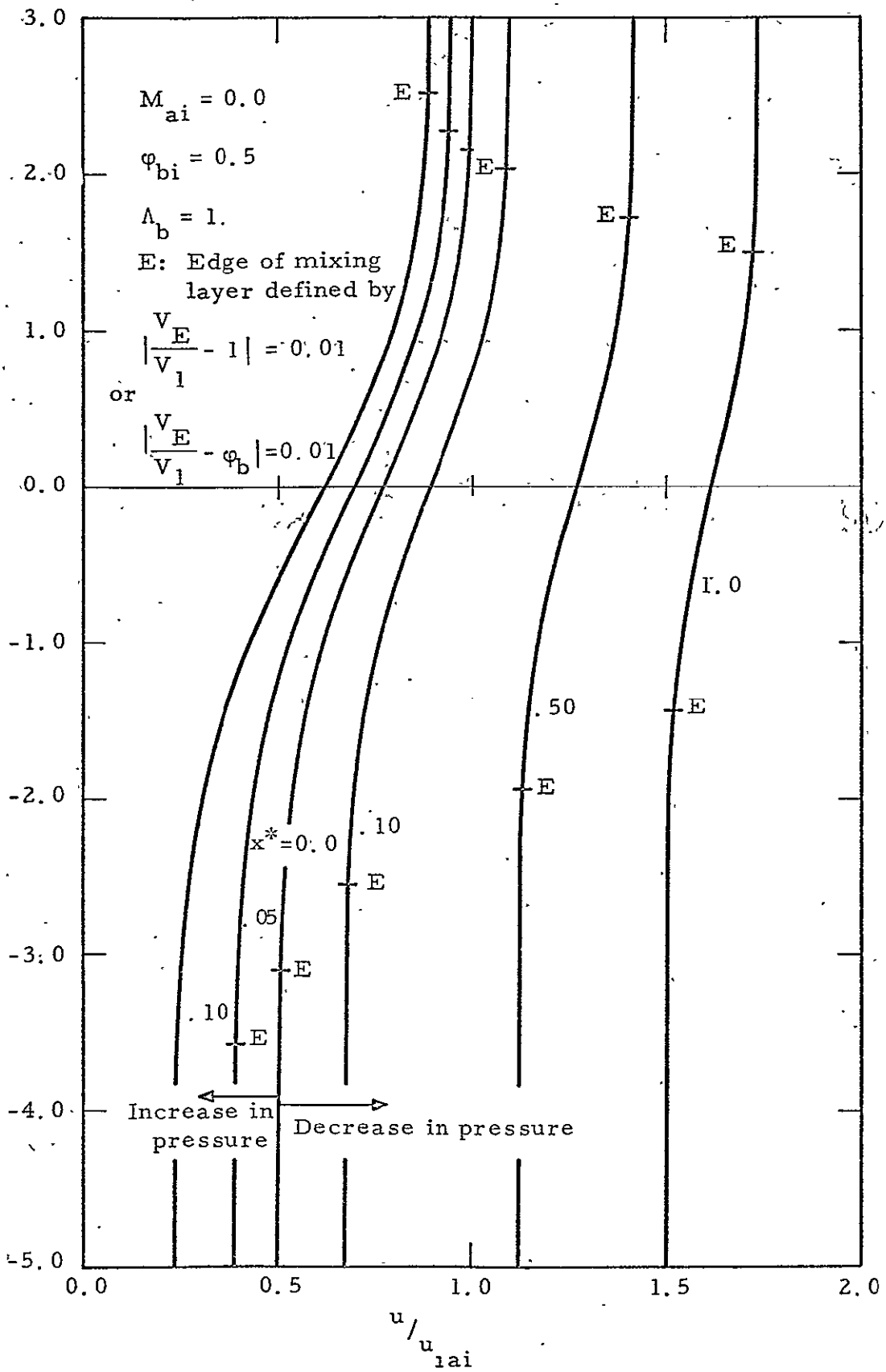

Figure 10a Velocity profiles in variable pressure mixing region

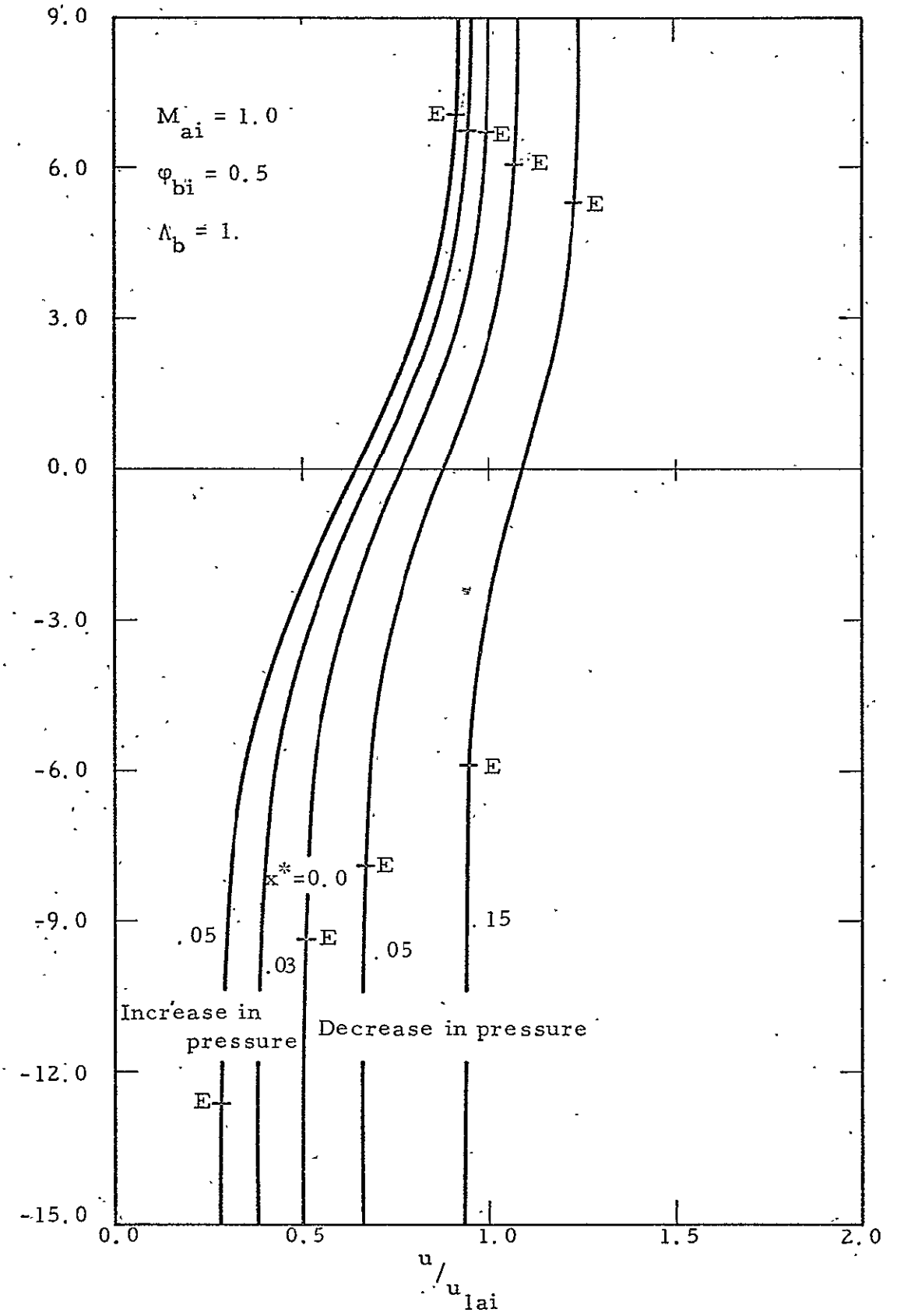

Figure 10b Velocity profiles in variable pressure mixing region

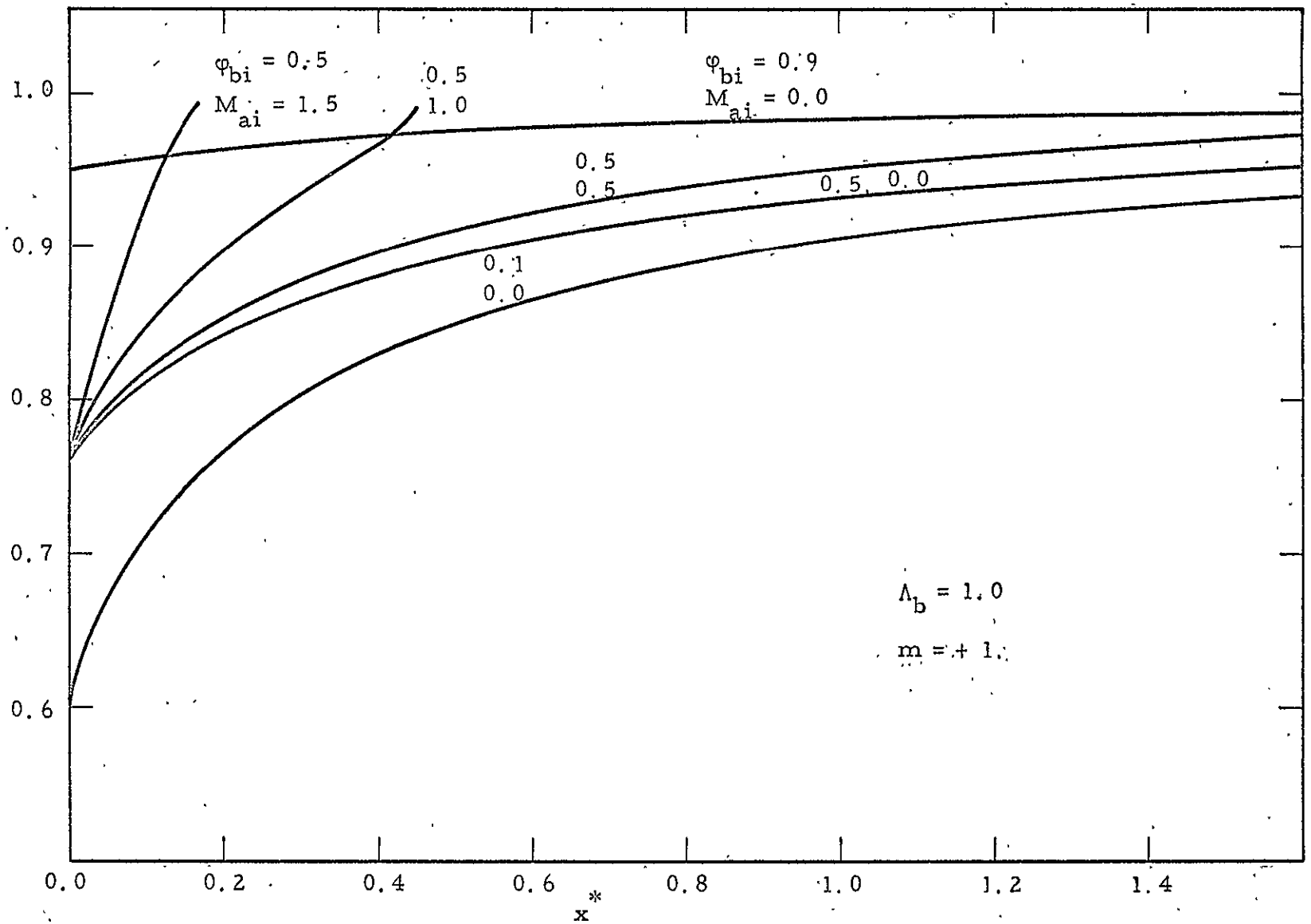

Figure 11 Coefficient a_1 as a function of x^* for various velocity ratios and Mach numbers

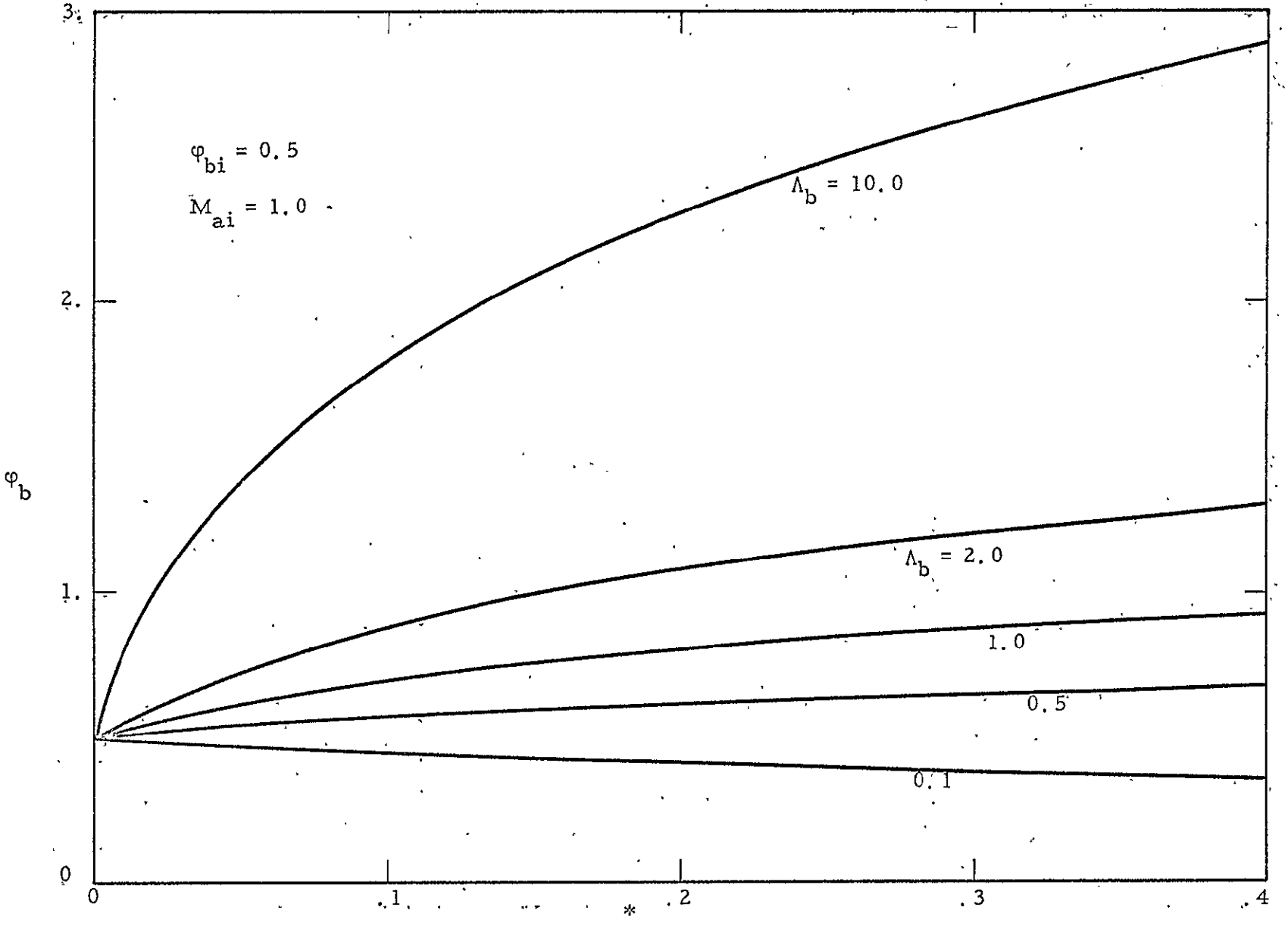

Figure 12 Local freestream velocity ratio as a function of x*

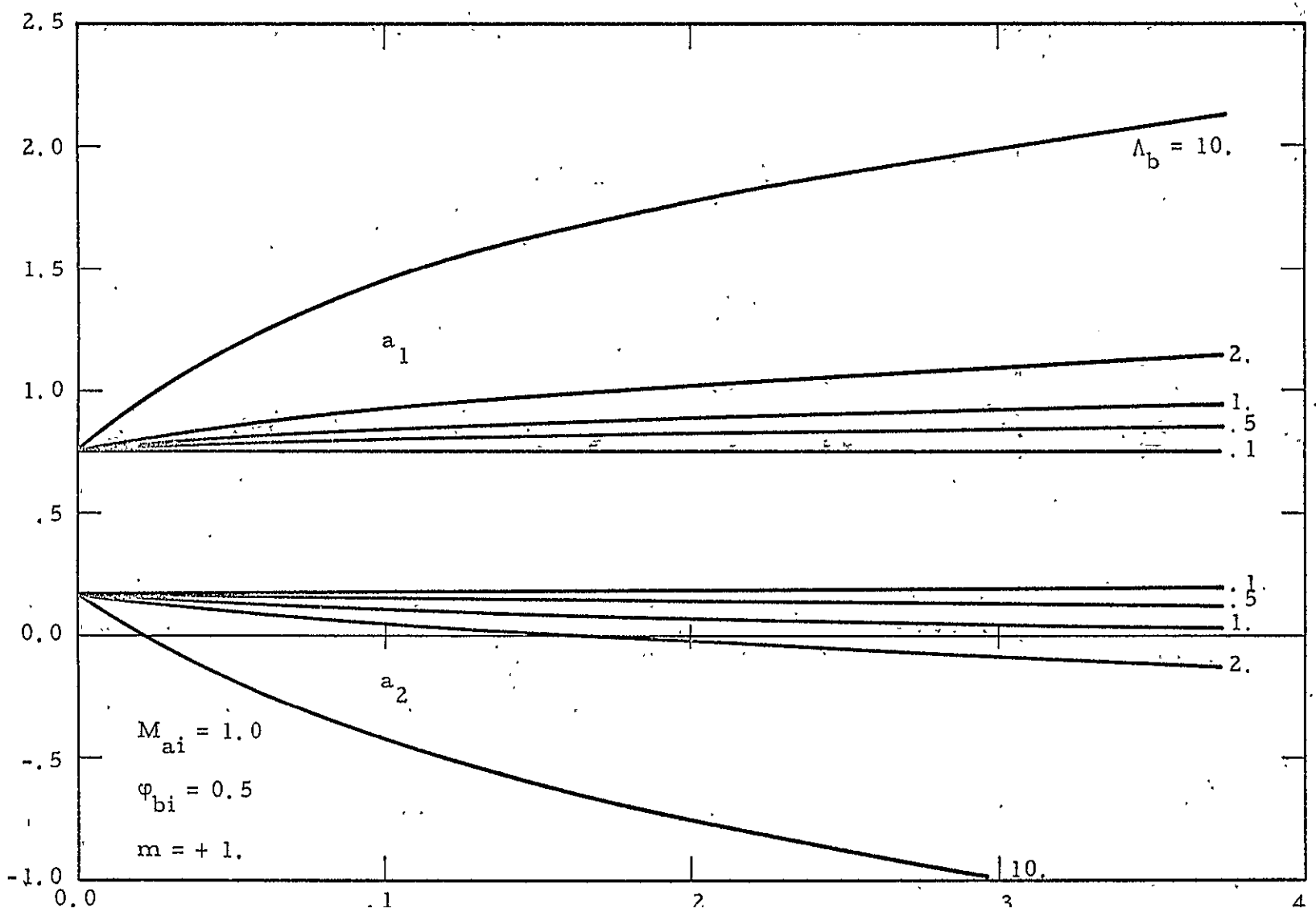

Figure 13a Coefficients a_1 and a_2 as a function of x* for various total temperature ratios

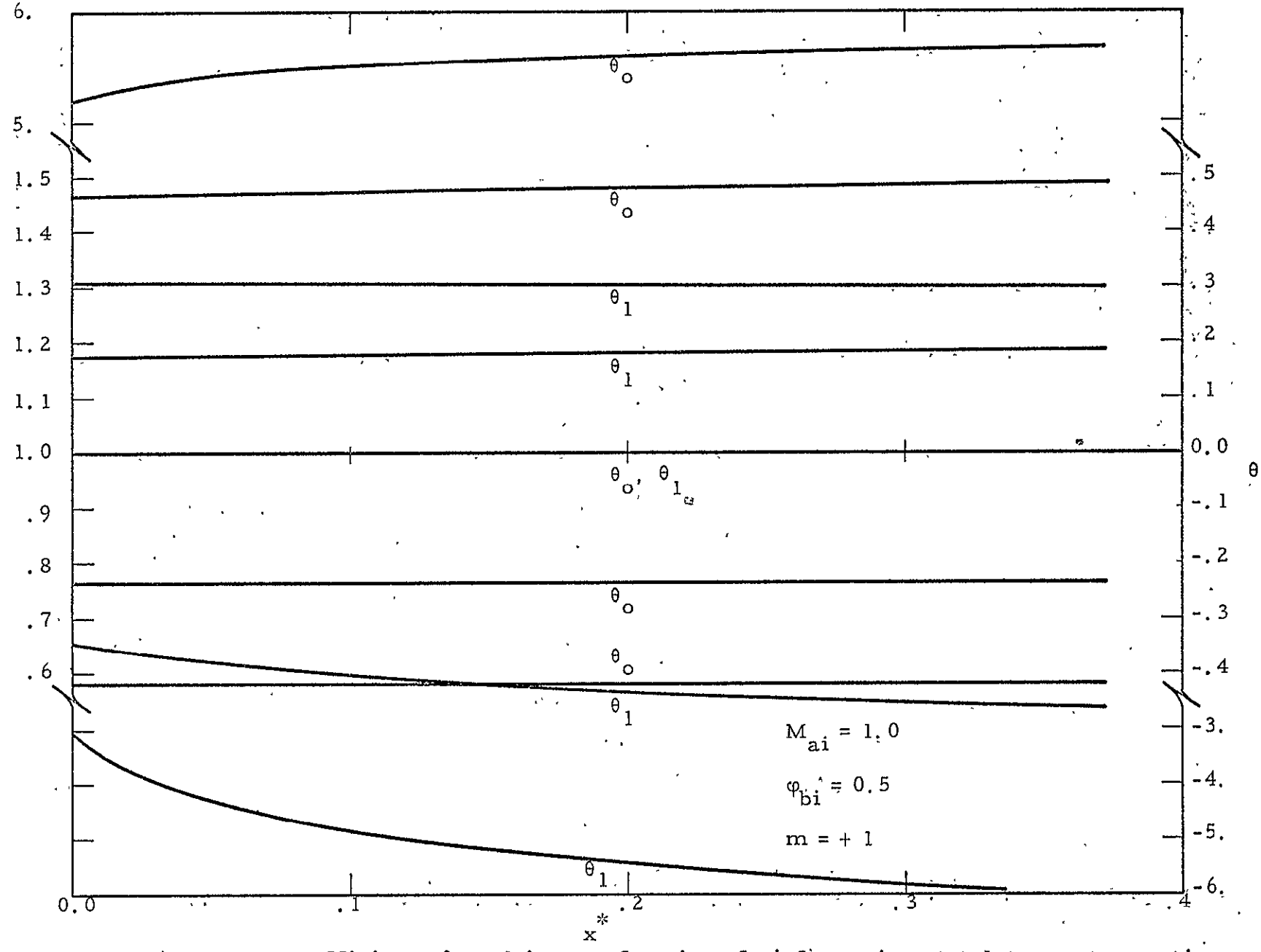

Figure 13b Coefficients θ_0 and θ_1 as a function of x* for various total temperature ratios

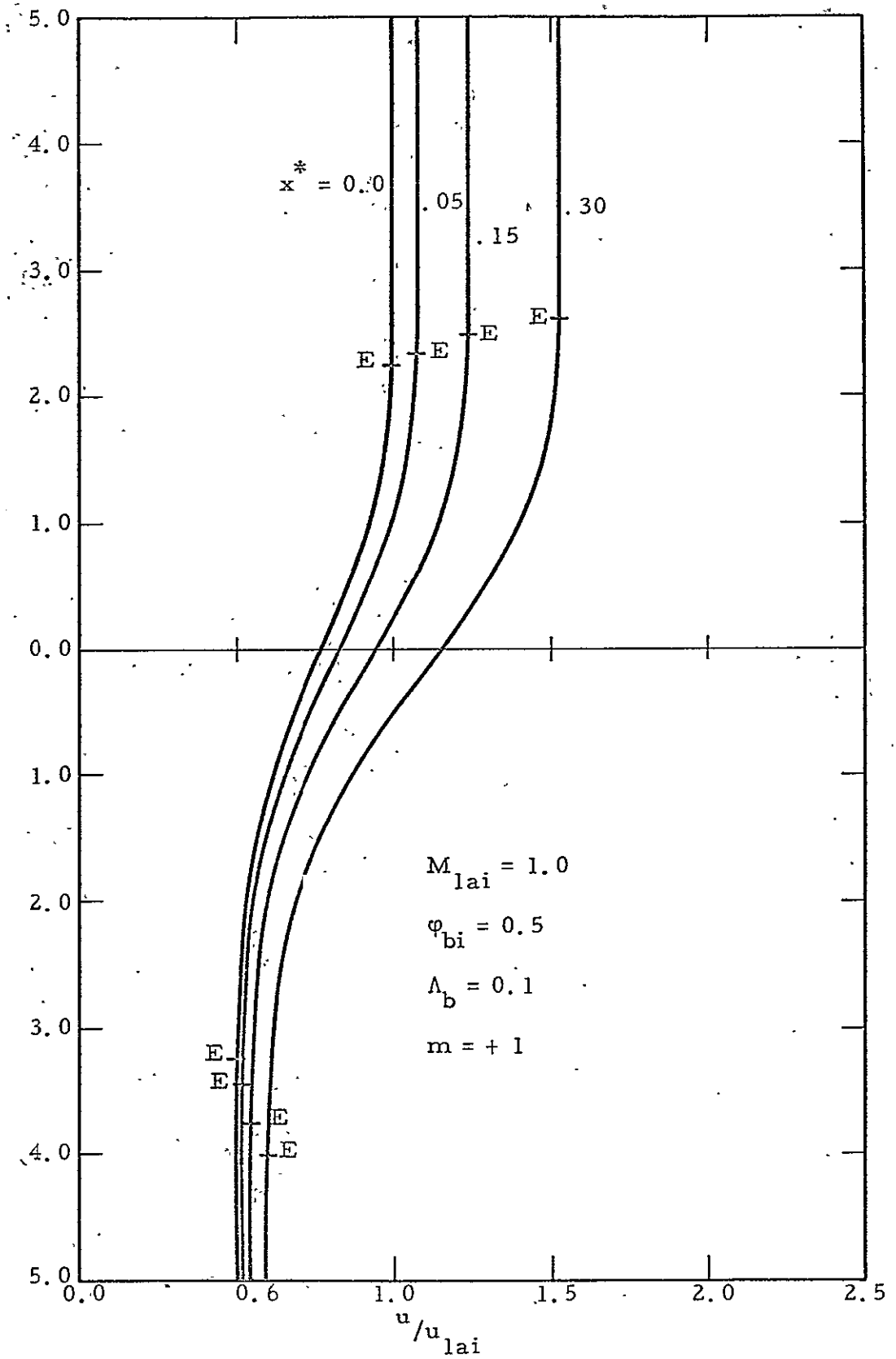

Figure 14a Velocity profiles for Λ_b = 0.1

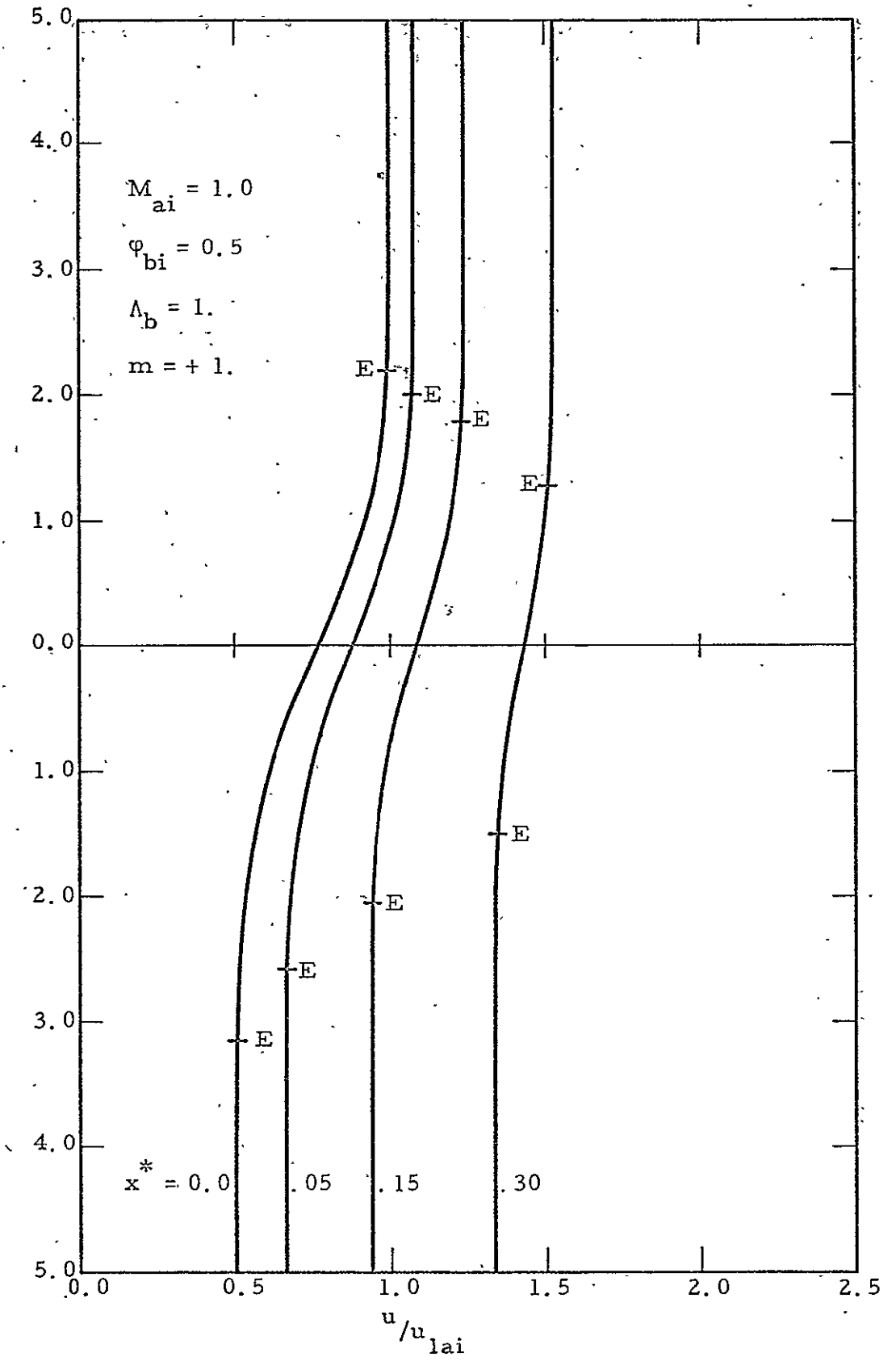

Figure 14b Velocity profiles for Λ_b = 1.0

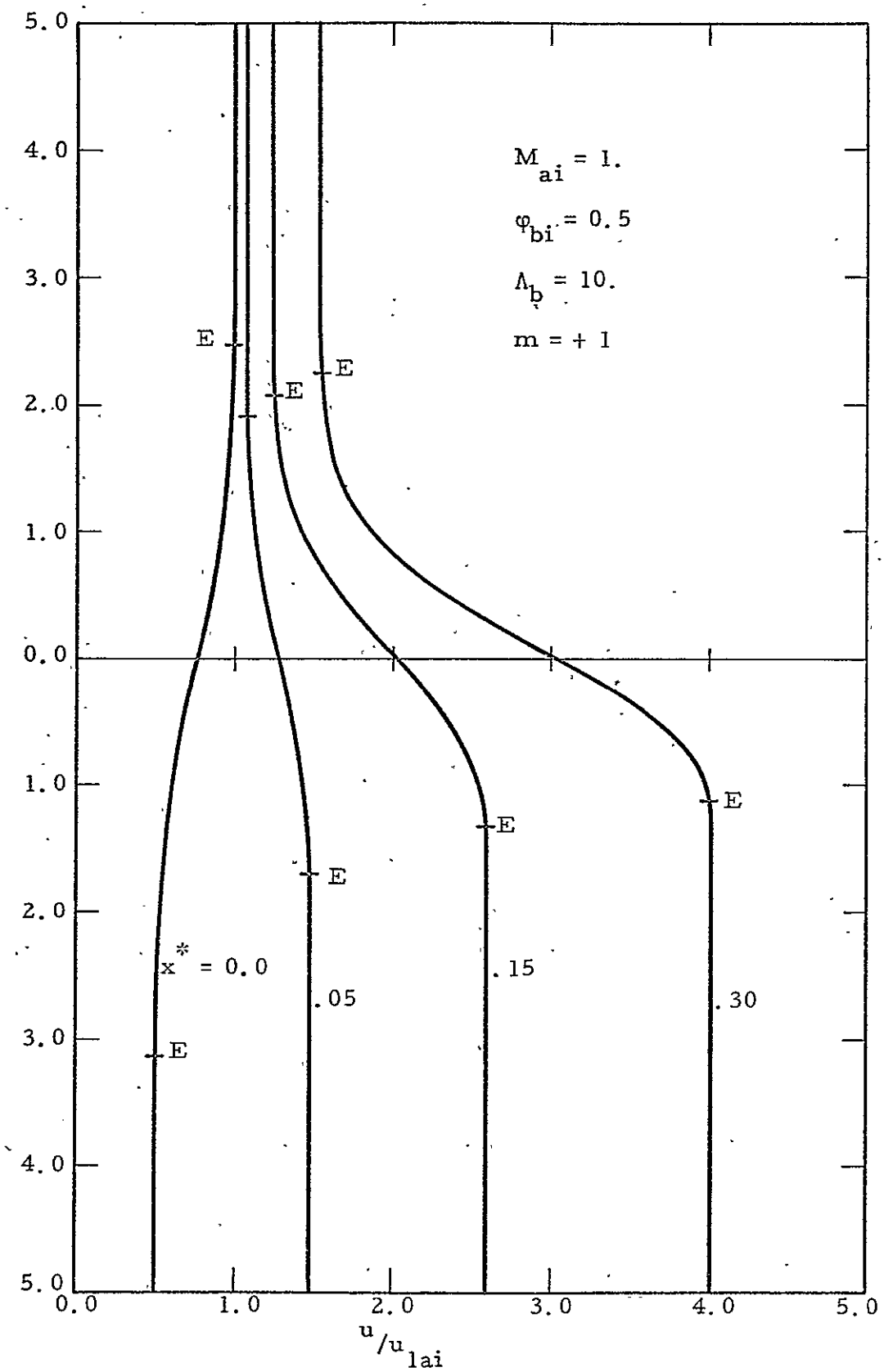

Figure 14c Velocity profiles for Λ_b = 10

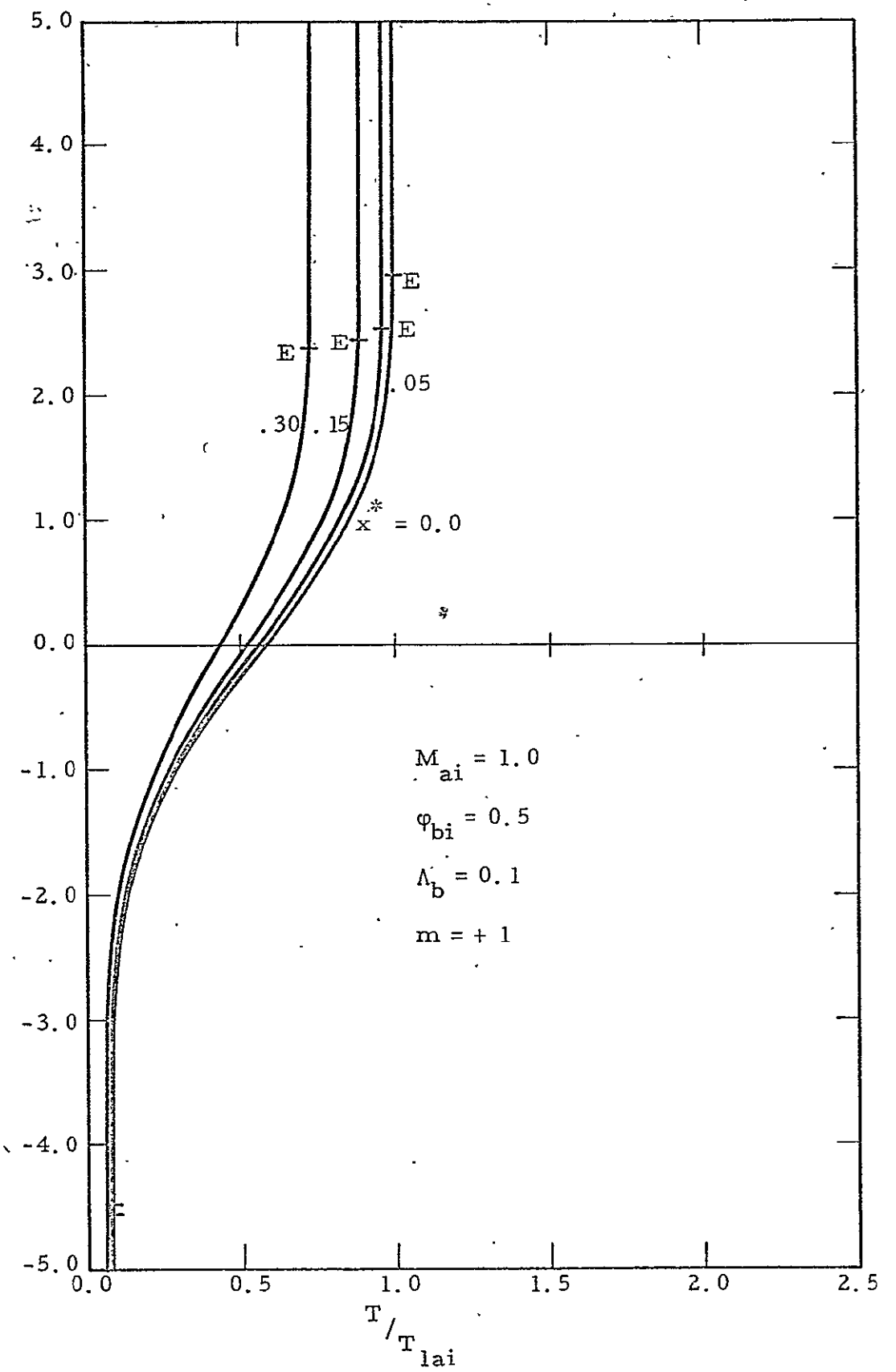

Figure 15a Temperature profiles for $\Lambda_b = 0.1$

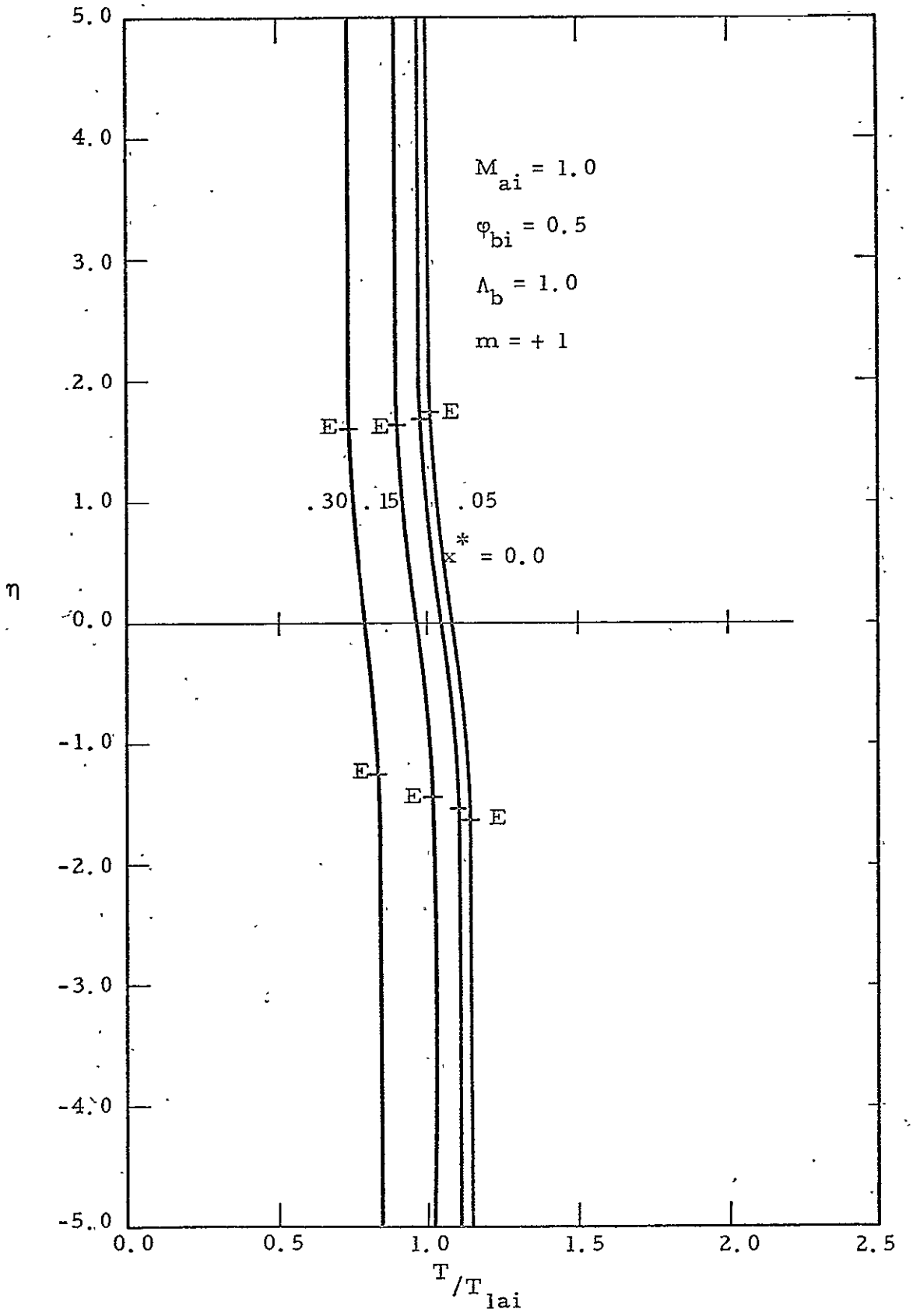

Figure 15b Temperature profiles for $\Lambda_b = 1.0$

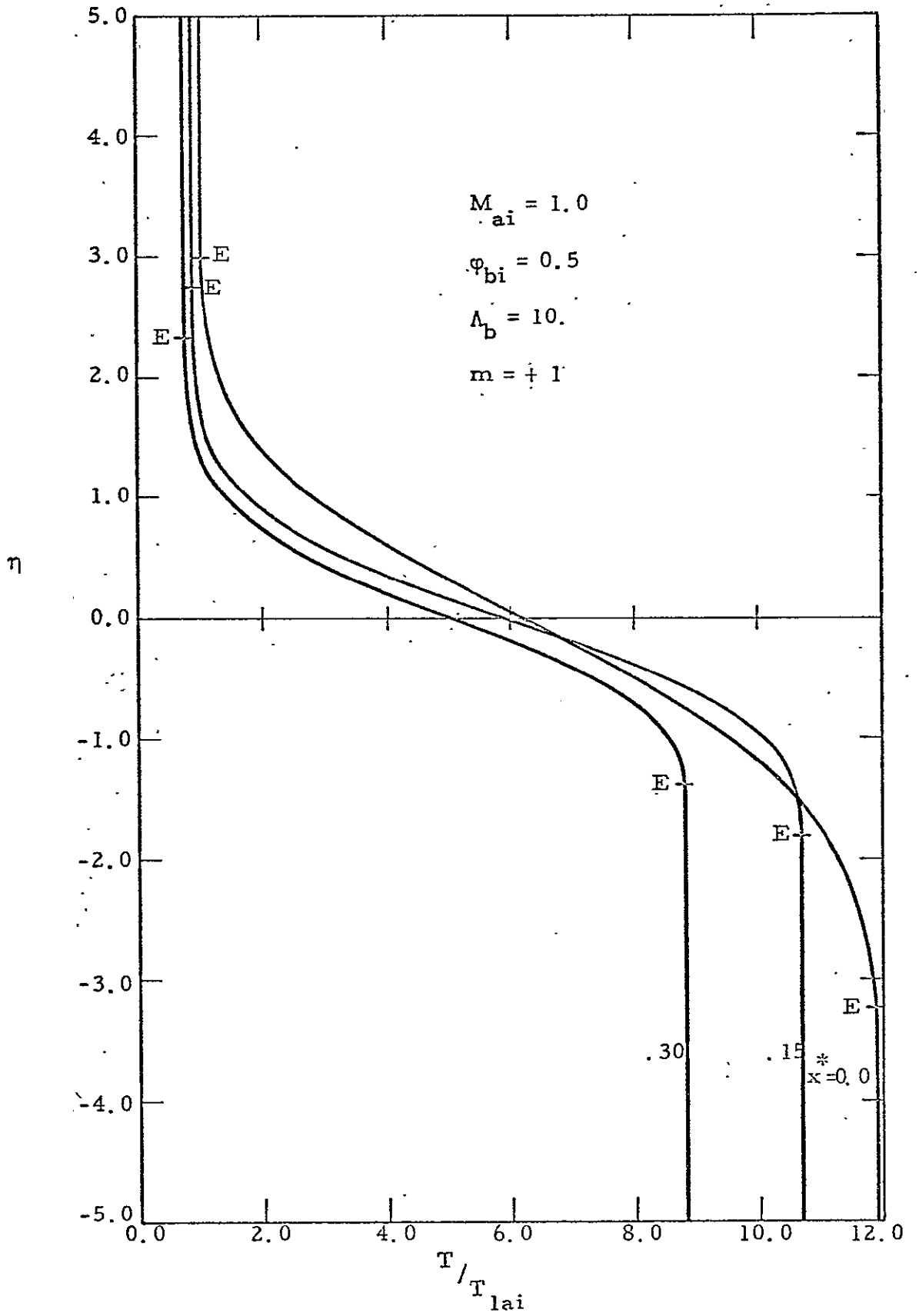

Figure 15c Temperature profiles for Λ_b = 10

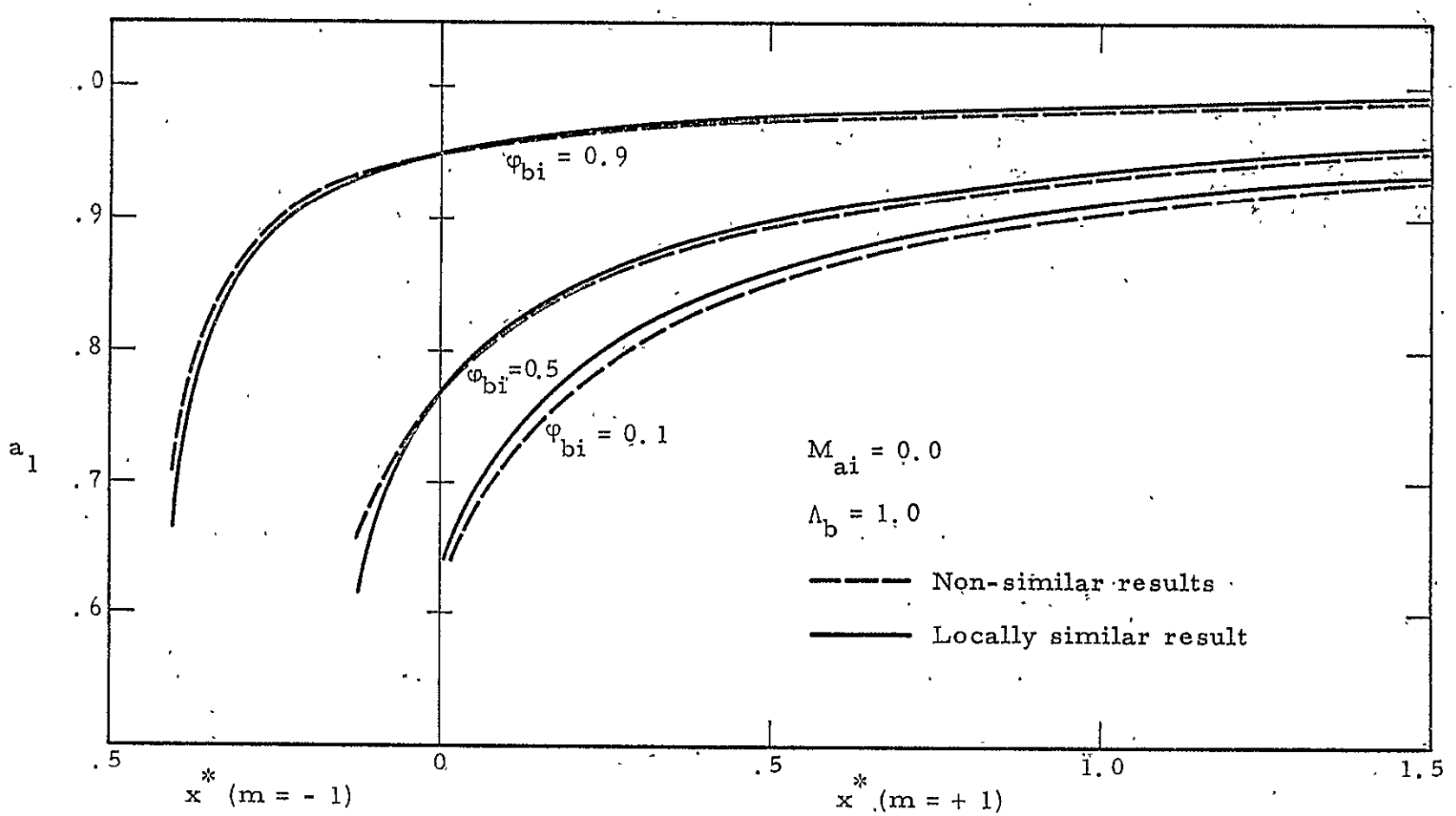

Figure 16a Comparison of a_1 as a function of x^* for the locally similar and non-similar solutions

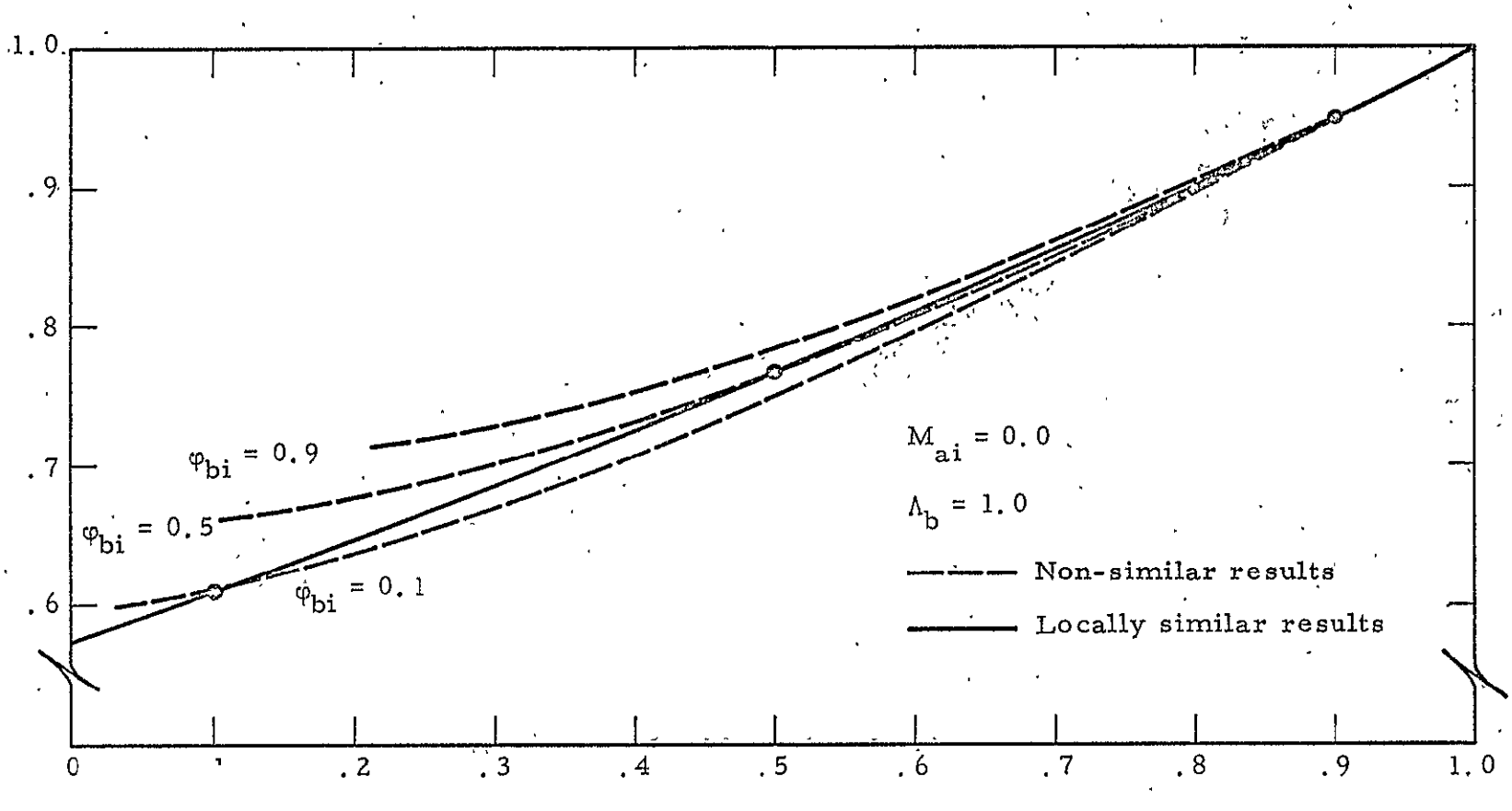

Figure 16b Comparison of a_1 as a function of ϕ_b for the locally similar and non-similar solutions

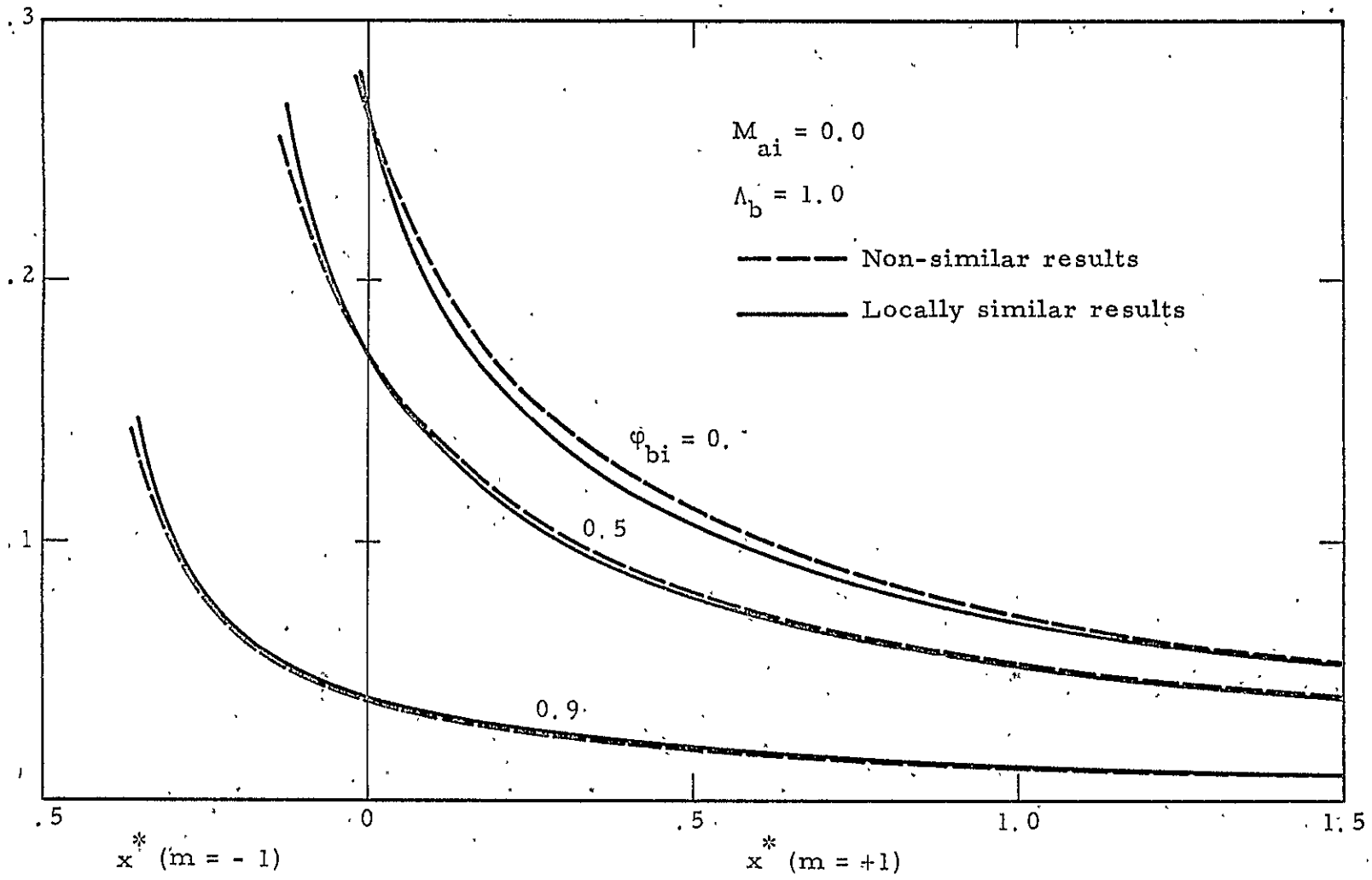

Figure 16c Comparison of a_2 as a function of x^* for the locally similar and non-similar solutions

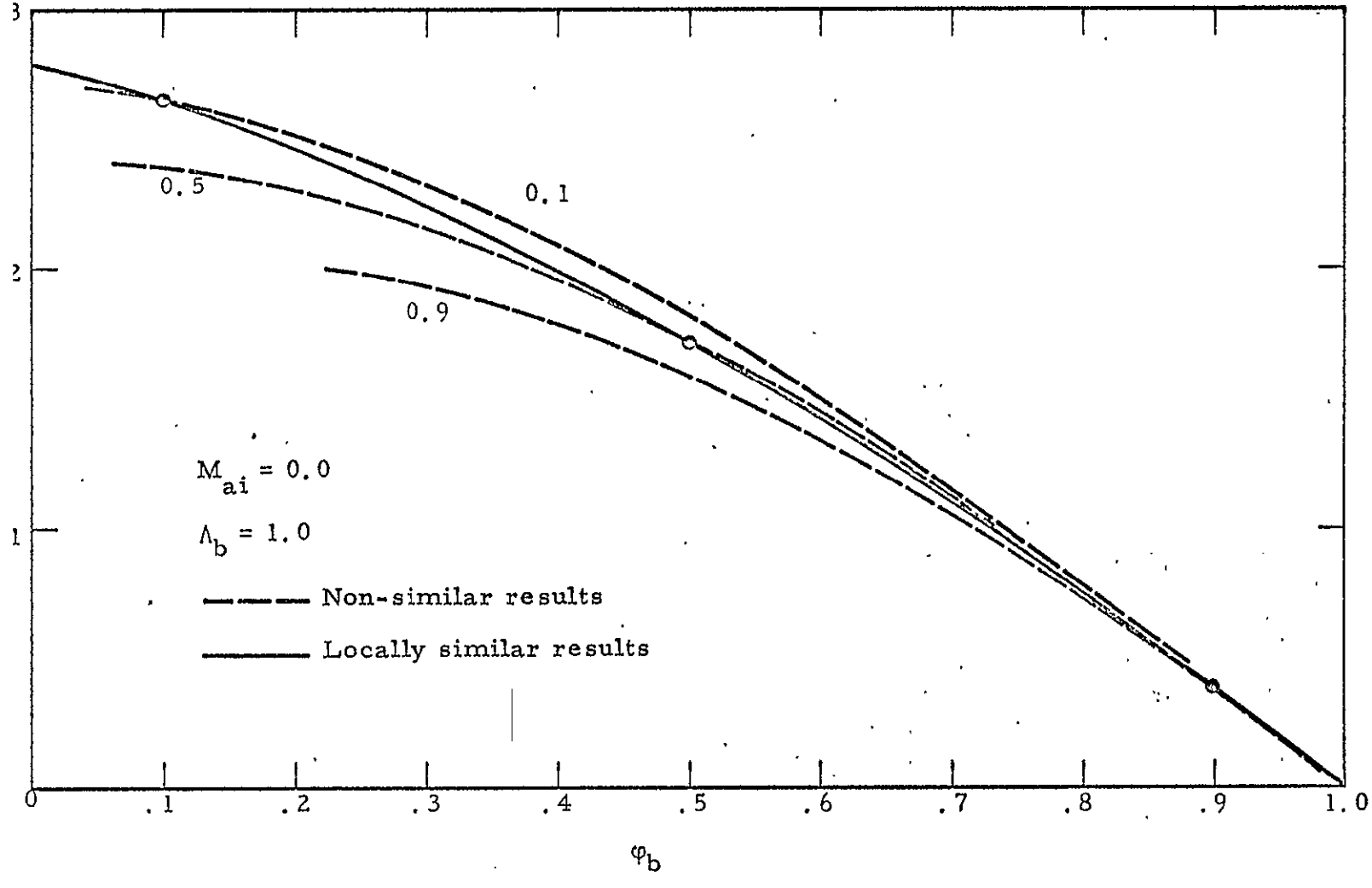

Figure 16d Comparison of a_2 as a function of ϕ_b for the locally similar and non-similar solutions

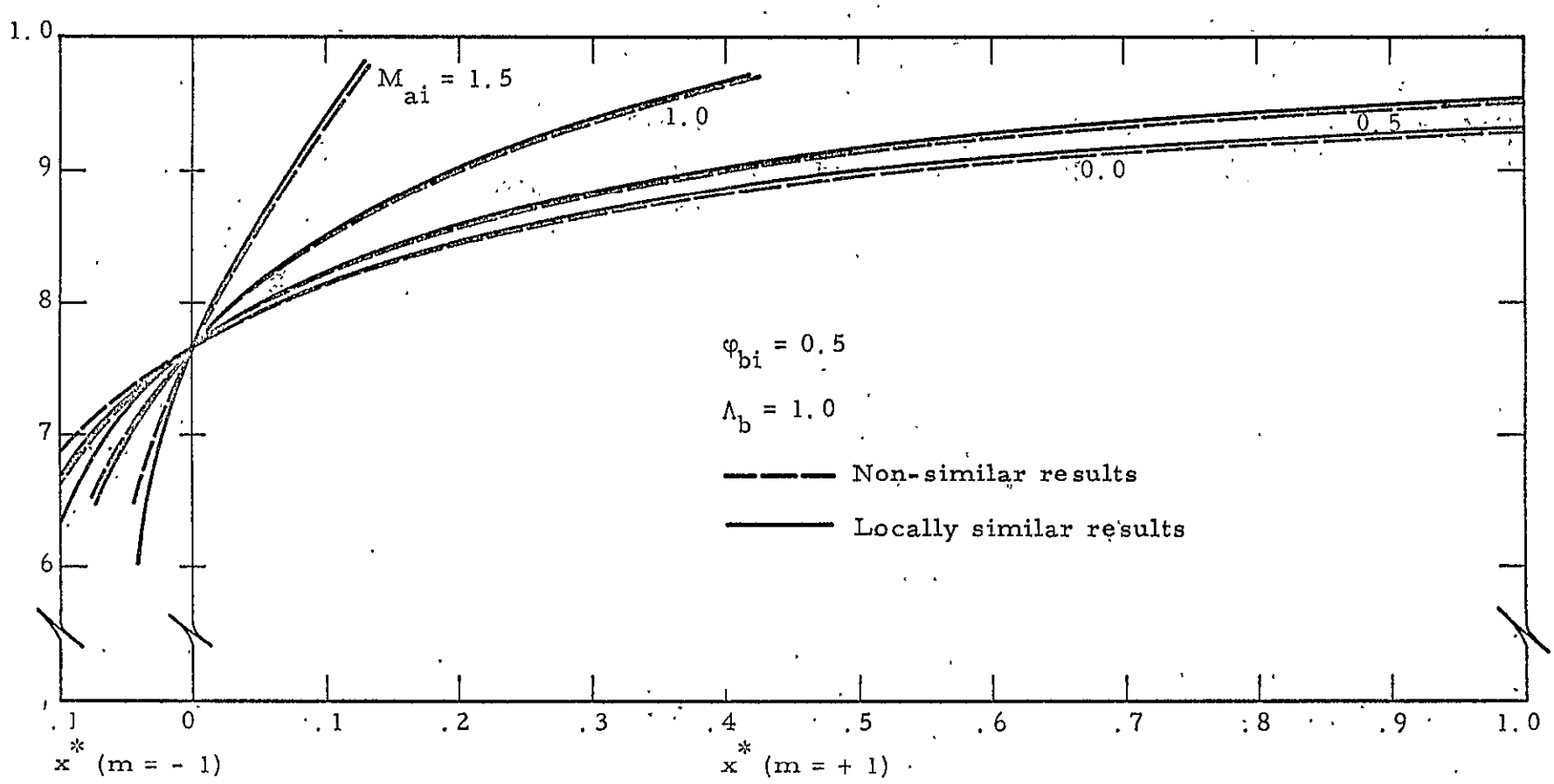

Figure 17a Comparison of a as a function of x* for the locally similar and non-similar solutions

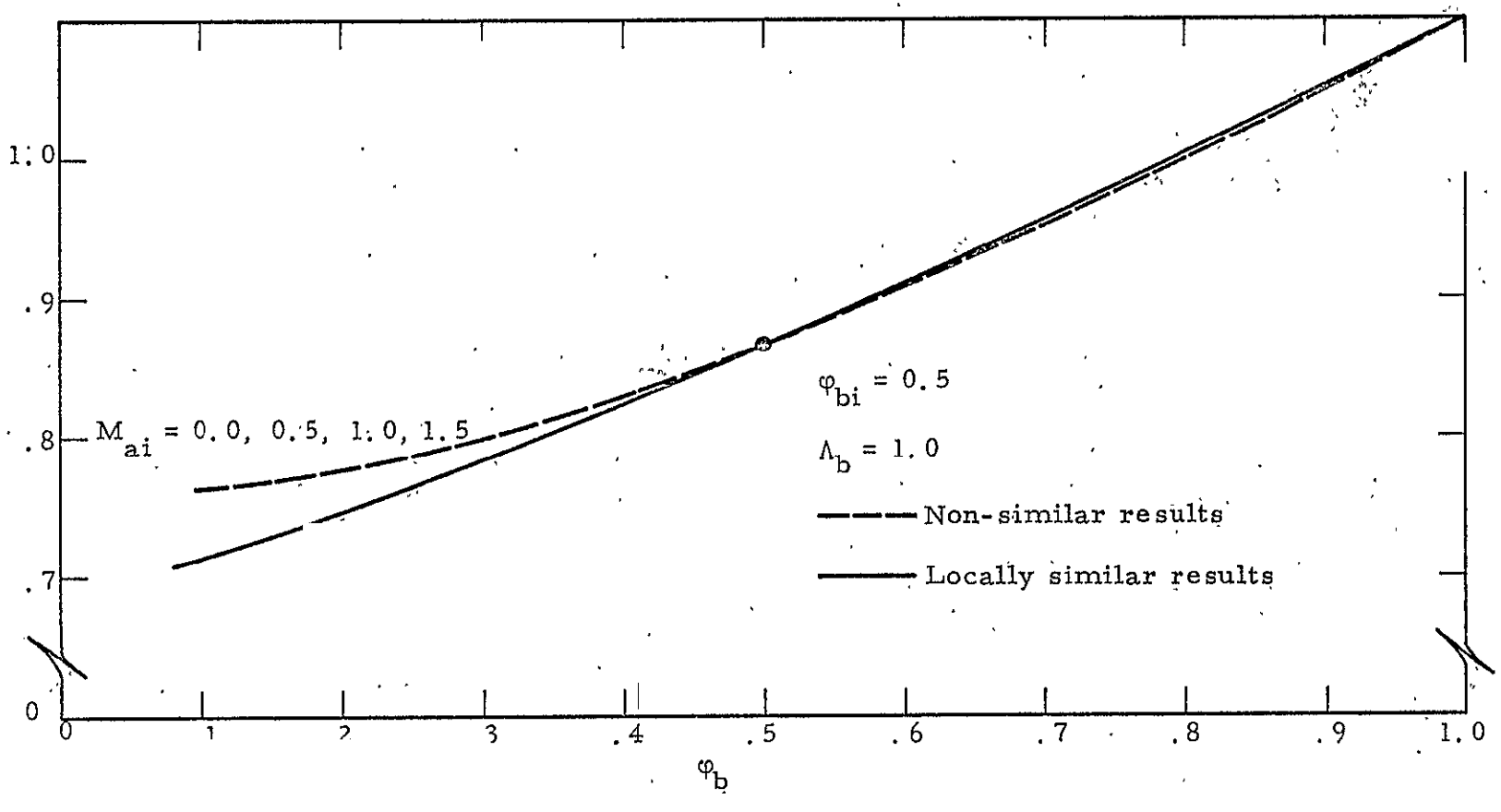

Figure 17b Comparison of a_1 as a function of ϕ_b for the locally similar and non-similar solutions

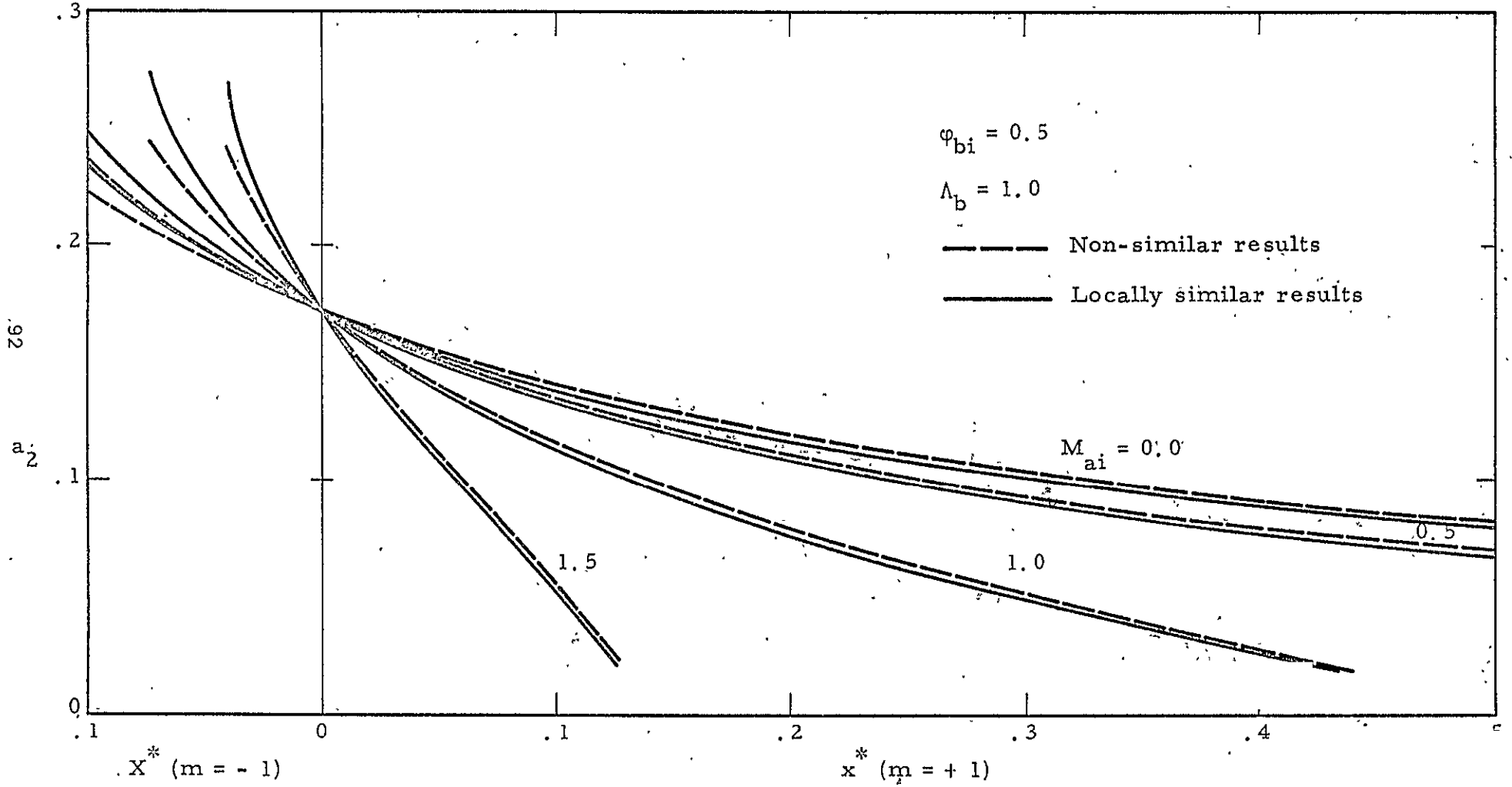

Figure 17c Comparison of a_2 as a function of x^* for the locally similar and non-similar solutions

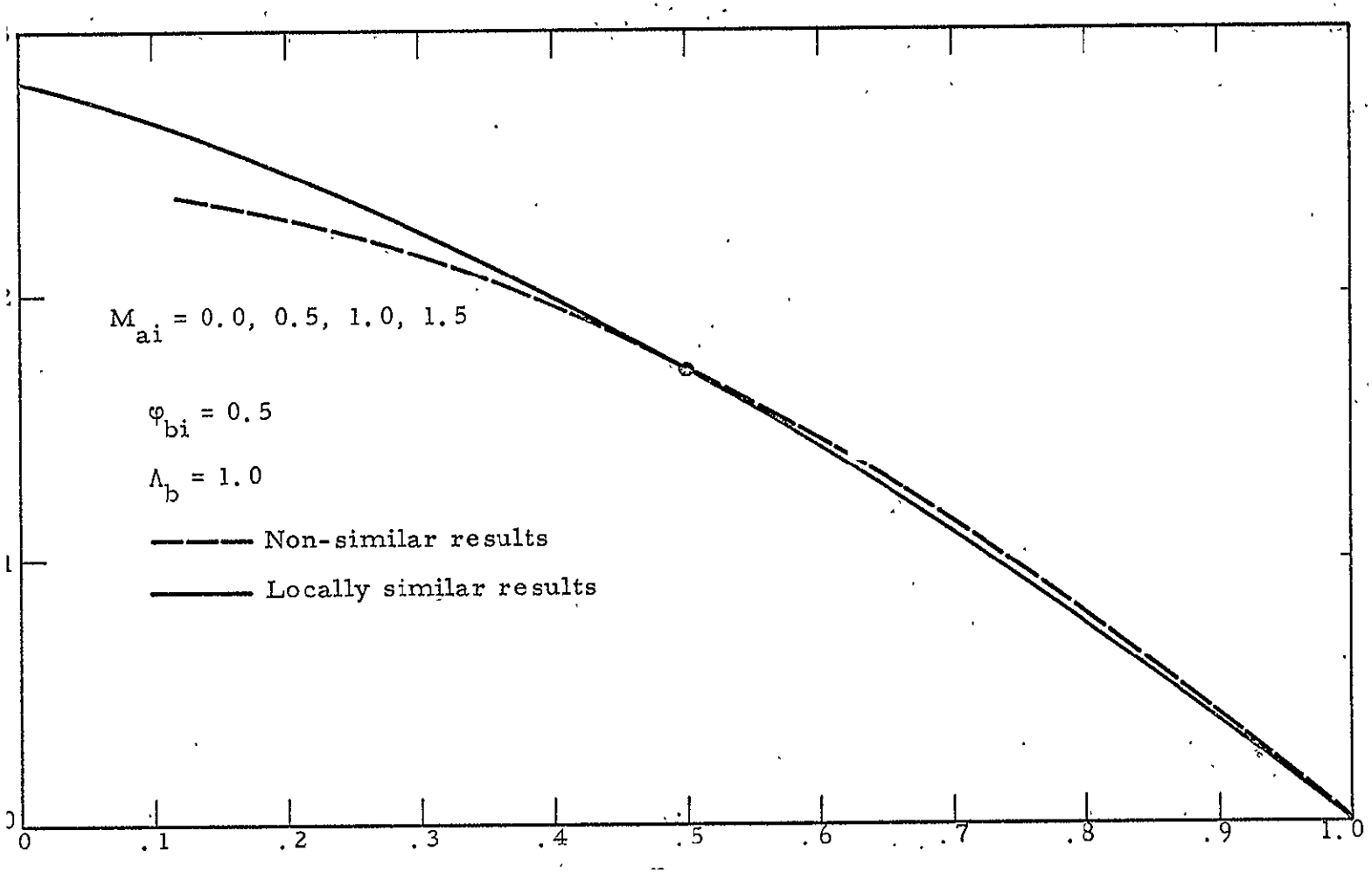

Figure 17d Comparison of a_2 as a function of ϕ_b for the locally similar and non-similar solutions

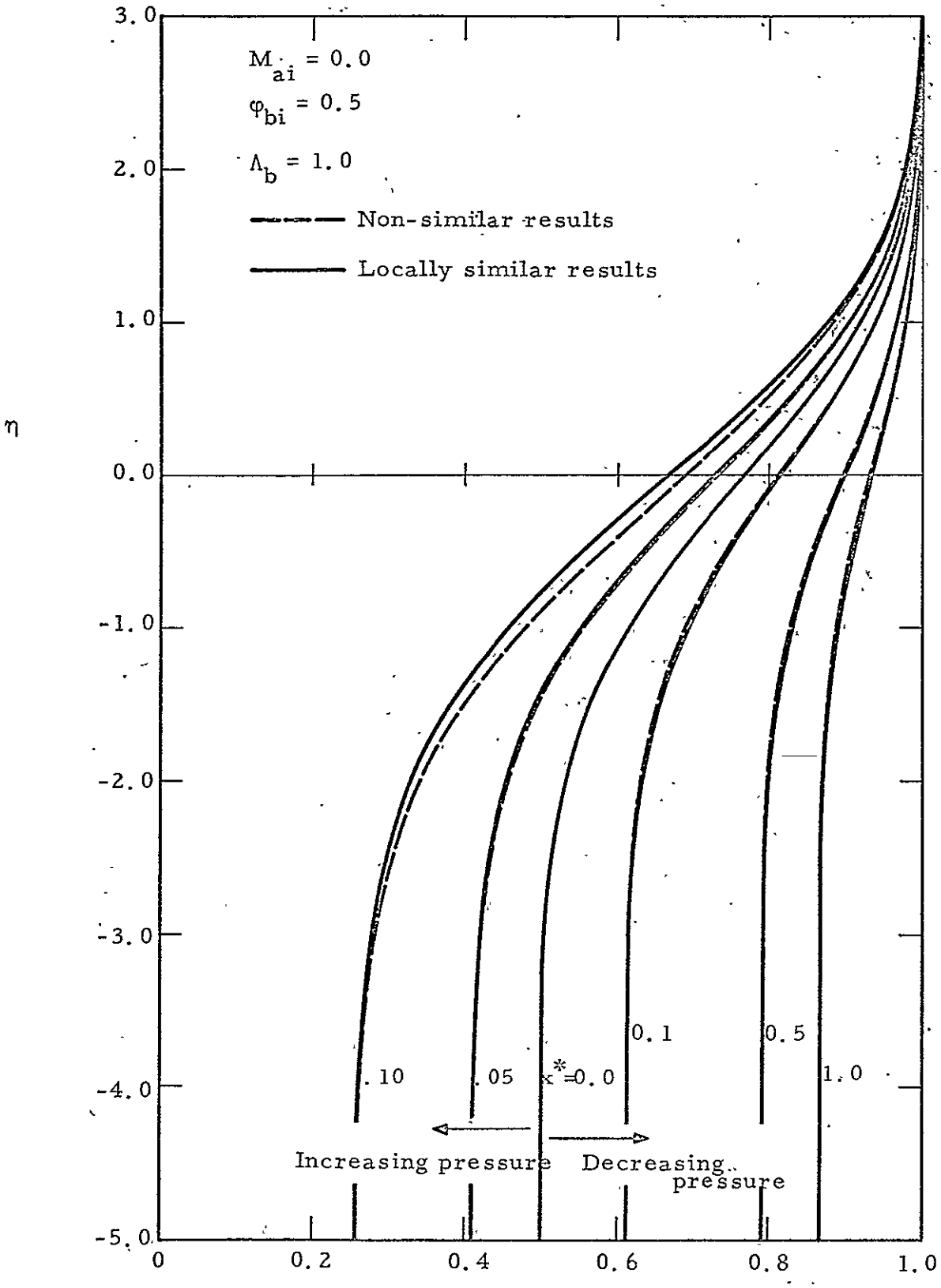

Figure 18a Comparison of velocity profiles for the locally similar and non-similar solutions

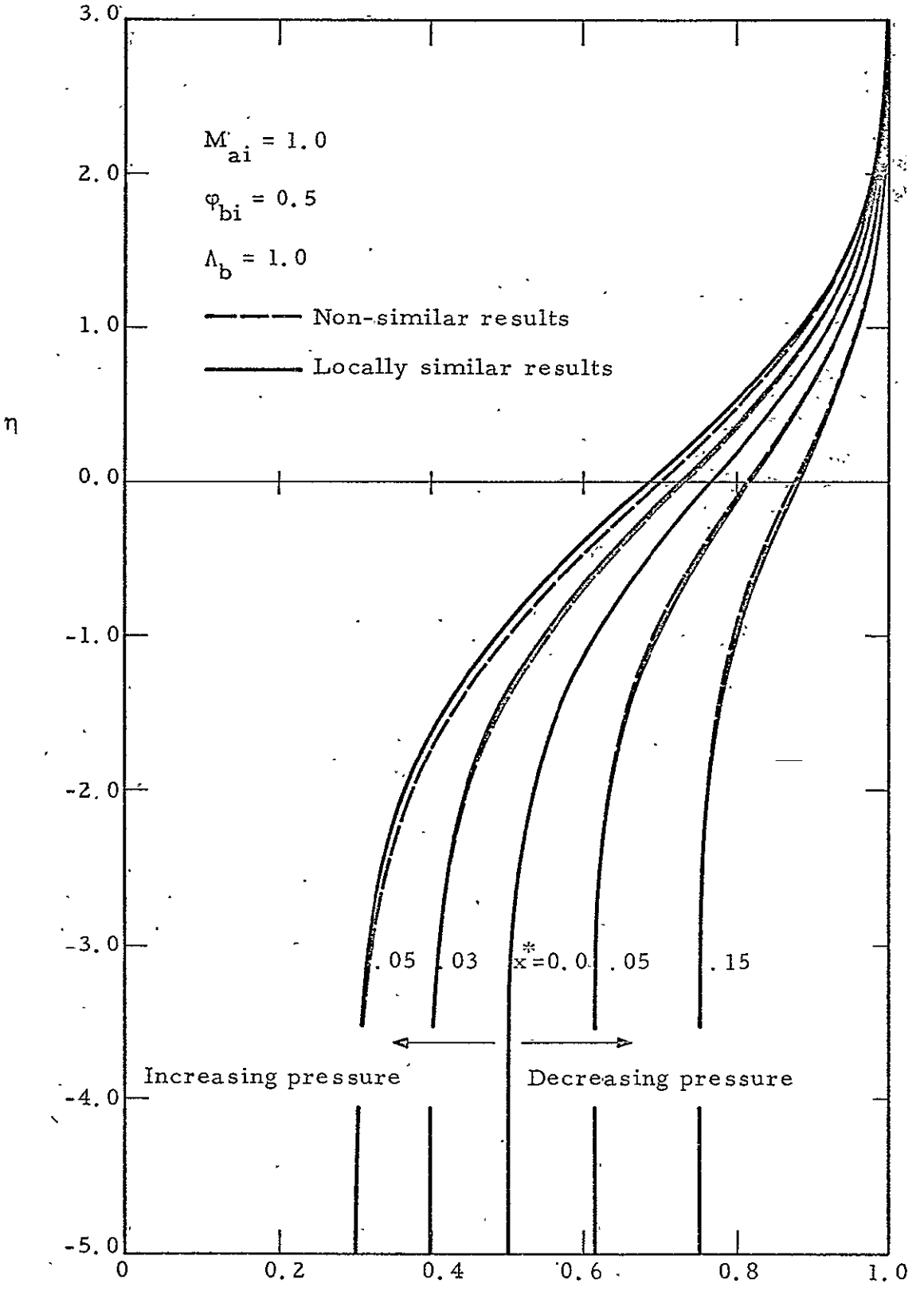

Figure 18b Comparison of velocity profiles for the locally similar and non-similar solutions

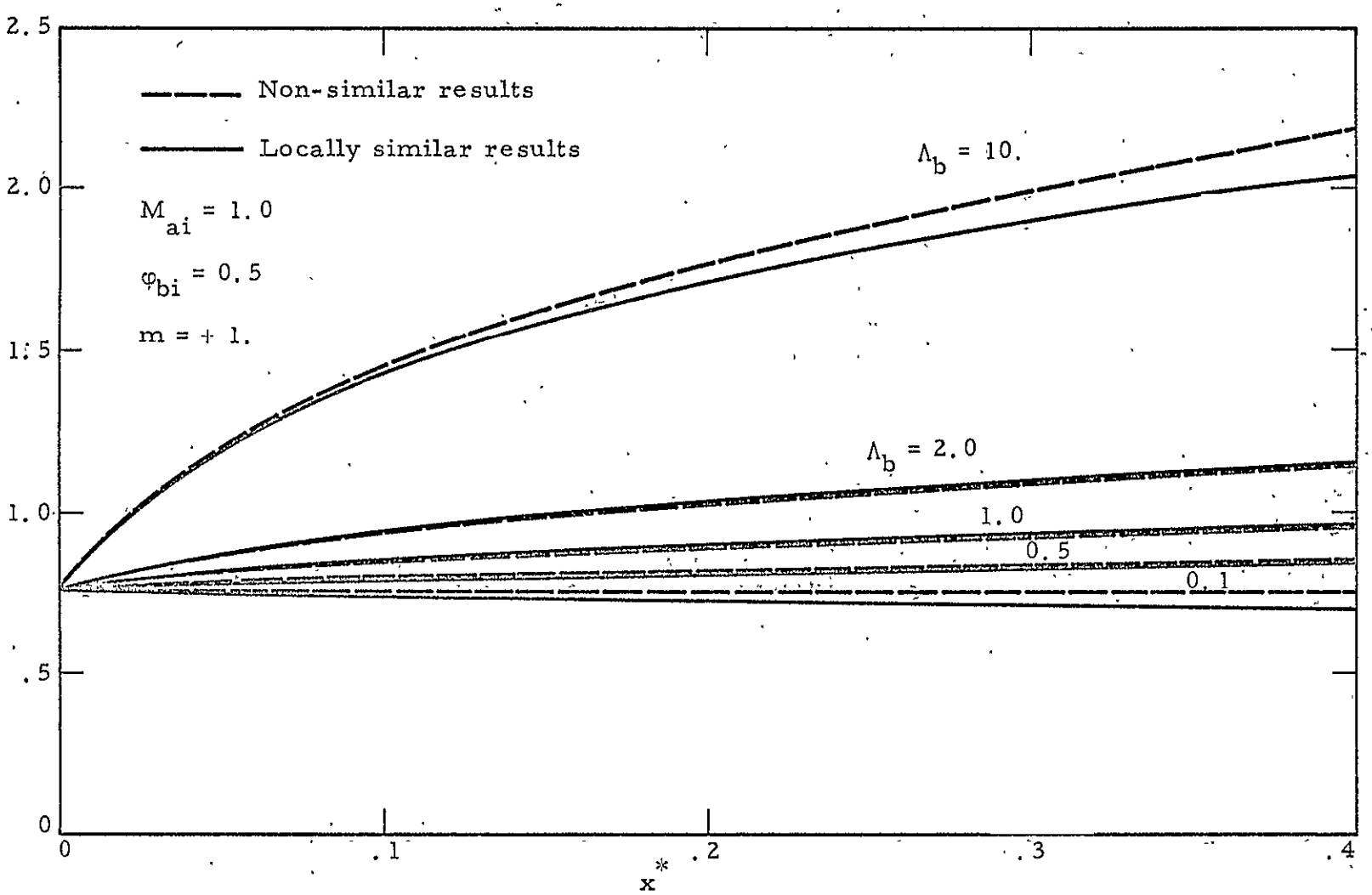

Figure 19a Comparison of a_1 as a function of x* for the locally similar and non-similar solutions

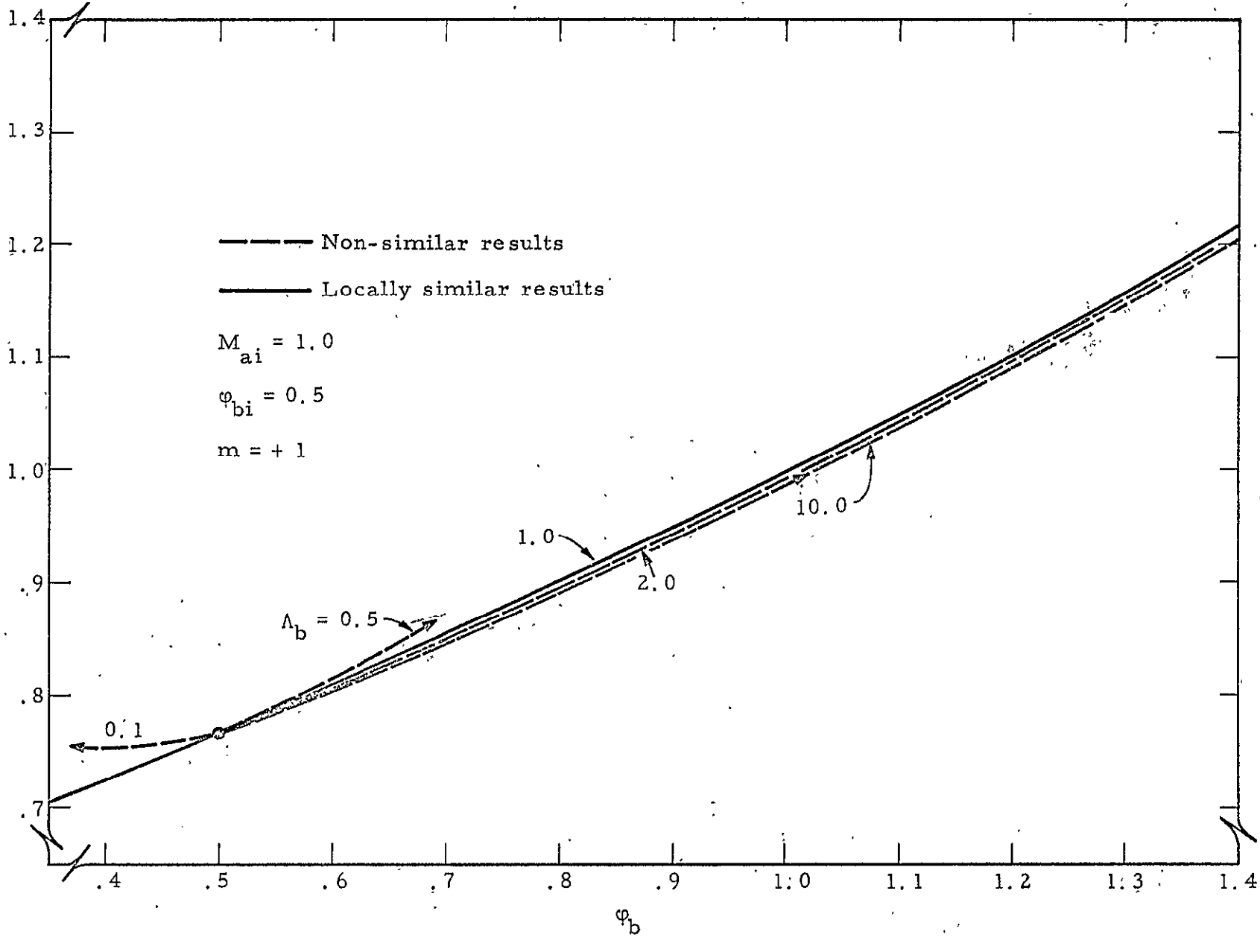

Figure 19b Comparison of a_1 as a function of ϕ_b for the locally similar and non-similar solutions

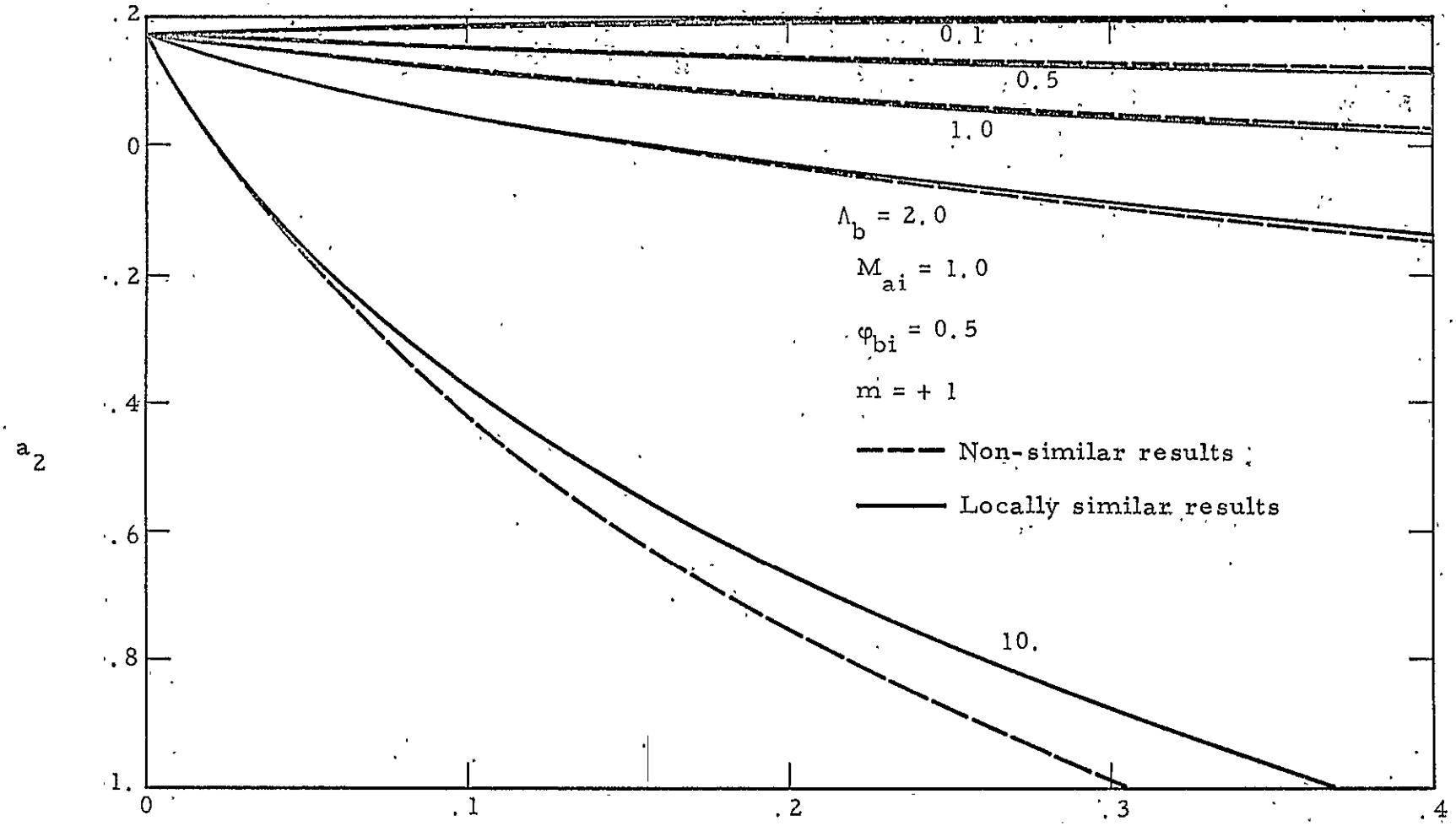

Figure 19c Comparison of a_2 as a function of x* for the locally similar and non-similar solutions

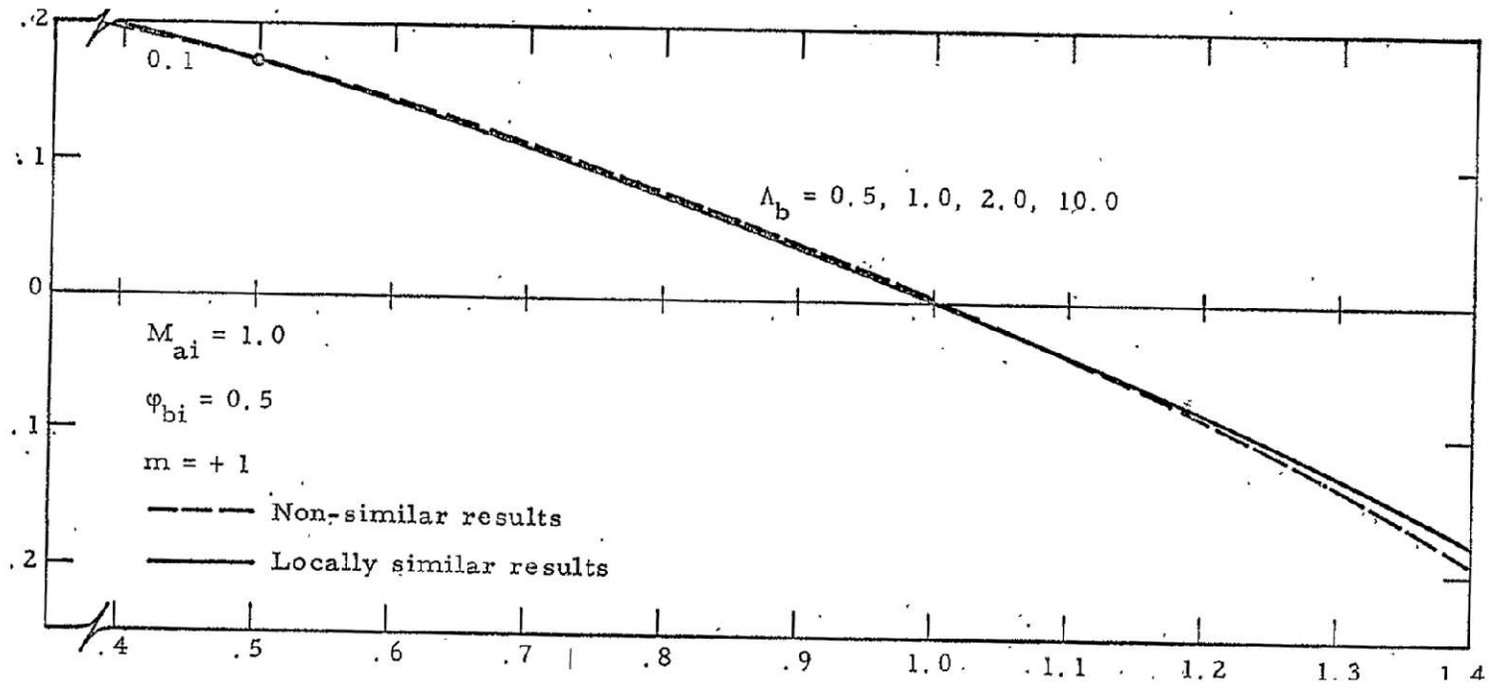

Figure 19d Comparison of a_2 as a function of ϕ_b for the locally similar and non-similar solutions

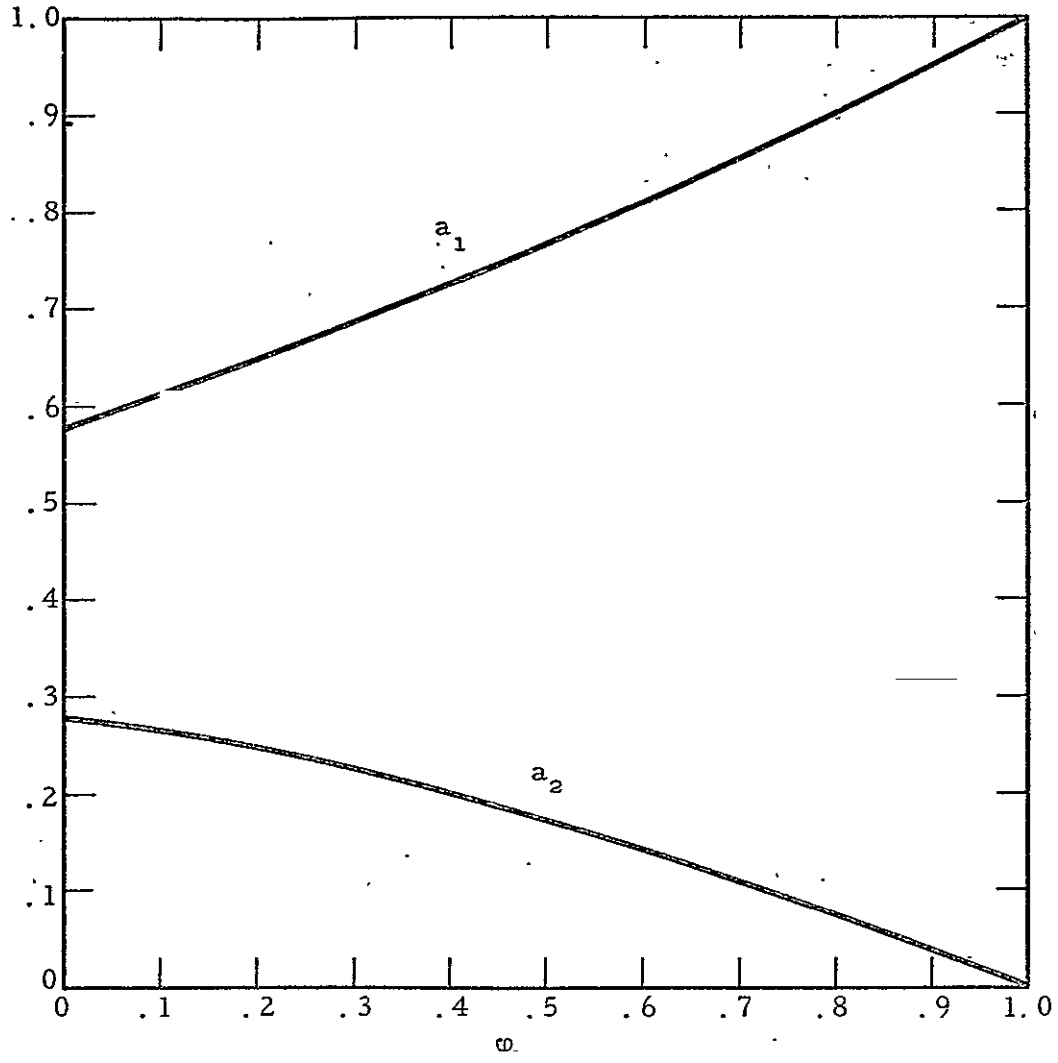

Figure 20 Coefficients a_1 and a_2 (for three terms from Eq. 3.9) as a function of velocity ratio for isobaric similar mixing

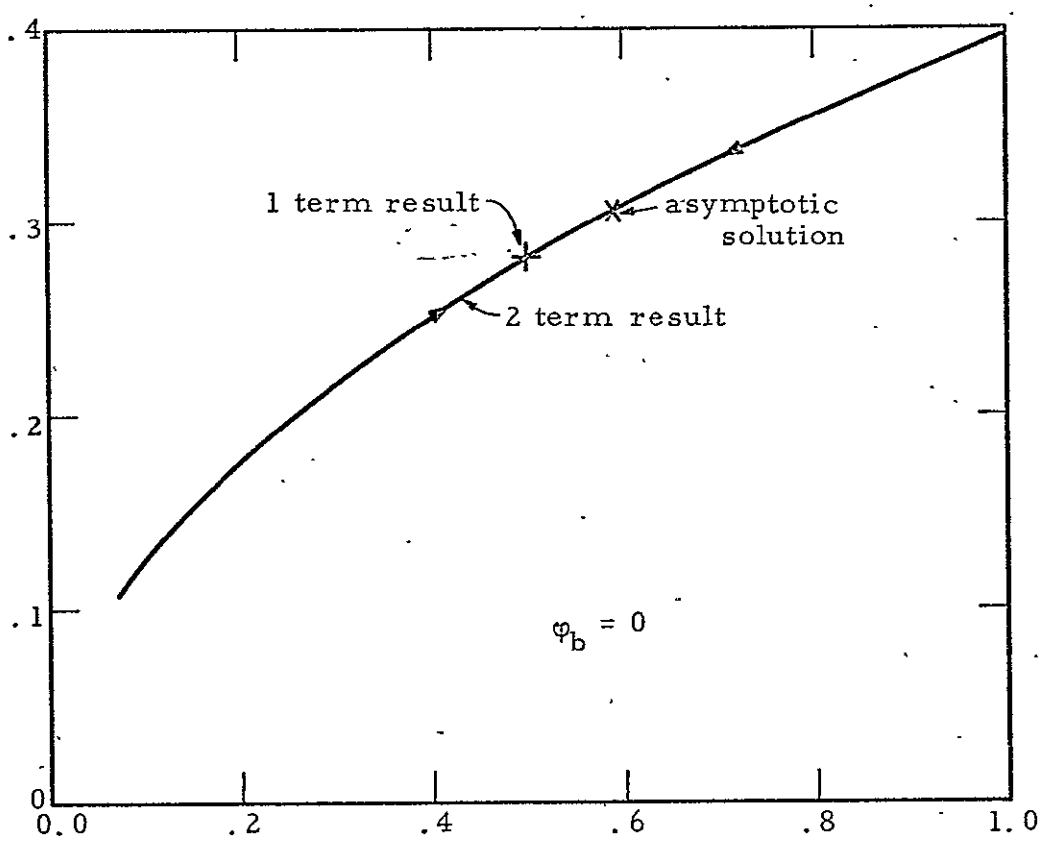

Figure 21 One- and two-term results for isobaric non-similar mixing

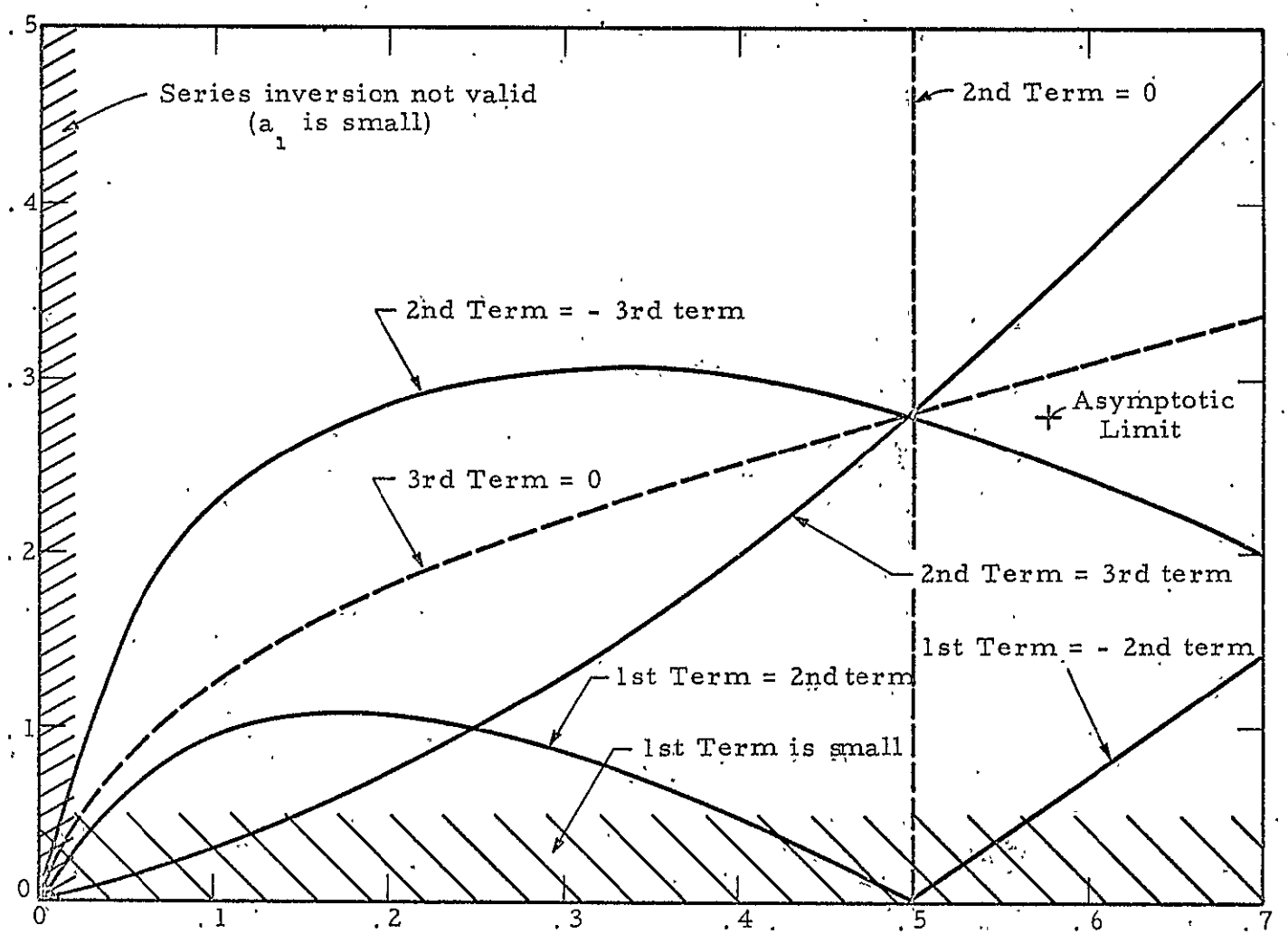

Figure 22 Illustrations of regions of good, slow, and poor convergence in a_1, a_2 plane

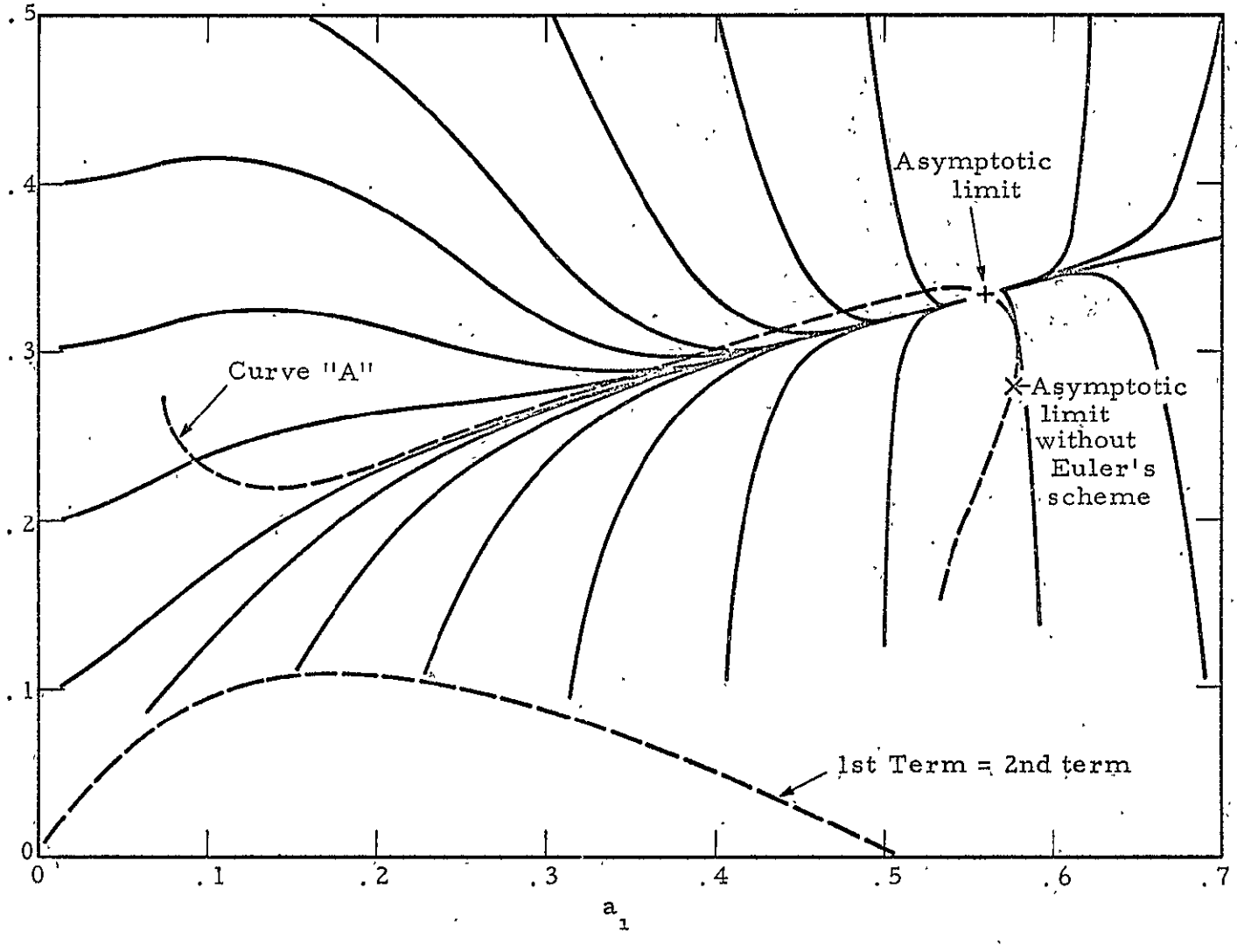

Figure 23 Integral curves using Euler's summation scheme

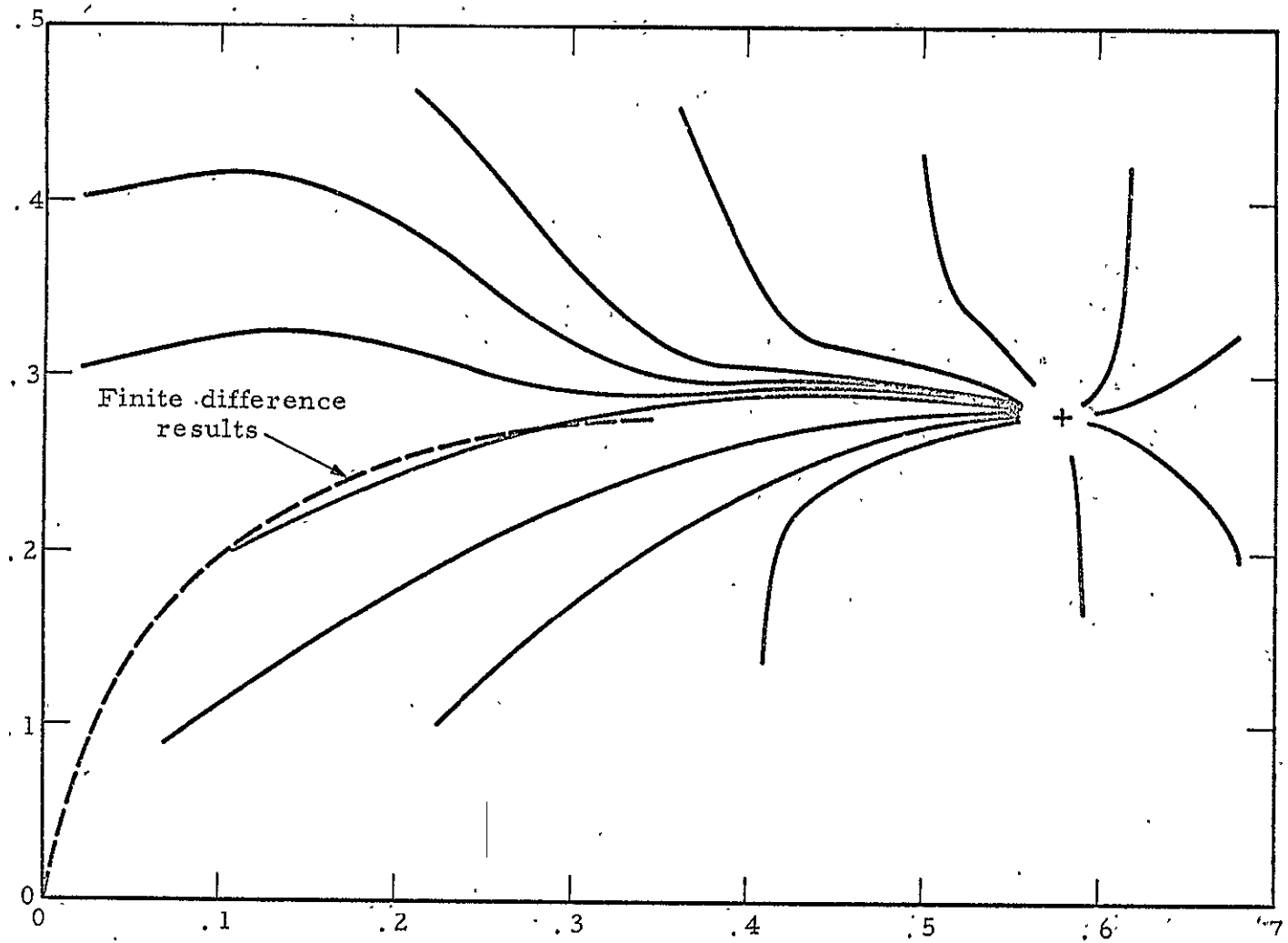

Figure 24 Integral curves and comparison with finite difference results

APPENDIX

Finite Difference Calculation of a Developing Jet Mixing Region

The solution to the problem of incompressible, constant pressure jet mixing with an intial velocity profile at $\xi = \xi_o$ can also be obtained by using a finite difference technique in the von Mises plane. The momentum equation for laminar flow

$$u \frac{\partial u}{\partial x} + v \frac{\partial u}{\partial y} = \nu \frac{\partial^2 u}{\partial y^2} \tag{A1}$$

can be transformed into

$$\frac{\partial u}{\partial x} = \nu \frac{\partial}{\partial \psi} \left(u \frac{\partial u}{\partial \psi} \right) \tag{A2}$$

in the von Mises plane, where $\partial\psi/\partial y = u$, $-\partial\psi/\partial x = v$ have been defined and introduced. Defining

$$X^* = \frac{X}{L} , \phi = \frac{u}{u_o} , \psi^* = \frac{\sqrt{Re_L}}{Lu_o} \psi, \tag{A3}$$

where L is an arbitrary reference length, u_o is a reference velocity, and Re_L is the Reynolds number based on L, u_o, and $\nu (Re_L = Lu_o/\nu)$, the momentum equation becomes

$$\frac{\partial \phi}{\partial x^*} = \frac{\partial}{\partial \psi^*} \left(\phi \frac{\partial \phi}{\partial \psi^*} \right) \tag{A4}$$

Using an implicit finite difference scheme, the derivatives can be written as

$$\frac{\partial \phi}{\partial x^*} = \frac{\phi_j^{i+1} - \phi_j^i}{\Delta x^*}$$

and

$$\frac{\partial}{\partial \psi^*}\left(\phi \frac{\partial \phi}{\partial \psi^*}\right) = \frac{\phi \frac{\partial \phi}{\partial \psi^*}\Big)_j^{i+1} - \phi \frac{\partial \phi}{\partial \psi^*}\Big)_{j-1}^{i+1}}{\Delta \psi^*} \tag{A6}$$

with

$$\phi \frac{\partial \phi}{\partial \psi^*}\Big)_j^{i+1} = \frac{\phi_{j+1}^i + \phi_j^i}{2} \frac{\phi_{j+1}^{i+1} - \phi_j^{i+1}}{\Delta \psi^*}$$

and

$$\phi \frac{\partial \phi}{\partial \psi^*}\Big)_{j-1}^{i+1} = \frac{\phi_j^i + \phi_{j-1}^i}{2} \frac{\phi_j^{i+1} - \phi_{j-1}^{i+1}}{\Delta \psi^*}$$

where linearization has been applied to the above expressions. The differential equation, written in finite difference form becomes

$$\left(\phi_j^i + \phi_{j-1}^i\right) \phi_{j-1}^{i+1} - \left(\frac{1}{A} + \phi_{j+1}^i + 2\phi_j^i + \phi_{j-1}^i\right) \phi_j^{i+1} + \left(\phi_{j+1}^i + \phi_j^i\right) \phi_{j+1}^{i+1} = -\frac{\phi_j^i}{A} \tag{A7}$$

with

$$A = \frac{\Delta x^*}{2(\Delta \psi^*)}$$

When this expression is applied to any point i, j, only three unknown values of ϕ^{i+1} appear in the equation. Therefore, when

Eq. (A7) is written for the n unknown nodes, n equations coupling (n + 2) unknowns result. This system can be written in the matrix form $A\bar{X} = B$, where the n X n square matrix A is seen to be a tri-diagonal matrix.

The boundary conditions will eliminate two unknowns from the above linear system of equations (the largest and smallest index in j). Thus, with given initial conditions, the velocity profile can be established at new locations by solving the matrix equation

$$A\bar{X} = B$$

This method was, of course, programmed on a digital computer and used to calculate the velocity profiles for the problem of one stream jet mixing. The initial profile was that measured by Schubauer at the separation point of a low speed flow past an elliptic cylinder. This profile and its ξ value were also determined by Meksyn.

A total of 71 points was used for the initial profile in the x^*, ψ^* plane, and this number was increased as the width of the mixing region grew. To interpret the results from the calculations in the a_1, a_2 plane, one has to realize that the velocity gradient in the ξ,η plane is

$$\frac{\partial u}{\partial y} = \frac{u_{1a}}{L}\sqrt{\frac{Re_L}{2\xi}}\, f_{\eta\eta}$$

with

$$a_1 = f_\eta(\xi, \eta = 0)$$

$$a_2 = f_{\eta\eta}(\xi, \eta = 0)$$

and from the results obtained from the x^*, ψ^* plane

$$\frac{\partial u}{\partial y} = \frac{u_o}{L} \sqrt{Re_L'}\, \phi \frac{\partial \phi}{\partial \psi^*}$$

where Re_L and Re_L' are based on u_{1a} and u_o, respectively, L being the minor axis of the elliptic cylinder. From the measurements of Schubauer at the separation point

$$u_{1a} = 1.25\, u_o^*$$

while $a_1 = \phi_d^i$, the value of a_2 (the velocity gradient at the dividing streamline in the ξ,η plane) then becomes

$$a_2 = \sqrt{\frac{2\xi_o}{1.25(\Delta\psi^*)^2} + 4A(i-1)}\; \frac{\phi_d^i}{\sqrt{1.25}}\; \frac{\phi_{d-1} - \phi_{d+1}^i}{2}$$

where subscript d refers to the dividing streamline (identified by $\psi^* = 0$). The results of these numerical calculations are presented in Fig. 24.

---

†Note that due to the difference in the reference velocities between the two formulations the ξ_o obtained by Meksyn and the velocity profile have to be corrected before the results may be plotted in the a_1, a_2 plane.